

# Modeling and optimization of building HVAC systems

Jin, Guang Yu

2011

Jin, G. Y. (2011). Modeling and optimization of building HVAC systems. Doctoral thesis, Nanyang Technological University, Singapore.

<https://hdl.handle.net/10356/49960>

<https://doi.org/10.32657/10356/49960>

# **Modeling and Optimization of Building HVAC Systems**

**Jin Guang Yu**

**School of Electrical & Electronic Engineering**

A thesis submitted to the Nanyang Technological University  
in fulfillment of the requirement for the degree of  
Doctor of Philosophy

**2011**

### **Statement of Originality**

I hereby certify that the work embodied in this thesis is the result of original research and has not been submitted for a higher degree to any other University or Institution.

---

Date

---

Jin Guang Yu

# Acknowledgements

First and foremost, I would like to express my sincere gratitude to my supervisor, Associate Professor Dr. Cai Wenjian, for his enthusiastic encouragement, excellent guidance and inspiration throughout the duration of this research.

I would like to sincerely thank my wife, my parents and my relatives for their continuous encouragement, understanding and steadfast support.

Special thanks are also dedicated to my seniors and colleagues, Dr. Lu Lu, Dr. Ding Xudong and Dr. Wang Yaowen and technicians at the Instrumentation & System Engineering Laboratory and the Process Instrumentation Laboratory for their help and encouragement during the course of my study.

Finally, I would like to thank the School of Electrical and Electronic Engineering, Nanyang Technological University for providing the experimental environment, research facilities and opportunity for this study.

# **Abstract**

This thesis presents the development of hybrid modeling methodologies for HVAC component static/steady-state models and dynamic/transient models, and the development and implementation of a model-based optimization approach for building heating, ventilating, and air conditioning (HVAC) systems, especially for the out-building section. Firstly, through component characteristic analysis, hybrid HVAC component models associated with cooling loads, operating variables and energy consumption characteristics for heat exchangers and energy consuming devices are established. All the model parameters can be derived from manufacturers' specification data or on-site testing and measurement data. Secondly, the nonlinear constraint optimization problem for HVAC out-building section which consists of a refrigeration cycle and a condenser water loop is formulated by considering the system level and component level characteristics and interactions among all components and their associated variables. The optimization of both the refrigeration cycle and the condenser water loop is realized using a PSO based optimizer, with the target of minimizing the total power consumption of the HVAC system. Simulation studies of the proposed system optimization approach are conducted to compare the control accuracy, computation time and memory requirement of the proposed PSO based optimizer with those of the GA based optimizer using the same models. The results show that the system optimization approach using PSO based optimizer is able to achieve the same control accuracy yet requiring less computation time and memory compared to the system optimization approach using a GA based optimizer. Then the proposed hybrid model-based system optimization approach using a PSO based optimizer is implemented in the laboratorial centralized HVAC system to validate and evaluate the energy performance of the proposed method compare to traditional ones. The results of

experimental tests show that the proposed method indeed improves the system performance significantly.

The main contribution of this thesis is to propose hybrid modeling methodologies to predict the steady-state as well as the transient performance of the HVAC component, which is the prerequisite for model-based control and optimization; and to develop a general feasible model-based system optimization approach to systematically optimize the energy consumption of a HVAC system out-building section instead of optimizing its individual components.

# Table of Contents

<b>Acknowledgements</b>	<b>i</b>
<b>Abstract</b>	<b>ii</b>
<b>Table of Contents</b>	<b>iv</b>
<b>Table of Chapters</b>	<b>v</b>
<b>List of Figures</b>	<b>ix</b>
<b>List of Tables</b>	<b>xii</b>
<b>Nomenclature</b>	<b>xiii</b>

# Table of Chapters

CHAPTER 1 INTRODUCTION .....	1
1.1 Background of HVAC Systems, EMCS and Supervisory Control.....	1
1.2 Motivation and Objectives .....	4
1.3 Major Contributions .....	6
1.4 Organization of the Thesis .....	7
CHAPTER 2 LITERATURE REVIEW .....	9
2.1 Modeling .....	10
2.1.1 Static cooling tower models.....	12
2.1.2 Dynamic cooling coil models .....	13
2.1.3 Dynamic cooling tower models .....	15
2.1.4 Composite models for the refrigeration cycle.....	16
2.2 Model –Based System Optimization for HVAC Systems .....	19
2.2.1 Physical model-based system optimization .....	22
2.2.2 Black-box model-based system optimization .....	27
2.2.3 Hybrid model-based system optimization .....	34
2.3 Summary .....	36
CHAPTER 3 STATIC MODEL OF COOLING TOWERS.....	39
3.1 Introduction.....	39
3.2 Hybrid Cooling Tower Model .....	39
3.2.1 Mechanism analysis of mechanical cooling towers.....	39
3.2.2 Merkel’s model .....	40
3.2.3 NTU-effectiveness method .....	42
3.2.4 Stoecker’s model.....	45
3.3 Hybrid Model.....	46

3.4 Parameter Identification .....	49
3.5 Model Validation .....	52
3.6 Summary .....	58
CHAPTER 4 DYNAMIC MODELS OF COOLING COILS AND COOLING	
TOWERS .....	62
4.1 Introduction.....	62
4.2 Hybrid Cooling Coil Model .....	62
4.2.1 Modeling based on heat transfer mechanism.....	62
4.2.2 Modeling based on energy and mass conservation.....	65
4.2.3 Dynamic modeling.....	68
4.3 Hybrid Cooling Tower model.....	71
4.3.1 Modeling based on heat transfer mechanism.....	71
4.3.2 Modeling based on energy and mass conservation.....	74
4.3.3 Dynamic modeling.....	78
4.4 Parameter Identification.....	78
Step 1 Steady state identification.....	79
Step 2 Dynamic identification .....	80
4.5 Model Validation .....	83
4.5.1 Model validation of a cooling coil.....	84
4.5.2 Model validation of a cooling tower.....	88
4.6. Summary .....	91
CHAPTER 5 COMPOSITE MODEL OF REFRIGERATION CYCLES .....	
5.1 Introduction.....	92
5.2 Composite Model.....	93
5.2.1 Evaporator model.....	94

5.2.2 Compressor model .....	100
5.2.3 Expansion valve model .....	102
5.2.4 Condenser model .....	102
5.3 Model Validation .....	107
5.4 Summary .....	109
CHAPTER 6 HVAC SYSTEM OPTIMIZATION – OUT-BUILDING SECTION....	110
6.1 Introduction.....	110
6.2 Formulation of Model-Based Optimization.....	113
6.2.1 Objective function.....	113
6.2.2 Physical limitation constraints of components .....	115
6.2.3 Interaction constraints between components .....	116
6.3 Optimization Based on PSO Algorithms .....	127
6.3.1 Initialization .....	127
6.3.2 Construction of the fitness function.....	128
6.3.3 Updating velocity and position .....	129
6.3.4 Termination.....	130
6.3.5 PSO implementation .....	130
6.4 Optimization Based on Genetic Algorithms (GA).....	132
6.4.1 Encoding .....	133
6.4.2 Construction of the fitness function.....	134
6.4.3 Evolutionary operation.....	136
6.4.4 Termination.....	137
6.4.5 GA implementation.....	138
6.5 Comparison Study of Two Optimization Methods.....	139
6.5 Summary .....	143

CHAPTER 7 REAL SYSTEM IMPLEMENTATION .....	144
7.1 Introduction.....	144
7.2 Description of Experimental HVAC System.....	145
7.3 Implementation of System Optimization Approach .....	148
7.4 Experimental Study of Energy Performances.....	152
7.5 Summary.....	164
CHAPTER 8 CONCLUSIONS AND FUTURE WORK.....	165
8.1 Conclusions.....	165
8.2 Future work.....	166
Author's publication .....	169
References.....	170

# List of Figures

Figure 1.1 Scheme of a typical building HVAC system.....	2
Figure 1.2 Control structure of supervisory control and EMCS for HVAC systems .....	3
Figure 2.1 Classification of nonlinear optimization techniques for HVAC system optimization .....	20
Figure 3.1 Mechanical draft counter-flow and cross-flow tower .....	40
Figure 3.2 Conceptual scheme of the counter-flow cooling tower.....	44
Figure 3.3 Heat exchange scheme using an electric analogy.....	46
Figure 3.4 Comparison between the calculated data and the real data on February 03 <sup>rd</sup> , 2006.....	53
Figure 3.5 Comparison between the calculated data and the real data on February 04 <sup>th</sup> , 2006.....	54
Figure 3.6 Comparison between the calculated data and the real data on February 10 <sup>th</sup> , 2006 with the model parameters identified on February 3 <sup>rd</sup> , 2006 .....	55
Figure 3.7 Comparison between the calculated data and the real data on March 03 <sup>rd</sup> , 2006 with the model parameters identified on February 3 <sup>rd</sup> , 2006 .....	56
Figure 3.8 Comparison between the calculated data and the real data on March 03 <sup>rd</sup> , 2006 with new identified model parameters .....	57
Figure 4.1 A typical finned-tube cooling coil.....	63
Figure 4.2 Heat transfer mechanism of coil.....	64
Figure 4.3 Temperature changes in the X direction.....	67
Figure 4.4 Temperature and enthalpy profiles of cooling coil.....	67
Figure 4.5 Temperature changes towards the Z and X direction.....	75
Figure 4.6 Directions of water and air flows, levels and sections in the cooling tower .	76
Figure 4.7 Temperature changes in the X direction.....	76

Figure 4.8 Temperature changes in the Z direction .....	77
Figure 4.9 An AHU and a cooling coil of the pilot plant .....	84
Figure 4.10 Time varying temperature and mass flow rate of inlet air and chilled water .....	85
Figure 4.11 Comparison of six-parameter model calculations with the measured data .	86
Figure 4.12 Comparison of five-parameter model calculations with the measured data	86
Figure 4.13 Increase of the mass flow rate of water from 48kg/s to 80 kg/s.....	89
Figure 4.14 Increase of the mass flow rate of inlet air from 175kg/s to 250 kg/s .....	89
Figure 4.15 Cooling tower water supply temperature step rise from 35.5 to 38.5 C.....	90
Figure 5.1 Schematic diagram of a vapour-compression water –cooled chiller.....	93
Figure 5.2 Thermodynamics of the refrigeration cycle .....	94
Figure 5.3 Schematic diagram of evaporator .....	95
Figure 5.4 Heat transfer mechanism of evaporator.....	96
Figure 5.5 Schematic diagram of a condenser .....	103
Figure 5.6 Heat transfer mechanism of condenser.....	104
Figure 5.7 Comparison between modeled COP and measured COP .....	108
Figure 6.1 Block diagram of HVAC out building section .....	111
Figure 6.2 Performance of a cooling tower .....	119
Figure 6.3 Optimal operating points at different wet-bulb temperatures.....	120
Figure 6.4 Pressures & refrigerant flow for decreasing cooling load with constant condensing pressure control.....	123
Figure 6.5 Pressures and refrigerant flow for decreasing cooling load with optimal condensing pressure control.....	123
Figure 6.6 Power consumption and COP for decreasing cooling load with constant condensing pressure control.....	124

Figure 6.7 Power consumption and COP for decreasing cooling load with optimal condensing pressure control.....	124
Figure 6.8 Trade-offs between compressor power and fan power [96] .....	126
Figure 6.9 Optimization procedure of PSO based optimizer .....	132
Figure 6.10 Optimization procedure of GA based optimizer .....	139
Figure 6.11 Schematic of the laboratorial HVAC out-building section .....	140
Figure 7.1 Experimental setup .....	147
Figure 7.2 Implementation procedures of the proposed system optimization approach .....	149
Figure 7.3 Wet-bulb temperature and building cooling load profile for a typical day .	155
Figure 7.4 Implementation procedures of the fixed approach method .....	157
Figure 7.5 Condenser water supply temperatures and wet-bulb temperatures for a typical day.....	159
Figure 7.6 Total power consumptions for a typical day .....	162
Figure 7.7 Operating numbers of chillers and cooling towers.....	163

## List of Tables

Table 3.1 Comparison of different cooling tower models .....	60
Table 4.1 Estimated parameters of the six-parameter and five-parameter model ( $\ell = 0.8$ ) .....	85
Table 4.2 Performances of the six-parameter model and the five-parameter model .....	87
Table 4.3 Estimated parameters of the four-parameter model.....	88
Table 4.4 Performances of the model in different scenarios .....	90
Table 5.1 Details of the experimental chiller.....	107
Table 5.2 Model accuracy.....	109
Table 6.1 Parameters of the pilot HVAC system under study .....	141
Table 6.2 Typical test conditions, and optimization results using different optimization techniques .....	142
Table 7.1 Measurements and defined initial settings for system component models...	149
Table 7.2 Building envelop parameters of the studied building .....	154
Table 7.3 Comparison of one day total electricity consumption using different control strategies .....	162

## Nomenclature

$A$	heat transfer area ( $\text{m}^2$ )
$A_a$	heat transfer area of air side convection ( $\text{m}^2$ )
$A_{crw}$	heat transfer area of cooling tower water side convection ( $\text{m}^2$ )
$A_{chw}$	heat transfer area of chilled water side convection ( $\text{m}^2$ )
$A_{imp}$	impeller outlet area ( $\text{m}^2$ )
$a_0 \sim a_9$	parameter (dimensionless)
$a$	interfacial contact area of the surface of water droplets per unit volume of the cooling tower ( $\text{m}^{-1}$ )
$b_0 \sim b_9$	parameter (dimensionless)
$C$	constant (dimensionless)
$C_s$	derivative of saturation air enthalpy with respect to temperature
$C_{pa}$	specific heat of moist air [ $\text{J}/(\text{kg } ^\circ\text{C})$ ]
$C_{pa,e}$	equivalent ideal gas specific heat [ $\text{J}/(\text{kg } ^\circ\text{C})$ ]
$C_{pw}$	specific heat of water under constant pressure [ $\text{J}/(\text{kg } ^\circ\text{C})$ ]
$c_1 \sim c_9$	parameter (dimensionless)
$D$	diameter of the round passage or equivalent diameter for other shapes (m)
$D_{calculation}$	calculated data (dimensionless)
$D_{real}$	real experimental data (dimensionless)
$d_k$	search direction (dimensionless)
$d_1 \sim d_n$	parameter (dimensionless)
$e_1 \sim e_n$	parameter (dimensionless)

$F(u_k)$	error between the real values and model predicting values (dimensionless)
$F$	film coefficient ( $W/m^2\text{ }^\circ C$ )
$f_1 \sim f_n$	parameter (dimensionless)
$h$	enthalpy (J/kg)
$h_{a,i}$	enthalpy of inlet air (J/kg)
$h_{a,o}$	enthalpy of outlet air (J/kg)
$h_s$	enthalpy of saturated air at the temperature of the wetted surface (J/kg)
$h_{s,w,i}$	saturation air enthalpy at the temperature of inlet water (J/kg)
$h_{s,w,o}$	saturation air enthalpy at the temperature of outlet water (J/kg)
$J(u_k)$	Jacobian matrix of $u_k$ (dimensionless)
$k$	thermal conductivity [ $W/(m^2\text{ }^\circ C)$ ]
$k_\omega$	mass transfer coefficient [ $kg/(m^2\text{ s})$ ]
Le	Lewis number (dimensionless)
$M$	number of operating points to determine Stoecker's model (dimensionless)
$Me_M$	Merkel number (dimensionless)
$\dot{m}$	mass flow rate (kg/s)
$\dot{m}_a$	mass flow rate of air (kg/s)
$\dot{m}_{chw}$	mass flow rate of chilled water (kg/s)
$\dot{m}_{ctw}$	mass flow rate of cooling tower water (kg/s)
$\dot{m}_{cw}$	mass flow rate of condenser water (kg/s)
$N$	number of operating points to determine the proposed model (dimensionless)

$N_{ch}$	number of chillers in the out building section (dimensionless)
$N_{ct}$	number of cooling towers in the out building section (dimensionless)
$NTU$	number of transfer units (dimensionless)
$n$	number of experimental data (dimensionless)
$P$	power(kW), refrigerant pressure (kPa)
PLR	part load ratio (dimensionless)
$P_i$	refrigerant pressure at state point $i$ (kPa)
$p$	pressure ( $kPa$ )
$Q$	heat transfer rate (kW)
$\dot{Q}_{rej}$	heat rejection rate of the cooling tower (W)
$q$	heat exchange quantity of element ( $W$ )
$R$	heat transfer resistance ( $^{\circ}C/W$ )
$R_a$	heat transfer resistance of air convection ( $^{\circ}C/W$ )
$R_{ctw}$	heat transfer resistance of cooling tower water convection ( $^{\circ}C/W$ )
$R_{chw}$	heat transfer resistance of chilled water convection ( $^{\circ}C/W$ )
$T$	temperature ( $^{\circ}C$ )
$T_{chwe}$	chilled water entering temperature ( $^{\circ}C$ )
$T_{chwl}$	chilled water leaving temperature ( $^{\circ}C$ )
$T_{CWS}$	condenser water supply temperature ( $^{\circ}C$ )
$T_{CWR}$	condenser water return temperature ( $^{\circ}C$ )
$T_{CTWS}$	cooling tower water supply temperature ( $^{\circ}C$ )
$T_{CTWR}$	cooling tower water return temperature ( $^{\circ}C$ )

$T_{wb,i}$	wet-bulb temperature of ambient air ( ° C )
$T_{wb,o}$	wet-bulb temperature at the outlet air of the cooling tower ( ° C )
$U$	heat transfer coefficient [W/ (m <sup>2</sup> ° C)]
$UA$	actual heat transfer coefficient-area product (W/ ° C)
$U_{imp}$	tip speed of impeller (m/s)
$u_k$	value of $c_1 \sim c_3$ of the $k^{th}$ iteration (dimensionless)
$u$	velocity of mass flow (m/s)
$V$	volume (m <sup>3</sup> )
$V_{ref}$	volumetric flow rate of refrigerant (m <sup>3</sup> /kg)
$v$	average fluid velocity (m/s)
$v_i$	specific volume of refrigerant at state point $i$ (m <sup>3</sup> /kg)
$W_{in}$	mechanical work input to compressor (kJ/kg)
$z$	elevation (m)
$\beta$	angle of impeller (rad)
$\delta$	throttling rate(dimensionless)
$\varepsilon$	effectiveness of heat transfer exchanger (dimensionless)
$\varepsilon_a$	heat transfer effectiveness in Braun's model (dimensionless)
$\eta_{pol}$	efficiency of polytropic compression
$\eta_m$	combined motor and transmission efficiency of compressor
$\lambda_k$	control coefficient in Levenberg-Marquardt method (dimensionless)
$u$	fluid viscosity (m/s)
$\xi$	index of reversible polytropic expansion
$\pi$	system pressure ratio (dimensionless)

$\rho$	fluid density (kg/m <sup>3</sup> )
$\tau$	a certain time interval (s)
$\omega$	ratio of the minimum heat capacity flow rate to the maximum heat capacity flow rate (dimensionless)

### **Subscripts**

<i>a</i>	air
<i>chw</i>	chilled water
<i>i</i>	inlet
<i>o</i>	outlet
<i>tube</i>	tube
<i>ma</i>	moist air
<i>wb</i>	wet-bulb
<i>total</i>	sum of variables
<i>com</i>	compressor
<i>ev</i>	evaporator
<i>cd</i>	condenser
<i>ct</i>	cooling tower
<i>ref</i>	refrigerant
<i>ctw</i>	cooling tower water
<i>cw</i>	condenser water
<i>fan</i>	cooling tower fan
<i>op</i>	optimal
<i>pump</i>	condenser pump
<i>sat</i>	saturated refrigerant



# CHAPTER 1 INTRODUCTION

## *1.1 Background of HVAC Systems, EMCS and Supervisory Control*

A building's heating, ventilation and air conditioning (HVAC) system can be generally described as a system for transporting heat and moisture between the inside building and the outside environment. HVAC is particularly important in the design of medium to large industrial and commercial buildings such as skyscrapers or hotels where comfort and healthy living conditions are regulated through temperature and humidity, as well as with "fresh air" from outdoors.

The scheme of a typical building water cooled HVAC system is shown in Figure 1.1., which can be divided into five heat transfer loops [1]:

- **The indoor air loop** includes fans, cooling coils, terminal units, dampers, ducts, and controls. The air in the conditioned space is driven by fans through cooling coils and then distributed to terminal units. Dampers are used to control airflows to the terminal units and fans are used to keep a certain air pressure in the ducts. The cooling and ventilation loads are transferred from the conditioned space to the chilled water.
- **The chilled water loop** includes pipes, pumps, cooling coils, evaporators, valves, and controls. The chilled water contained in pipes is driven by pumps to circulate between the cooling coils and the evaporators. Valves are used to control the water flow to the cooling coils. The heat is transferred from air handling units (AHUs) to the evaporators.
- **The refrigerant cycle** consists of evaporators, compressors, condensers, expansion valves and controls. The refrigerant extracts heat through the evaporators by changing phase from liquid to vapour. The compressors turn the refrigerant into a high pressure and high temperature state. The compressed high temperature refrigerant is cooled in the condensers. The high pressure gas-state

refrigerant is ejected by expansion valves back to the evaporators again with phase change. The heat is transferred from the evaporators to the condensers.

- **The condenser water loop** includes cooling towers, condensers, pumps and controls. The condenser water in the refrigeration cycle is delivered to cooling towers by pumps. The heat is transferred from the condensers to the cooling towers.
- **Finally, the outdoor air loop** includes fans, cooling towers, and controls. The outdoor air is driven by fans to go through cooling towers and to exchange heat with the cooling tower water. The heat is transferred from the cooling towers to the ambient environment.

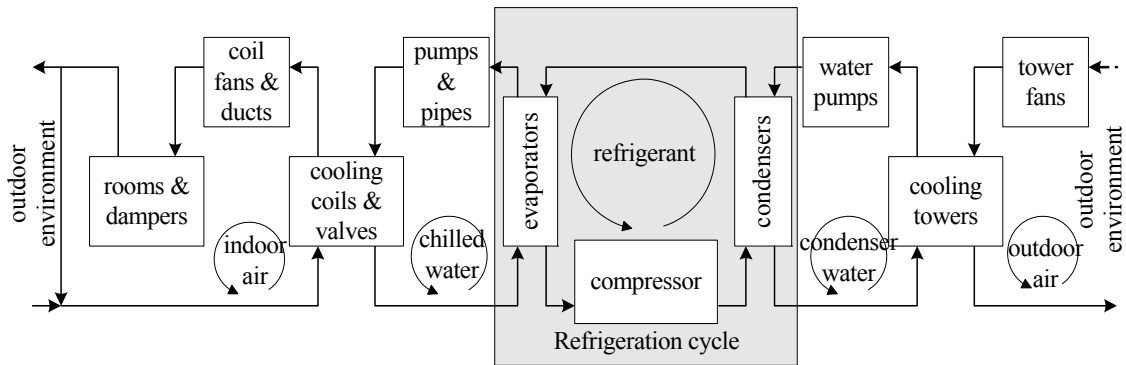


**Figure 1.1 Scheme of a typical building HVAC system**

Energy management and control system (EMCS) technology for HVAC system has evolved over the past three decades from pneumatic and mechanical devices to direct digital controls (DDC) or computer-based controllers and systems. Today's EMCSs for HVAC system consist of electronic devices with microprocessors and communication capabilities and utilize powerful, low cost microprocessors and standard communication protocols.

Supervisory control for HVAC systems aims at seeking the minimum energy input or operating cost to provide the satisfied indoor comfort and healthy environment, taking into account the ever-changing indoor and outdoor conditions as well as the

characteristics of HVAC systems. It is the total system monitoring and overall control of the local subsystems.

EMCSs integrated with a supervisory control strategy using model-based system optimization approach provides a two-level control structure; i.e., local control and system optimization, as illustrated in Figure 1.2[2].

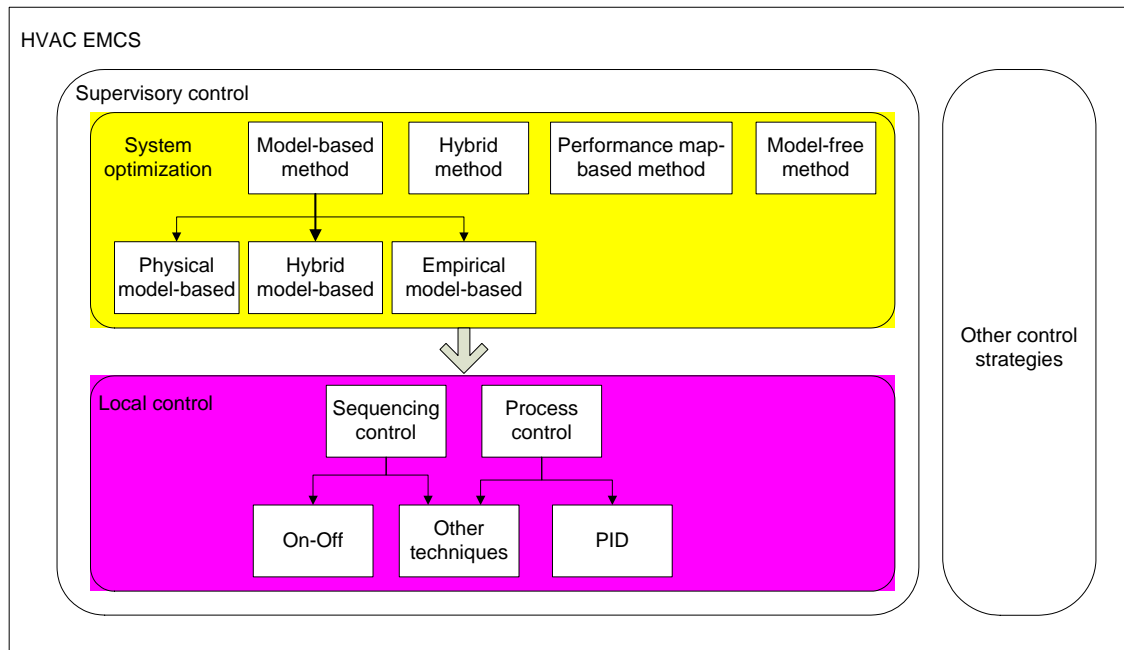


**Figure 1.2 Control structure of supervisory control and EMCS for HVAC systems**

Local control is at the lower level in the EMCS structure, comprising of the basic control and automation that allow the HVAC systems to operate properly and provide adequate services. Local control can be further subdivided into two groups, including sequencing control and process control. Sequencing control defines the order and conditions associated with bringing equipment online or moving them offline. The typical sequencing control in HVAC systems includes chiller sequencing control, cooling tower sequencing control, pump sequencing control, fan sequencing control, etc. Process control is used to adjust the control variables to guarantee the operation robustness and keep track of well-defined objective set points regardless of disturbances by using measurements of state and/or disturbance variables. The typical process

control algorithm used in the HVAC field is proportional integral derivative (PID) control [2].

System optimization is at the higher level of the EMCS structure aiming at on-line seeking the optimal or near optimal operating set points which make the HVAC system operate with a minimal energy consumption or operating cost to provide on demand cooling load, taking into account the ever-changing indoor and outdoor conditions as well as the characteristics of HVAC systems. Different from the local control, system optimization requires an overall consideration of the system level characteristics and interactions among all components and their associated variables. The knowledge of the system level characteristics and interactions can be utilized to formulate a well-defined cost function or objective function, which would lead to improved system response and reduced overall system operating energy consumption or cost without violating the operating constraints of each component.

## ***1.2 Motivation and Objectives***

Among building energy service systems, HVAC systems are the most energy consuming facilities, and account for about 55% of the total electrical usage in Singapore [3]. Consequently, operation and control of HVAC systems have significant impact on the energy or cost effectiveness of buildings.

The growing concerns on energy conservation, sustainability and eco-friendly development have motivated extensive research on various aspects of HVAC system optimization approaches. The study on modeling as well as optimizing the HVAC systems is one of the fastest growing areas that contribute to energy savings and improve HVAC system operating performance.

In an effort to reduce energy costs, the performance of individual components in building HVAC systems, such as chillers, pumps, fans, and heat exchangers, has been

greatly improved for decades. Nowadays, the effort of improving the efficiency of individual components becomes expensive and limited; however, a big potential for energy savings lies in maximizing the efficiency of the overall system through system optimization. Unfortunately, as there are always numerous components in a large-scaled HVAC system and hundreds of cross coupled control set points to be controlled and monitored, it is extremely difficult to consider all of them as a whole for optimization without simple yet accurate models as well as powerful optimization techniques. For example, in a typical multi-chiller HVAC system, the thermal processes and associated power consumption taking place in the out-building section, can be broken down as follows: sensible/latent energy flows of the refrigerant, chilled water and condenser water in the refrigeration cycle; sensible/latent energy flows of the water and air in the cooling tower; conversion of evaporating and condensing refrigerant into the compressor electrical power consumption with respect to the chilled water temperature and condenser water temperature through the refrigeration cycle; and conversion of water and air flow rate into pump and fan electrical power consumption with respect to the ambient wet-bulb temperature and condenser water temperature entering the cooling tower, etc. Due to the fact that these thermal processes and the corresponding operating variables which directly relate to the component power consumption characteristics are simultaneously undergoing changes and interacting with each other, a system approach is required to accurately model these processes, the power consumption characteristics and their interactions. It is only then feasible to find improved control strategies to the problem of optimizing the thermal processes in the HVAC system.

During the past thirty years, tremendous efforts have been made on modeling or simulating the HVAC system for the purpose of developing system optimization approaches. However, the consensus is that most EMCSs integrated with supervisory

control for HVAC system in practice have not performed to their full potential with respect to its optimization functions. One of the main reasons for poor performance is the fact that HVAC processes are most likely optimized at the local loop level, which does not include system level process-to-process interactions. Another reason is the lack of suitable simple yet accurate and comprehensive HVAC component and system models which can be easily mastered and used by the HVAC engineers. Thus, the challenge of performing system optimization for the overall system relies on the sophisticated HVAC component and system models as well as the compatible global optimization techniques which could make the over-all system optimization possible.

To address the above problems, this thesis will focus on 1) developing simple yet accurate HVAC component models using hybrid methods 2) formulating and resolving the global optimization problem of energy savings in a HVAC system out-building section 3) the application of EMCS implemented with the proposed system optimization approach for the HVAC out-building section.

### ***1.3 Major Contributions***

The major contributions of this thesis include the modeling of individual components, formulating and solving the optimization problem, and implementing of the proposed system optimization approach into the EMCS for a laboratorial centralized HVAC plant for the purpose of validating and evaluating the proposed methods. The main achievements are summarized below:

- Development of a hybrid static model for cooling towers based on energy balance principles and heat and mass transfer analysis. The developed model is useful for studying interactions among chiller condenser, cooling tower, and operating variables. The model can be used to perform various energy management and optimization strategies.

- Development of hybrid dynamic models for the cooling coils and the cooling towers. The developed models can be used to simulate the HVAC system local control performance or designing local controllers.
- Development of a composite model for the refrigeration cycle of chillers for the HVAC system optimization. The developed model is used to study interactions among cooling tower, evaporator, condenser, compressor and operating variables.
- Development of model-based system optimization approaches using PSO and GA for energy savings of HVAC out-building section and for algorithm performance comparison studies.
- Implementation and validation of proposed system optimization approach using PSO as the optimization technique for the HVAC out-building section.

#### ***1.4 Organization of the Thesis***

This thesis is organized into 8 chapters. Chapter 1 introduces the general information of building HVAC systems and EMCS followed by the motivations, objectives and major contributions. Chapter 2 reviews the studies and research work on HVAC system modeling, and research and applications of model-based optimization in EMCS for HVAC systems. Chapter 3 develops a static model of cooling towers using a hybrid method. Chapter 4 develops dynamic models for cooling coils and cooling towers based on a similar hybrid modeling method. Chapter 5 presents a hybrid composite model for the refrigeration cycle with a component-based method for model-based optimization. Chapter 6 proposes the optimization method for building HVAC systems, focusing on using Particle Swarm Optimization (PSO) and the Genetic Algorithm (GA) to resolve the energy minimization problem of the HVAC out-building section, respectively. Simulation studies are conducted to compare the control accuracy, computation time and memory requirement of these two optimization techniques. In

Chapter 7, the system optimization approach based on the developed models is implemented into the EMCS for a centralized HVAC pilot plant. Experimental studies are conducted to evaluate the operating energy saving of the proposed approach by compared to that of the conventional method. Chapter 8 concludes the thesis and discusses potential future work.

## CHAPTER 2 LITERATURE REVIEW

Over the last three decades, HVAC system optimization methods have been developed enormously thanks to the innovation of information, computer and EMCS integration technologies. According to the classification in Figure 1.2, the methods of HVAC system optimization can be divided into four categories, namely, model-based, hybrid, performance map-based, and model-free optimization methods.

This thesis will focus on the model-based optimization methods. The fundamental asset of a model-based system optimization method is its modeling. On one hand, establishing static models to simulate component or system performances enables us to understand the behavior of a HVAC system under different operating conditions, and to calculate system energy consumption; thus the cost of operating a system without constructing and operating an actual system. On the other hand, constructing the dynamic models enables us to understand the system's transient responses to the ever-changing demands, environment, and control settings of the actual systems, and thus design the local controller to make the EMCS to perform sophisticated local loop controls.

Another essential constituent of the model-based system optimization approaches is the development of the optimization technique. The purpose of an optimization technique is to seek the optimal control settings (i.e., operation modes and/or set points) by taking into account the system operating constraints which lead to minimal system power consumption or operating cost while still satisfying the cooling demand.

In this chapter, the literature review of the related works is divided into three sections. Section 2.1 reviews the existing static and dynamic models for HVAC components; Section 2.2 reviews the applications and research work on HVAC system

optimization based on the combinations of various kinds of models and various kinds of optimization techniques; finally, the objectives of this thesis are summarized in section 2.3.

## **2.1 Modeling**

HVAC component modeling has attracted a great amount of research interests as it can be utilized for controller design, simulation and optimization depending on the characteristics of the model types. According to the different characteristics, the existing models can be classified into two categories: i) static models, also known as steady-state models, and ii) dynamic models, also known as transient models. A static model does not account for the element of time, while a dynamic model does. Static models predict the performance of the HVAC component/system at steady-state operating condition. Dynamic models typically are represented with difference equations or differential equations, and used to predict the performance of the HVAC component/system during the transient period. According to the different methods in developing the models, each category can be further classified into i) physical models, also known as theoretical models, ii) black-box models, also known as empirical models and iii) hybrid model, also known as gray-box models.

Just as the name implies, the physical models strictly rely on fundamental physical laws and principles, such as the general principles of thermodynamics and heat and mass transfer to predict pressure, temperatures and fluid flow rates within each component of the HVAC system. Physical models require information on the physical dimensions, properties, and processes that determine the performance of the equipment, and the interactions among components of the equipment. Most of the required information can be obtained from physical descriptions of the equipment and its components, thus few or no performance test data are needed. Usually, these physical

models have high accuracy in prediction and high control reliabilities within their allowed working conditions since the basic assumptions and laws utilized in the model development are effective and valid within their allowed ranges. However, most such models are rather complicated. And an iteration process is usually required in calculating the results, which may cause instability and divergence as well as high computational cost and memory demand. These drawbacks may constitute serious obstacles to their real-time applications.

Different from physical model approaches, the black-box models use a simple “black box” concept that is partially supported by physical laws or totally ignores physical laws [4]. Statistical analysis with or without the support of general engineering principles are used to select input and output variables that are important in representing the modeled equipment and its role in an entire system. This model approach directly relates the input variables to the output variables and uses regression analysis to fit the equations with discrete performance data obtained from the HVAC equipment manufacturer, in-laboratory tests, or data generated from the more complex models. Black-box models can be used to predict equipment performance within the range of available test data for the particular equipment operating in a specific environment. The simplicity and ease-of-use of these models make them particularly suitable to be used in adaptive control modeling, where the parameters required can be updated based on the on-line measurement. However, models cannot be used to forecast performance outside the limited range of test data, or for other similar type of equipment operating in different environments. This is the main drawback of this model approach and largely limits the flexibility in real world applications.

To achieve a wide operating range as in the physical models but still keep a simple structure as in the black-box models, engineers and researchers have made great efforts

in recent years to develop hybrid models for HVAC equipment and systems. Generally, two methods are used to develop hybrid models. One is through numerical analysis, by which the prior knowledge of the system or testing process can be incorporated as constraints on the model parameters or variables. The other is through a specific model structure based on physical relations, which describe the behaviors of the process or system. The main advantage of hybrid models is that the complexity of the model structure and computational cost to achieve the optimal solutions are greatly reduced, while at the same time, the parameters in the models still retain certain physical significance and can be used for extrapolation outside the range of the test data covered.

In the following sections, we will firstly review the existing models for these HVAC components including the static models for a cooling tower, the dynamic models for cooling coils and cooling towers and the composite model for the whole refrigeration cycle. The development of hybrid models for HVAC main components, including cooling tower, cooling coil and the whole refrigeration cycle will be presented in Chapters 3~5.

### **2.1.1 Static cooling tower models**

A HVAC cooling tower is employed to reject heat from an operating refrigeration cycle to the environment. Heat rejection in cooling towers is accomplished by heat and mass transfer between hot water droplets and ambient air. Much attention is currently being paid to cooling tower designs as they are important factors in energy conservation of HVAC systems [5-7]. As such, there have been substantial research interests in modeling of static performance of cooling towers [8-15].

The first milestone work may be traced back to 1925, when Merkel [8] developed a practical model for cooling tower operation, where the water loss of evaporation is neglected and the Lewis number ( $Le$ ) is assumed to be one in order to simplify the

analysis. The model has since been the basis for most modern cooling tower analysis and a revised form was adopted by a software package for energy calculation [16]. However, the Merkel method does not accurately represent the physical characteristics of the heat and mass transfer process in the cooling tower fill [17]. HVAC1Toolkit [16] developed the equations necessary to apply the Effectiveness-NTU method directly to counter-flow cooling towers. This approach is particularly accurate and simplifies the method of solution when compared with a more conventional numerical procedure. The drawback of the Effectiveness-NTU method is that the heat transfer coefficient-area product is difficult to determine and requires detailed geometric information of cooling towers. Besides, an iterative computational procedure is a must when the operating point changes. Bernier [11] proposed a one-dimensional cooling tower model for idealized spray-type towers based on the analysis of heat and mass transfer process in cooling towers at water droplet level. This particular model is useful for cooling tower designers, but little information is provided to plant operators for cooling towers already in operation. Soylemez [14] presented a method for estimating the size and performance of forced draft countercurrent cooling towers backed with experimental results. Then again, this model also needs iterative computation and is not suitable for online optimization.

### **2.1.2 Dynamic cooling coil models**

Cooling coils of Air Handling Units (AHUs) are the interface between the HVAC out-building section (primary plant) and the in-building section (secondary plant/air distribution system). As the heat exchanger, a cooling coil is an important component in a HVAC system which plays an essential role to transfer the cooling load from the air loop to the chilled water loop by forcing air flow over the coil and into the space to be conditioned [18-20].

The design of efficient controllers for AHU largely depends on the availability of good dynamic models of a cooling coil. It is important that the dynamic models are developed from fundamental principles for the purpose of comparison, validation and more importantly for i) finding global optimal dynamic operating strategies using modern control theory and ii) simulating the control performance of the EMCS. So far, various approaches have been suggested to model the transient performance of the cooling coil, and these approaches can be generally placed into two categories: 1) finite difference models and 2) lumped parameter models. The finite difference approach results in a large number of equations and it is suitable only for numerical simulation. For this approach, Myers et al. [21] and Kabelac [22] used the governing differential equations to study the dynamic response of a cooling coil by the assumption that one fluid has an infinite capacitance. Gartner and Daane [23] found transfer function relations for different coil parameters. Bocanegra [24] and Khan [25] developed a model to analyze the performance of a counter-flow cooling and dehumidification coil. Yao [26] presented a rigorous analysis of the effect of a perturbation of the relevant parameters on the thermal quality of a cooling coil under different initial conditions. The obstacle of applying these models to industrial applications is that modeling methodologies require comprehensive information on the structure of the cooling coil and physical properties of the fluids, such as the fin and the tube thickness, diameter and spacing, which are often unavailable from manufacturers' specifications. Another drawback is that they require intensive computation and can potentially lead to numerical instabilities.

The lumped parameter approach involves fewer equations, but frequently ignores some dynamics due to the complex heat exchanger behavior. Specifically, the entire cooling coil dynamics is often modeled as a single system, and the important dynamics

associated with the moving boundary between the wet surface region and the dry surface region are ignored. Lebrun et al. [27] derived a first-order differential equation on the basis of an energy balance to represent the dynamics of a coil with lumped thermal mass. This approach has been used by several authors for simulation purposes, and occasionally for controller design purposes [28]. Extending this approach, Bi and Cai et al. [29] presented a lumped parameter empirical model through a robust identification method and applied the modeling method to the HVAC control loop auto-tuning [30]. Wang and Hibara [31] presented a distinct method (also called equivalent dry-bulb temperature method) to simplify the calculation in each region. This method is examined in Wang et al. [18]’s work. They showed the potential that the complex heat and mass transfer characteristics of the cooling coil could be further simplified yet still predicts the system correctly.

### **2.1.3 Dynamic cooling tower models**

As mentioned in section 2.1.1, a cooling tower is an important heat exchanger in the HVAC system which rejects heat carried by water through heat exchange with the ambient air to the environment; its performance has big implications on the total energy consumption of the overall process. Ideally, the cooling tower should be controlled such that the condenser water supply temperature will follow the set points regardless of the ever-changing operating conditions, i.e., the cooling tower water supply temperature and flow rate, and the ambient air wet bulb temperature. However, this requirement can hardly be satisfied for a long period of time in practice. The main problem is the lack of an effective model to derive the control laws for the constantly changing operating conditions. Therefore, a simple yet effective dynamic model which can be applied to a wide range of operating conditions is necessary for deploying the optimal control strategies for the cooling towers.

For dynamic modeling, the existing cooling tower models are mainly derived by finite difference approach, which may results in a large number of governing equations [32-37]. Similarly, the obstacle for these models to be applied in practice is that modeling methodologies require comprehensive information on the structure of the cooling tower and the physical properties of the fluids, such as the fill structure, spraying nozzles distribution, etc. which are often unavailable in manufacturers' specifications. Another drawback is that they require great computational effort and potentially cause numerical instabilities. To overcome these difficulties, Al-Nimr proposed a simple mathematical model to describe the dynamic thermal behavior of cooling towers [38-39]. An analytical solution can be obtained by the perturbation technique to solve the governing equations of the model for the hot water and cold air temperatures. However, the detailed relationship between the control variables and the manipulated variables was not revealed in the formulae.

#### **2.1.4 Composite models for the refrigeration cycle**

Vapor-compression refrigeration cycles are the essential component in a building HVAC system, and their operation consumes the majority of the electricity. The refrigeration cycle consists of four major components: evaporator, compressor, condenser and expansion valve (EX valve), where the evaporator and compressor can be regarded as the heat exchangers, the compressor is the power-consumption device and the expansion valve is the throttling device. Many refrigeration cycle models have been developed using various principles and a variety of purposes [40-56].

For example, Braun et al. [40] developed a thermodynamic model for the refrigeration cycle of a centrifugal refrigeration cycle with variable speed control. The model is useful for predicting the power requirement, the cooling capacity, and also the conditions at which compressor surge develops. Both heat exchanger models neglected

pressure drops. The model neglected the effect of sensible cooling of the superheated refrigerant on the condensing heat transfer coefficient. The boiling heat transfer coefficient in the evaporator was also evaluated using correlations for boiling on a single tube.

Ng et al.[41] developed a simple thermodynamic model using regression analysis for a centrifugal refrigeration cycle which was experimentally validated with data from an air-conditioning plant with a computer management system. The model successfully predicted two distinct operating regimes for the refrigeration cycle where: (i) the refrigeration cycles operate at high load and high efficiency; and (ii) the refrigeration cycles operate at low load and low efficiency due to the throttling action of the guide vanes.

Van Houte and Van den Bulck [42] developed a steady-state model for a centrifugal refrigeration cycle where each heat exchanger was split into three specific regimes i.e. saturated refrigerant liquid, two-phase refrigerant, and superheated refrigerant gas. The log mean temperature- difference (LMTD) method is used for simulating changes in the heat-transfer coefficients of the evaporator and air-cooled condenser at part load.

Browne and Bansal [43] proposed a static model for water-cooled centrifugal refrigeration cycles. Their method is based on physical laws and heat-transfer coefficients determined using the number of transfer units-effectiveness (NTU-e) approach through a “bundle average” method for the evaporator and condenser. Later Browne and Bansal [44] extended this model to develop an improved model using a unique “elemental” methodology to account for the variation in the heat transfer coefficients throughout the heat exchangers. This kind of model is able to predict a wide range of conditions and operating capacities of a refrigeration cycle.

A finite-time thermodynamic model for the refrigeration cycle was developed by Gordon et al. [45, 46]. This proposed model is universal enough to carry out a diagnostic case study and to deal with the performance of refrigeration cycles with reciprocating or centrifugal type compressors.

Bourdouxhe et al. [47] established a toolkit for primary HVAC system energy calculations. The toolkit contains subroutine programs to model a water-cooled refrigeration cycle operating at full and part load separately. Both the evaporator and condenser are modeled using the NTU-e method with constant heat-transfer coefficients (UA). And semi-empirical models are applied to determine the power input to the centrifugal compressors when the capacity control is done by adjusting the open position of the inlet guide vanes at constant speed [47 – 51].

Chan and Yu [52-56] developed thermodynamic models for air-cooled refrigeration cycles with different types of compressors. The log mean temperature difference (LMTD) is used for simulating changes in the heat-transfer coefficients of the evaporator and condenser at part load. These models include an algorithm to evaluate the heat-rejection second flow required for any given cooling capacity based on a set point condensing temperature. This algorithm is particularly important in modeling precisely the heat-rejection characteristics of condensers and in assessing the controllability of the condensing temperature under various operating conditions.

All above mentioned thermodynamic models for the refrigeration cycles have the drawback of requiring complex iterative computation or requiring data of the heat exchangers that are generally considered confidential by the manufacturers and are often unavailable to HVAC engineers, especially when using the NTU-e or the LMTD method to calculate the heat-transfer coefficient. Hence, a much better modeling approach would be to predict the performance, i.e. the coefficient of performance (COP)

and to have simple model structure which only requires manufacturer's specification data and input variables that can be easily acquired, e.g. the chilled water temperature and flow rate entering the evaporator, the condenser water temperature and flow rate entering the condenser, and the evaporating and condensing pressure. This leads to the hybrid composite model for the refrigeration cycle which will be given in Chapter 5.

## ***2.2 Model –Based System Optimization for HVAC Systems***

Based on the knowledge of the system utilized to formulate the optimization problem, model-based system optimization approaches can be further divided into physical model-based, black-box model-based, and hybrid model-based system optimization approaches. Because of the inherent characteristics of highly nonlinearity and interactions of the operating equipment, the optimization problems of building HVAC systems are often characterized with discretization, nonlinearity, and high constraints. Hence, only nonlinear optimization techniques are suitable for such applications.

During the past three decades, much research has been done on the development and application of various nonlinear optimization techniques in HVAC systems [57-61]. These efforts have resulted in significant achievements, which provide HVAC professionals or designers with an opportunity to effectively use reliable and efficient optimization techniques for their applications.

A classification according to Figure 2.1 summarize the nonlinear optimization techniques into three categories [2], i) nonlinear local optimization techniques and nonlinear global optimization techniques. As their names implied, the nonlinear local optimization techniques seek the local optimum, and nonlinear global optimization techniques seek the global optimum, however, the nonlinear global optimization techniques cannot always converge to the global optimal solutions due to the complexity of the optimization problems.

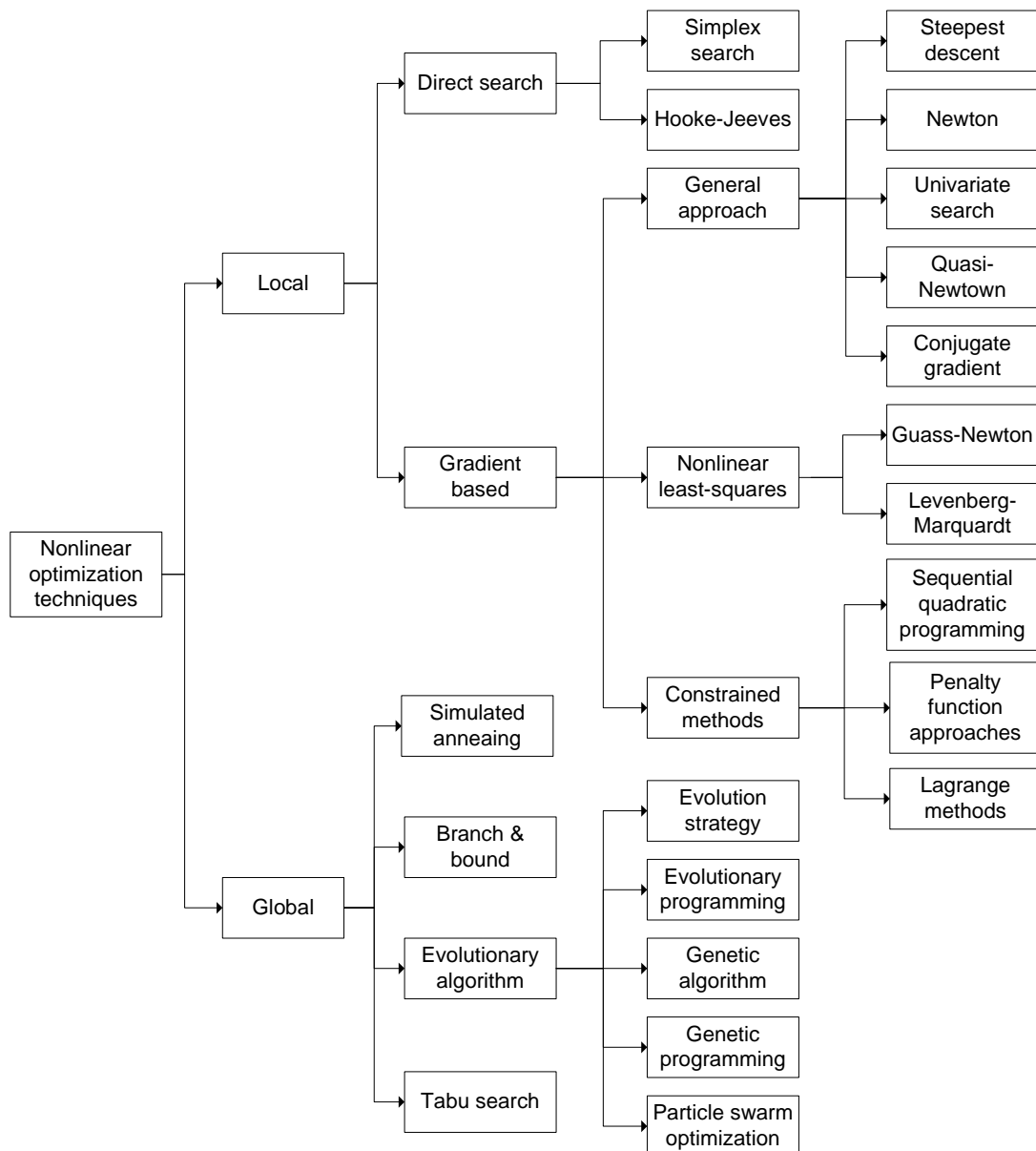


**Figure 1.1 Classification of nonlinear optimization techniques for HVAC system optimization**

It is worth to point out that, as a subcategory of the nonlinear global optimization techniques, the evolutionary algorithms (EA) have drawn much attention these years, especially with the advance of computing techniques and computer hardware. Evolutionary algorithms get their inspiration from natural selection and survival of the fittest in the biological world. They initiate a search from a “population” of solutions. Each iteration process consists of a competitive selection that discards poor solutions. The solutions with high “fitness” are “recombined” or “updated” with other solutions by swapping parts of a solution with another. Solutions are also “mutated” by making a small change to a single element of the solution. Recombination and mutation are used to generate new solutions that are biased towards regions of the search space for which good solutions have already been identified [62].

The existing evolutionary algorithms include evolutionary strategy (ES), evolutionary programming (EP), genetic algorithm (GA), genetic programming (GP) and particle swarm optimization (PSO). They all share similar basic static models, but are considerably different in the way of their representation of an individual solution (binary or real-valued), the means of their selection (stochastic or deterministic), and the essentials of the evolution process.

In practice, however, optimization techniques should be selected based on the combination of the complicity and characteristics of the HVAC system under study as well as the number of optimization variables involved in a particular optimization problem. The selected optimization technique should have guaranteed the required control accuracy with less computational cost and memory demand subject to the limitation and requirement of practical applications.

The different combinations of models and optimization techniques lead to differences of control accuracy and implementation feasibility of the model-based

system optimization methods. Based on the work of Wang and Ma [2], this section reviews the research, development as well as the applications of model-based system optimization approaches in building HVAC systems in the last three decades according to the classification of models used.

### **2.2.1 Physical model-based system optimization**

So far, there are quite a number of studies utilizing dynamic and/or static governing equations as well as physical models, which are derived based on the fundamental laws of energy, mass and heat transfer, momentum and flow balance, etc., to formulate the system optimization problems for the supervisory control strategies of EMCS in building HVAC systems.

Kaya et al. [63] introduced a thermal model based on the governing equations for the space along with an index of energy consumption. On top of this model, they used a static optimization technique, namely the generalized reduced gradient method, to develop a system optimization approach consisting of controlling temperature, humidity, and velocity simultaneously to keep the room at the comfort region and to minimize the corresponding energy expenditure. The method implemented static and dynamic optimization schemes and included the interdependence of those three parameters. The optimization theory was then utilized to develop the new control policies. A comparison between the proposed method and a conventional method under a common baseline was demonstrated by experiments. The experimental results showed that the control performance and energy efficiency can be much more improved through controlling temperature, humidity and velocity simultaneously rather than independently. Their work indicated that the control strategy that takes into consideration control variable interactions among the system and components systematically can result in more energy

saving when compared to the control strategies considering the control variables separately.

Cumali [64] formulated the optimization problem for building HVAC systems based on the physical component models, and then he employed a global optimization technique to develop optimal control and operation strategies. The results showed that projected and/or augmented Lagrange multiplier methods did not perform well because of the equality constraints used in the problem formulation, while generalized reduced gradient methods appeared to provide consistent results if one starts with a reasonable initial solution.

By deriving governing equations from the principles of conservation of mass and energy, House et al. [65] and House and Smith [66] described a systematic approach for optimization of building HVAC systems. The approach considered the interactions among the system equipment, the multi-zone building system, and their associated variables. The optimization problem was resolved by a nonlinear sequential quadratic programming method, in which the continuous control variables were discretized in the time domain to transform the infinite dimensional optimization problem to a finite dimensional form. Using discrete values for the state and control variables, the cost function was integrated numerically based on the trapezoidal rule. The drawback of the sequential quadratic programming method is that it has to start from initial guesses for the solutions and the convergence speed is affected by its initial guesses.

Zaheer-Uddin and his collaborators have made considerable contributions in the optimal and sub-optimal optimization approaches of building HVAC systems [67-70]. These optimal and sub-optimal optimization approaches were developed based on physical models. The simulation results demonstrated that these optimal and sub-optimal optimization approaches, in which multiple control variables were optimized

simultaneously, can improve the system response and operational efficiency. They also demonstrated that a multistage optimization technique is an effective and useful tool for computing optimal set points profiles for building systems subject to time-of-day operating schedules.

Koeppel et al. [71] investigated the system performance and optimization approaches for a direct-fired LiBr absorption refrigeration cycle system using simulation. They used detailed and simplified component models to predict the system energy and environment performance. A global optimization algorithm, simulated annealing, was employed to determine the optimal control settings under different control options. Their results showed that the optimal operation schedule for absorption refrigeration cycles can be determined from the optimization investigation under the simulation environment.

Kota et al. [72] investigated the performance of the differential dynamic programming (DDP) technique which can be applied to dynamic optimization of building HVAC systems. Based on the mass and energy conservation principles, they derived the state equations utilized to describe the HVAC system. In their study, they compared their optimization result with that obtained from a nonlinear programming (NLP) technique using the sequential quadratic programming (SQP) method. They demonstrated that DDP is more efficient compared to NLP for the example problems, while NLP is more robust and can treat constraints on the state variables directly.

Henze et al. [73] described the development and simulation of a predictive optimal controller for thermal energy storage systems. The optimal strategy based on the dynamic programming method minimizes the cost of operating the cooling plant over the simulation horizon. The particular case of an ice storage system was investigated in a simulation environment. Various predictor models were analyzed with respect to their

performance in forecasting cooling load data and information on ambient conditions (dry-bulb and wet-bulb temperatures). The predictor model provides load and weather information to the optimal controller in discrete time steps. An optimal storage charging and discharging strategy was planned at every time step over a fixed look-ahead time window utilizing newly available information. The first action of the optimal sequence of actions was executed over the next time step and the planning process was repeated at every following time step. The effect of the length of the planning horizon was investigated. Various utility rate structures were analyzed to cover a range of potential real-time pricing scenarios. The predictive optimal controller was then compared to conventional control heuristics. And the simulation results showed that this optimal controller can achieve a significant performance benefit over the conventional controls in the presence of complex rate structures, while requiring only a simple predictor.

Later, Henze et al. [74] demonstrated a physical model-based predictive optimization of an active and passive building thermal storage inventory in a test facility in real time using time-of-use differentiated electricity prices without demand charges. In their study, the building was modeled in the transient systems simulation program, TRNSYS, while Matlab and its optimization toolboxes were used to interface with the building simulation program. The experimental results showed that the savings associated with passive building thermal storage inventory were small because the test facility utilized was not an ideal candidate for the investigated control technology.

Wang and Jin [75] presented a system optimization approach for variable air volume (VAV) air-conditioning systems in which simplified physical models were utilized to predict the overall system performance, and a genetic algorithm (GA) was used to resolve the optimization problem of multiple control variables. It was the first application of GA in solving an optimal control problem formulated using a system

approach in the HVAC field. The simulation results showed that this online supervisory control strategy can improve the overall system energy and environment performance since it took into consideration the system level characteristics and interactions among the system variables.

Xu and Wang et al. [76] extended the work of Wang and Jin [75] to develop a model-based system optimization approach for multi-zone VAV air-conditioning systems aiming at optimizing the total fresh air flow rate by compromising the thermal comfort, indoor air quality and total energy consumption. The proposed optimization approach is based on a constructed cost function relating all the optimization objectives including the thermal comfort, the indoor air quality and the total energy consumption, while the cost function is calculated based on the prediction of system responses using simplified models. The genetic algorithm (GA) was again used for optimizing the temperature set point of critical zones in the optimization process. This approach was evaluated in a simulated building and air-conditioning environment under various weather conditions. Test results showed that the genetic algorithm is a convenient tool for optimizing the temperature set point for online optimization applications by minimizing the total cost with the aim of optimally estimating the total ventilation rate in multi-zone air-conditioning systems.

Based on the physical models of building and plant equipment, Zhang and Hanby [77] presented a model-based system optimization approach for renewable energy systems in buildings. The objective of the optimization problem was to minimize the net external energy consumption of the system subject to a series of constraints. An evolutionary algorithm was then used to seek the optimal and near-optimal control settings. Simulation results indicated that significant improvements in system operation are possible as compared to the existing rule-based control scheme.

These above studies demonstrated that the energy or cost efficiency, the in-building environment performance and the system response of the building HVAC system can be improved by using physical model-based system optimization approaches. However, many parameters in the governing equations are uncertain, and many parameters in the detailed physical models require detailed information of the system or process of concern. In practice, the parameter online identification and performance prediction of these governing equations and physical models in the supervisory control strategies often require many iterations, which may result in high computational cost and memory demand, as well as control instability. All of these characteristics are the major obstacles that may seriously prevent the online control applications of physical model-based supervisory control strategies.

### **2.2.2 Black-box model-based system optimization**

There are also a number of studies that utilize black-box models to construct the system optimization approaches in the HVAC field. One popular technique is artificial-neural-networks (ANNs)-based optimization.

ANNs are networks of highly interconnected neural computing elements that have the ability to respond to input stimuli and to learn to adapt to the environment [78]. ANNs do not require detailed information about the system; they learn the relationships between input and output variables by studying the historical data. The main advantages of ANNs are their abilities to map nonlinear functions, to learn and generalize by experience, as well as to handle multivariable processes in HVAC system. These merits make ANNs feasible for control applications. The research and development on ANNs in building HVAC systems started at the early 1990s.

Curtiss et al. [79] and Massie [80] developed ANNs-based optimization approach to minimize the total energy consumption of building HVAC systems. They proposed an

optimization approach consisting of two networks, a training network and a predictor network, working in parallel. The training network was used to learn the relationship between the various controlled and/or uncontrolled variables and the total power consumption of HVAC systems. The training network weights were then passed to the predictor network where they were used as an activation function of the predictor network. The predictor network subsequently found optimal values for the controlled variables that can minimize the overall system operating cost. Bradford [81] adopted the method introduced by Curtiss et al. [79] to deploy online optimization of a cooling plant without storage. The historical data from a test building are used to train the ANNs. The output of the networks was the total power consumption of the HVAC system. The network was configured with two hidden layers of three and two nodes, respectively. These three studies demonstrated that an ANNs-based optimization approach can greatly reduce the operating cost of building HVAC systems and it is also robust in finding optimal solutions at any given working condition since such an optimizer does not rely on any assumptions of the system or process of concern.

Curtiss et al. [82] used HVAC system performance data collected in the laboratory to train ANN models and discussed the results of a proof-of-concept experiment in which ANNs were used for both local and global optimization of a commercial building HVAC system. The experimental results obtained from the laboratory testing showed that significant energy savings are possible when the proposed optimization approach is used.

Gibson [83] installed both GA based and ANNs based optimizers at the central cooling system of a building in a high school to compare their performances. The system operation results showed that both GA and ANNs are effective techniques for online optimization. However, the important lessons learned by the authors showed that

great care should be given since GA and ANNs cannot always provide the desirable solutions.

Chow et al. [84] introduced the concept of integrating a neural network with GA in the optimization of an absorption refrigeration cycle system. The neural network was used to model the system characteristics of the absorption unit and GA is applied as a global optimization tool. The results from the case studies showed that considerable energy can be saved since such an optimizer allows an overall consideration of the interactions among the systems and their controlled variables.

Xu et al. [85] presented an optimization-based methodology to control HVAC units in stochastic settings. Considering the difficulties related to tuning the parameters for different buildings, a neural network was used to predict the dynamics of HVAC systems instead of using system dynamic governing equations. A Lagrangian relaxation method was used to obtain near-optimal solutions with quantified quality. Numerical testing and prototype implementation results showed that this method is significantly better than other existing methods.

The above studies using ANNs-based supervisory control strategies demonstrate that ANNs could be a choice for the optimization of building HVAC systems. Energy or cost savings are possible when such ANNs-based optimizers are used. However, most of these studies were presented from the view point of academic research, the practicability and effectiveness of the real-time application of ANNs-based optimization approach still need to be proved and improved. Since ANNs operate as black-box models, they have the inherent deficiency that they are only reliable at the operation conditions in the range of training data covered. Hence, significant control errors might occur when the system operates outside the range of ANNs trained, and/or measurement faults, and/or component degradations occur. Moreover, the training of ANNs always

requires extensive computational cost and memory demand, which makes it almost impossible and unacceptable to apply adaptive control in practice to improve the prediction accuracies of ANN models. The online practical application of such methods needs to be implemented with great care [2].

Another general technique for black-box model-based optimization is empirical-relationship-based optimization.

Empirical relationships, including polynomial regression models and identification models, etc., could be the simplest way to formulate and construct the system and/or component models. Both inputs and outputs are known and measured from field monitoring. There are a few studies that use empirical relationship-based models to construct system optimization approaches.

Braun et al. [86-88] have devoted considerable efforts on developing optimal and near-optimal system optimization approaches using quadratic relationships for refrigeration cycle and water systems. These are addressed in detail in Chapter 41 of the 2003 ASHRAE Handbook—HVAC Applications [89]. These studies included the application of two basic methodologies for determining optimal or near-optimal values of the independent control variables in the building HVAC system that minimize the instantaneous operating costs of a refrigeration cycle plant. One was a component model-based nonlinear optimization algorithm, in which power consumptions of refrigeration cycles, cooling towers, chilled water pumps, as well as supply and return fans were expressed as quadratic relationships. This methodology was used as a simulation tool for investigating the system performance. The other was a system-based methodology for near-optimal optimization, in which an overall empirical cost function of total power consumption of a refrigeration cycle plant was developed using a

quadratic function. This method allowed a rapid determination of near-optimal control settings over a range of conditions.

Pape et al. [90] extended Braun's method to the overall HVAC system. The power consumption of the entire HVAC system was represented by a quadratic relationship in terms of control variables, loads, and ambient conditions. The optimal operating set points were determined by equating the first derivative of the power with respect to each control variable to zero. Braun's method was also further extended by Cascia [91] through simplifying the component models and providing the equations for determining the set points of near-optimal control. All component power consumptions (e.g., refrigeration cycles, pumps, fans) were expressed as a function of temperature difference between chilled-water supply and return temperatures. The parameters in the model were determined from the direct measurements of total power consumption and temperature difference obtained from a direct digital control (DDC) system. This methodology was implemented at a small pilot cooling plant. A third-party energy accounting program was used to track the energy savings by the near-optimal control. The results showed a monthly energy reduction ranging from 3% to 14%. However, this strategy was based on the assumption that the condenser water flow rate is unchanged.

Cassidy and Stack [92] showed that varying the speed of cooling tower fans can reduce energy consumption at part load conditions. By considering the effects of the condenser water flow rate on the performance of the refrigeration cycle condensers and cooling towers, Shelton and Joyce [93] recommended a fixed condenser water flow rate (1.5 gpm/ton) as a rule of thumb for system operation. Later, Kirsner [94] demonstrated that a high condenser water flow rate (3 gpm/ton) has good performance at full load condition, while a low condenser water flow rate (1.5 gpm/ton) has advantages at part load conditions.

Braun et al. [95] identified several guidelines for near-optimal optimization of chilled-water systems without significant thermal energy storage. They also identified that the optimization of a chilled water system was primarily a function of the total chilled water cooling load and ambient wet-bulb temperature. On top of these results, Braun and Diderrich [96] developed the near-optimal control strategy for cooling towers. The control algorithm for cooling tower was expressed as an open-loop control equation in terms of total chilled-water cooling load. Braun [97] further extended this method to develop a general control algorithm for cooling towers in cooling plants with refrigeration cycles. And Braun and Diderrich's method [96] was again used by Cascia [98] to develop a patent on determining the set points of near-optimal optimization for HVAC system with the simplified model. These near-optimal optimization approaches mentioned above are easy to implement for practical application, however the energy savings are not really significant compared to the "optimal" system optimization approaches.

Olson and Liebman [99] presented a mathematical programming approach for determining which available refrigeration cycle equipment to use to meet a cooling load as well as the optimal operating temperatures for the water flows throughout the system. First, an empirical model that is only dependent on cooling load was established to predict the power that would be required to cool the building with various combinations of equipment. Then, a mixed-integer, nonlinear formulation of the problem is developed. A heuristic approach for handling the integer variables is presented which allows optimal solutions to be obtained by solving a series of continuous problems using sequential quadratic programming (SQP). The results showed that computational cost can be reduced significantly by this approach.

Austin [100] utilized biquadratic polynomial models of refrigeration cycles and cooling towers to optimize the condenser water temperature set point. Based on the detailed analysis of refrigeration cycle and cooling tower performance characteristics, Austin emphasized that system modeling can help select the best combination of refrigeration cycles and condenser water temperature set points to meet different loads under various outdoor working conditions with the minimum energy input.

Ahn and Mitchell [101] developed a system optimization approach for a cooling plant. A quadratic regression equation was used to predict the power consumption of a total cooling system in terms of forcing function and controlled variables. The optimal control settings, e.g., supply air temperature, chilled-water temperature, condenser water temperature, etc., were selected to minimize the total system power consumption. The simulation result showed that minimum total system power consumption was a trade-off among power consumptions of different components. This method is simple and easy to implement. However, there are as many as 28 coefficients with no physical significance required to be identified from the monitoring data, which may result in significant prediction deviations for practical applications.

Yao et al. [102] investigated and established the empirical relationships among controlled variables, uncontrolled variables, and system performance of a large cooling system using site measurement data. A model of optimal operation for the system was established based on these empirical relationships. A system coefficient of performance (SCOP) was introduced to analyze the effects of energy savings of the cooling system. The results obtained from case studies showed that the energy saving was likely to reach as high as 10% by applying the optimal operation strategy to the cooling system.

Sun and Reddy [103] presented a general and systematic optimization approach, termed as complete simulation-based sequential quadratic programming (CSB-SQP), to

determine the optimal control strategy for building HVAC systems. Linear approximation with a Taylor expansion was utilized to formulate the system models. A case study on a simple cooling plant illustrated the accuracy, efficiency and robustness of this methodology.

These system optimization approaches using black-box relationships also demonstrate the energy- or cost-saving potentials in HVAC systems when such methods are utilized. Empirical relationship-based system optimization approaches are easy to implement in practical supervisory control of EMCS since the methodologies involved in such methods are relatively simple, and computation time is generally manageable. However, most existing approaches seem to lack generality because they were only validated for simulations or pilot tests with certain operating points. The application of such methods in large office or commercial buildings is lacking. The robustness of such methods is also a big issue in practice, especially when the systems operate at the range where the training data are not covered or system degradations or measurement faults occur. Although adaptive control can improve the prediction accuracies of these models to some extent, it is very dangerous to apply adaptive control to large and complicated HVAC systems at the current stage. More research is essentially needed to further validate the feasibilities of adaptive empirical relationship-based system optimization approaches in practice and special care should be given when such methods are used [2].

### **2.2.3 Hybrid model-based system optimization**

A few studies using hybrid models are reviewed in this section. Actually it is quite difficult to clearly define what kinds of models hybrid models are. Occasionally, semi-physical models, simplified physical models and semi-empirical models can be regarded as hybrid models. In the study of Braun [104], the building model was a simplified physical model which can be regarded as a hybrid model, while refrigeration cycle plant

models were quadratic relationships. Simulation results of this study indicated that both operating costs and peak electrical use can be reduced significantly through optimal control of the intrinsic thermal storage within building structures. The proposed control methodology was employed by Simmonds [105] to minimize the system operating cost while maintaining the acceptable indoor comfort.

Lu et al. [106-109] presented a series of system optimizations for building HVAC systems. The interactive nature within and between components and their controlled variables in the system was considered. The objective function of global optimization was formulated based on mathematical models of the major components. The thermodynamic characteristics of the cooling coil and cooling tower were predicted with the hybrid models, which are simple yet accurate with some physical significance. The power consumption of refrigeration cycles was predicted using an empirical model, while the power consumption of water pumps and fans was modeled as a function of the ratio of water flow rate to the designed water flow rate and the ratio of airflow rate to the designed airflow rate. A modified genetic algorithm was utilized to search the optimal control settings. Simulation studies based on a small pilot-scale centralized HVAC plant showed that system level optimization can improve overall system operating performance significantly.

Fong et al. [110] proposed a simulation optimization approach for effective energy management of building HVAC systems. An empirical refrigeration cycle model and a hybrid cooling coil model were used to predict the system energy and environment performance, and then evolutionary programming was used to handle the discrete, nonlinear, and highly constrained optimization problems. The simulation exercises for the HVAC system in a subway station showed that 7% energy saving can be achieved

by optimizing the set points of chilled water temperature and supply air temperature on a monthly basis.

Braun [111] presented a simple control strategy for hybrid cooling plants that could be readily implemented with low installation costs. The refrigeration cycle performance was modeled by associating COPs with cooling capacities, while the cooling tower was modeled using an effectiveness hybrid model. This strategy was developed and evaluated using a simulation tool that could determine optimal control settings for specific simulated cooling plants. Braun [112] further developed a near-optimal control strategy for cool storage systems with dynamic electric tariff. This strategy used a hybrid model of the ice storage tank and an empirical model of the refrigeration cycle. This strategy was evaluated for ice storage tank using a simulation tool for different combinations of cooling plants, storage sizes, buildings, locations, and real-time electric tariff. The simulation results showed that 2% cost savings are possible with the use of optimal control.

Hybrid models-based system optimization approaches could be more suitable, and might be a feasible solution which can direct many advanced strategies to be applied in practice if the hybrid models are well developed and are combined effectively with other types of models in the system. However, most existing hybrid model-based system optimization approaches were evaluated by simulations, and their practical applications seemed to be inadequate. More research on application of hybrid model-based system optimization approaches in practice is highly needed.

## ***2.3 Summary***

In general, the previous studies have contained limitations when viewed in the context of (i) static hybrid HVAC component models with simple model structures

suitable for online system optimization; (ii) simple yet accurate transient hybrid models suitable for local control and/or constructing simulation platform; (iii) effective optimization algorithms suitable to the characteristic of the studied system and the optimization problem formulated based on the simple yet accurate hybrid HVAC component models; and especially, (iv) general and feasible hybrid model-based system optimization approach and its application in a real HVAC plant. The details are listed as follows:

- 1) Most models for cooling towers are physical models or black-box models which may not be suitable for online system optimization application.
- 2) Most models for cooling towers and cooling coil are of steady state type, which are not suitable for control analysis, because they do not consider the dynamics of the equipment.
- 3) Furthermore, few dynamic models for cooling towers and cooling coils are developed with the hybrid modeling methodologies for simulating and studying the transient response characteristics of the cooling coils and cooling towers which takes into account the variable air and water flow rate as well as time varying air and water temperature.
- 4) Little work has been done for analyzing the interactions among the energy consumption of the compressor, the condenser water supply temperature as well as the condensing and evaporating pressure within the refrigeration cycle. This kind of model and study are necessary for analysis of refrigeration cycle.
- 5) Little research has been done on using PSO to determine the global optimal set point profiles of a HVAC system subject to time varying weather and cooling loads,

which will be valuable in developing supervisory control strategies for energy efficient operation of a HVAC system.

Therefore, this thesis deals with the development of modeling methodologies for both static and dynamic semi-physical hybrid models for HVAC components and presents optimization techniques for global optimal operation of HVAC out-building section subject to realistic operating constraints. These hybrid models have the advantages of:

- 1) incorporation of theoretical and physical knowledge;
- 2) reliability over a wider range of operating conditions compared to empirical models;
- 3) less computational effort than the complex physical models.

The emphasis of this thesis is placed on

- i) the application of fundamental principles to develop an analytical component and system-level models of HVAC system using hybrid methods;
- ii) the application of an optimization technique such as the genetic algorithm (GA) and particle swarm optimization (PSO) to develop a methodology for determining the global optimal set point profiles for the local controller subject to realistic operating conditions which include the varying cooling load and varying weather condition; and
- iii) the application of the proposed system optimization approach to a real HVAC system to verify its effectiveness.

# CHAPTER 3 STATIC MODEL OF COOLING TOWERS

## ***3.1 Introduction***

In this chapter, we propose a simple yet accurate hybrid steady state cooling tower model for the purpose of energy conservation and management. Firstly, the mechanism of the cooling tower as well as the details of Merkel's model, the NTU-effectiveness model and Stoecker's model are introduced. Then, on the basis of Merkel's theory and the Effectiveness-NTU method, a new hybrid model is developed from an energy balance as well as heat and mass transfer analysis. Only three characteristic parameters are required to predict the steady state performance of heat transfer in cooling towers without iterative computation to calculate the heat rejection rate. The Levenberg-Marquardt method is employed to determine the three parameters by curve fitting the manufacturers' specification data or real time experimental data. Compared with the existing models, the proposed model is simple and accurate; therefore, it can be used for real time prediction of the performance of cooling towers. In Chapter 6, this model is integrated into the system models of HVAC out building section to formulate the system optimization problem for energy savings.

## ***3.2 Hybrid Cooling Tower Model***

### **3.2.1 Mechanism analysis of mechanical cooling towers**

Most popular cooling towers in HVAC systems are mechanical towers utilizing large fans to force air through circulated water. The water falls downward over fill surfaces which help increase the contact time between the water and the air, thus maximizing heat transfer between the two. Figure 3.1 shows a schematic representation

of two types of mechanical draft cooling towers: counter-flow and cross-flow. The principle of counter-flow is that the hot water flows downwards while the air is forced upwards by a fan. As the water flows further through the system, the air it encounters is fresher, in other words cooler and less saturated with moisture. On the other hand, the principle of cross-flow is that warm water flowing down through a cooling unit is cooled by air drawn upwards by a fan. Evaporation and direct heat exchange cause a rapid drop of temperature.

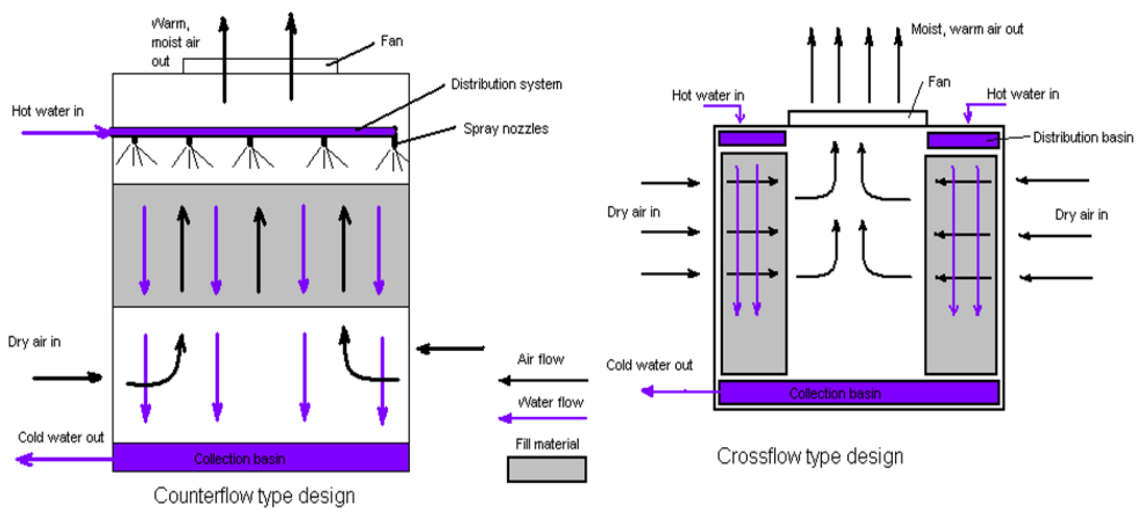


**Figure 3.1 Mechanical draft counter-flow and cross-flow tower**

Fills or packings are employed in cooling towers to increase the contact area and time between the water that needs to be cooled and the cooling air. There are basically three different types of fill designs: film, splash, and trickle type fills. A thin film of water runs down the film fill surface while the splash fill breaks the water stream into smaller droplets. The trickle film is basically a combination of film and splash type fill. However, Kloppers and Kröger's [17] revealed that the differences between the Merkel and Effectiveness-NTU approaches are independent of the fill type considered.

### 3.2.2 Merkel's model

The Merkel model relies on several critical assumptions:

1. the Lewis number ( $Le$ ) relating heat and mass transfer is equal to 1;
2. the air exiting the tower is saturated with water vapor and it is characterized only by its enthalpy;
3. the reduction of water flow rate by evaporation is neglected in the energy balance.

Eqs. (3.1) and (3.2) are obtained from mass and energy balances of the control volumes where air is in counter-flow with a downwards flowing water stream. For the Merkel theory it is assumed that the change in cooling tower water mass flow rate ( $\dot{m}_{ctw}$ ) due to evaporation is negligible, and

$$\frac{dh}{dz} = \frac{k_o a V}{\dot{m}_a} (h_s - h) \quad (3.1)$$

$$\frac{dT_{ctw}}{dz} = \frac{\dot{m}_a}{\dot{m}_{ctw}} \frac{1}{C_{pw}} \frac{dh}{dz} \quad (3.2)$$

where, Eqs. (3.1) and (3.2) describe, respectively, the change in the enthalpy of the air-water vapor mixture ( $h$ ) and the change in cooling tower water temperature ( $T_{ctw}$ ) as the air travel distance changes ( $z$ ). Eqs. (3.1) and (3.2) can be combined to yield upon integration the Merkel expression:

$$Me_M = \frac{k_o a V}{\dot{m}_{ctw}} = \int_{T_{CTWR}}^{T_{CTWS}} \frac{C_{pw}}{h_s - h} dT_{ctw} \quad (3.3)$$

where,  $Me_M$  is the tower characteristic, i.e. Merkel number, according to Merkel's approach.  $T_{CTWR}$  and  $T_{CTWS}$  denote the cooling tower water return temperature and cooling tower water supply temperature, respectively. It is often difficult to evaluate the surface area per unit volume of fill due to the complex nature of the two-phase flow in fills. It is, however, not necessary to explicitly specify the surface area per unit volume ( $a$ ) or the mass transfer coefficient ( $k_o$ ) as these are contained in the Merkel number which can be obtained from the right-hand side of Eq.(3.3).

It is not possible to calculate the true state of the air leaving the fill according to Eq. (3.3). Merkel assumed that the air leaving the fill is saturated with water vapor. This assumption enables the air temperature leaving the fill to be calculated.

### 3.2.3 NTU-effectiveness method

The NTU-effectiveness method is based on the same simplified assumptions as the Merkel method. The HVAC1Toolkit [16] presented a counter-flow cooling tower model of a typical NTU-effectiveness method. Based on this method, the total heat rejection rate ( $\dot{Q}_{ct}$ ) due to the direct contact between air and water under steady-state conditions is calculated as:

$$d\dot{Q}_{ct} = \frac{UdA}{C_{pa}}(h_s - h) \quad (3.4)$$

where,  $U$  denotes the heat transfer coefficient,  $A$  denotes the heat transfer area and  $C_{pa}$  denotes the specific heat of moist air, respectively. The first step in the modeling procedure is to assume that the moist air enthalpy can be defined by the wet-bulb temperature only and that the moist air can be treated as an equivalent ideal gas characterized by the following mean specific heat:

$$C_{pa,e} = \frac{\Delta h}{\Delta T_{wb}} = \frac{h_{a,o} - h_{a,i}}{T_{wb,o} - T_{wb,i}} \quad (3.5)$$

where,  $C_{pa,e}$  denotes the equivalent ideal gas specific heat,  $h_{a,o}$  and  $h_{a,i}$  denote the air enthalpy at the outlet and inlet of the cooling tower, and  $T_{wb,o}$  and  $T_{wb,i}$  denote the air wet-bulb temperatures at the outlet and inlet of the cooling tower, respectively.

The water side conductivity is much greater than the air side conductivity. Therefore, the wetted surface temperature is also assumed to be equal to the water temperature. On the basis of these assumptions, the expression of the total heat rejection rate becomes:

$$d\dot{Q}_{ct} = \frac{UC_{pa,e}}{C_{pa}} dA (T_{ctw} - T_{wb}) \quad (3.6)$$

An energy balance on the water and air sides gives:

$$d\dot{Q}_{ct} = \dot{m}_{ctw} C_{pw} dT_{ctw} = \dot{m}_a C_{pa,e} dT_{wb} \quad (3.7)$$

The water-side effectiveness of the cooling tower can be defined by analogy to the effectiveness of a simple heat exchanger:

$$\varepsilon = \frac{T_{CTWS} - T_{CTWR}}{T_{CTWS} - T_{wb,in}} \quad (3.8)$$

The combination of Eqs.(3.6) and (3.7) is integrated. The result of this integration is combined with Eq.(3.8) to provide the following expression of the cooling tower effectiveness:

$$\varepsilon = \frac{1 - e^{-NTU(1-\omega)}}{1 - \omega e^{-NTU(1-\omega)}} \quad (3.9)$$

where,

$$\omega = \frac{\dot{C}_{\min}}{\dot{C}_{\max}} \quad (3.10a)$$

$$\dot{C}_{\min} = \min(C_{pw}\dot{m}_{ctw}, C_{pa,e}\dot{m}_a) \quad (3.10b)$$

$$\dot{C}_{\max} = \max(C_{pw}\dot{m}_{ctw}, C_{pa,e}\dot{m}_a) \quad (3.10c)$$

$$NTU = \frac{C_{pa,e}}{C_{pa}} \cdot \frac{UA}{\dot{C}_{\min}} \quad (3.10d)$$

Then, the heat rejection rate is expressed by the following equation:

$$\dot{Q}_{ct} = \varepsilon \cdot \dot{C}_{\min} \cdot (T_{CTWS} - T_{wb,i}) \quad (3.11)$$

As can be seen, when  $\frac{\dot{m}_a}{\dot{m}_{ctw}} < \frac{C_{pw}}{\left(\frac{dh_s}{dT_{ctw}}\right)}$ , the  $NTU$  value according to the Merkel theory can

be given by:

$$NTU = \frac{\dot{m}_{ctw}}{\dot{m}_a} Me_M \quad (3.12)$$

From the derivation of Eq.(3.12), it is self evident that the value of  $NTU$  has a direct relationship with the tower characteristic ( $Me_M$ ). Consequently, Eq.(3.12) establishes the relationship between  $NTU$  and the physical variables in order to predict the performance of cooling towers. Nevertheless, the main influential factors are  $\dot{m}_a$  and  $\dot{m}_{ctw}$ , and  $T_{wb,i}$  and  $T_{CTWS}$  theoretically have no effect on the value of  $NTU$  and the tower characteristic  $Me_M$  [8]. Consequently, the cooling tower can be modeled, in the steady-state regime, by an equivalent classical counter-flow heat exchanger (Figure 3.2).

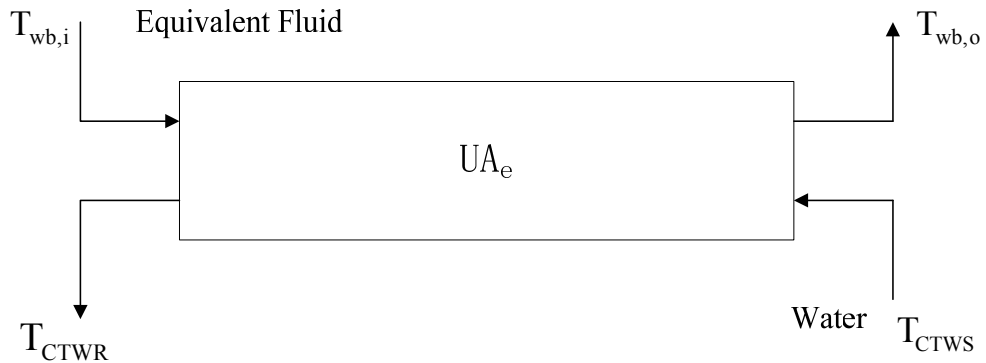


**Figure 3.2 Conceptual scheme of the counter-flow cooling tower**

The first fluid is water and the second fluid is an equivalent fluid entering the heat exchanger at temperature  $T_{wb,i}$  and characterized by the specific heat  $C_{pa,e}$ . The heat exchanger is characterized by a single parameter, its global equivalent coefficient-area product ( $UA_e$ ), which is related to the actual cooling tower heat transfer coefficient-area product by the following expression:

$$UA_e = \frac{C_{pa,e}}{C_{pa}} \cdot UA \quad (3.13)$$

Therefore, in the steady-state regime, the combination of the mass and heat transfer of water-vapor towards the air can be equivalent to the behavior of heat transfer by convection between water and moist air.

### 3.2.4 Stoecker's model

Apart from using NTU based on heat transfer theory, an entirely empirical model of a cooling tower was proposed by Stoecker [9]. In this model, the cooling tower was supposed to have a constant airflow rate and a water flow rate based on a polynomial approximation.

$$\dot{Q}_{ct} = \dot{m}_{ctw} C_{pw} (T_{CTWS} - T_{CTWR}) \quad (3.14)$$

$$T_{CTWR} = c_1 + c_2 T_{wb} + c_3 T_{wb}^2 + c_4 T_{CTWS} + c_5 T_{CTWS}^2 + c_6 T_{wb} T_{CTWS} + c_7 T_{wb}^2 T_{CTWS} + c_8 T_{wb} T_{CTWS}^2 + c_9 T_{wb}^2 T_{CTWS}^2 \quad (3.15)$$

If  $M$  operating points ( $M > 9$ ) are collected for model identification, Eq. (3.15) falls into a system of linear equations:

$$\Psi X = \Gamma + \Delta \quad (3.16)$$

where,  $\Delta$  is the error,  $X = \begin{bmatrix} c_1 \\ \vdots \\ c_9 \end{bmatrix}$ ,  $\Psi = \begin{bmatrix} 1 & T_{wb,1} & \cdots & T_{wb,1}^2 T_{CTWR,1}^2 \\ 1 & T_{wb,2} & \cdots & T_{wb,2}^2 T_{CTWR,2}^2 \\ \vdots & \vdots & \ddots & \vdots \\ 1 & T_{wb,M} & \cdots & T_{wb,M}^2 T_{CTWR,M}^2 \end{bmatrix}$ ,  $\Gamma = \begin{bmatrix} \dot{Q}_{rej,1} \\ \dot{Q}_{rej,2} \\ \vdots \\ \dot{Q}_{rej,M} \end{bmatrix}$  and

$$\Delta = \begin{bmatrix} \delta_1 \\ \delta_2 \\ \vdots \\ \delta_M \end{bmatrix}.$$

The best estimation  $X^*$  of  $X$  can then be obtained using a standard least-squares method as:

$$X^* = (\Psi^T \Psi)^{-1} \Psi^T \Gamma \quad (3.17)$$

### 3.3 Hybrid Model

Before developing the new hybrid cooling tower model, we use the follow reasonable assumptions:

1. heat and mass transfer occurs in a direction normal to the flow only;
2. the Lewis number ( $Le$ ) is a constant;
3. the reduction of water flow rate by evaporation is neglected in the energy balance;
4. the cross-sectional area of the tower and temperature distribution throughout the water stream at any cross section is uniform;
5. the saturation enthalpy is approximately linear with respect to wet-bulb temperature.

As we mentioned in the previous section, the cooling tower can be modeled, in the steady-state regime, by an equivalent classical counter-flow heat exchanger. Thus, during the process of heat transfer, heat is transferred from the water drops to the surrounding moist air by convection. As show in Figure 3.3, the equivalent heat transfer process can be classified into two parts: water convection and air convection.

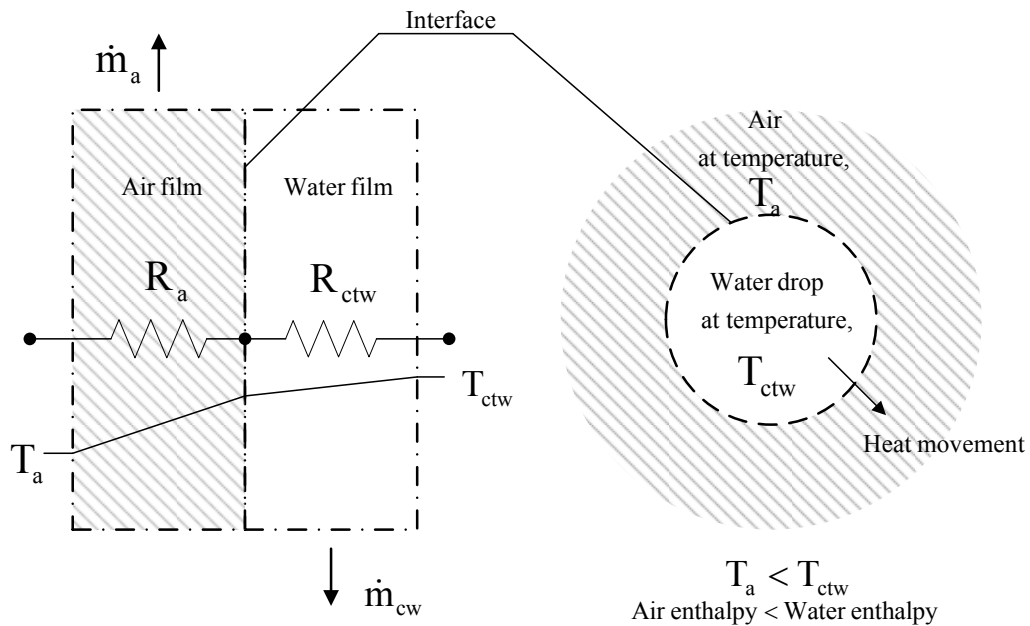


Figure 3.3 Heat exchange scheme using an electric analogy

The heat rejection rate can be calculated using the overall heat resistance ( $R$ ) according to heat transfer theory and the energy balance [113].

$$\dot{Q}_{ct} = \frac{T_{CTWS} - T_{wb,i}}{R} \quad (3.18)$$

When comparing Eq.(3.11) and Eq.(3.18), we can have another definition of the overall heat resistance:

$$R = \frac{1}{\varepsilon \cdot \dot{C}_{\min}} \quad (3.19)$$

Theoretically, the overall heat resistance ( $R$ ) consists of two parts: heat resistance due to the water convection ( $R_{ctw}$ ) and heat resistance due to the air convection ( $R_a$ ).

$$R = R_{ctw} + R_a \quad (3.20)$$

Convection heat transfer refers to the heat exchanged between an interface and the fluid moving over the interface. The amount of heat thus transferred depends on the nature of the interface and the fluid, the geometry of the cooling tower and the velocity of the fluid over the interface as well as the temperature difference.

As water and air in cooling towers are moved by pumps and fans, respectively, the type of heat transfer between water and air can be considered as forced convection. Assuming the uniform cross section area of the water flow is circular, with diameter ( $D$ ), by dimensional analysis [114], the heat resistance of water convection ( $R_{cw}$ ) and mass flow rate ( $\dot{m}_{cw}$ ) can be calculated as:

$$\frac{1}{R_{ctw}} = C \left( \frac{Dv\rho}{\mu} \right)^{e_1} \left( \frac{C_{pw}\mu}{k} \right)^{e_2} \cdot \frac{k}{D} \cdot A_{ctw} \quad (3.21)$$

$$\dot{m}_{ctw} = v \cdot \pi \cdot \frac{D^2}{4} \cdot \rho \quad (3.22)$$

where  $v$ ,  $\rho$ ,  $\mu$  and  $k$  denote the average velocity, density, viscosity and thermal conductivity of the cooling tower water flowing through the cooling tower, respectively. And the values of the constant  $C$  and the exponents  $e_1$  and  $e_2$  in Eq.(3.21) are difficult to be determined exactly.

For steady stable flow, it is reasonable to assume that the value of the heat transfer area of the cooling tower water side convection ( $A_{ctw}$ ), the cooling tower water density ( $\rho$ ) and the velocity ( $v$ ) remain constant. Moreover,  $\mu$ ,  $k$  and  $C_{pw}$  are approximately constants if the temperature difference is not too big (not greater than  $6^\circ\text{C}$  for water and  $50^\circ\text{C}$  for a gas) [115]. Replace  $v$  in Eq. (3.21) by Eq. (3.22), we obtain:

$$\begin{aligned} \frac{1}{R_{ctw}} &= \dot{m}_{ctw}^{e_1} \left[ \frac{4^{e_1} C}{\pi^{e_1}} \cdot \frac{C_{pw}^{e_2} \cdot k^{1-e_2}}{\mu^{e_1-e_2} \cdot D^{1+e_1}} \right] A_{ctw} = b_1 \dot{m}_{ctw}^{e_1} \\ b_1 &= \frac{4^{e_1} C}{\pi^{e_1}} \cdot \frac{C_{pw}^{e_2} \cdot k^{1-e_2}}{\mu^{e_1-e_2} \cdot D^{1+e_1}} \cdot A_{ctw} \end{aligned} \quad (3.23)$$

Following the same argument, the heat resistance of air convection can be expressed as:

$$\begin{aligned} \frac{1}{R_a} &= b_2 \dot{m}_a^{e_1} \\ b_2 &= \frac{4^{e_1} C}{\pi^{e_1}} \cdot \frac{C_{pe}^{e_2} \cdot k^{1-e_2}}{\mu^{e_1-e_2} \cdot D^{1+e_1}} \cdot A_a \end{aligned} \quad (3.24)$$

Substituting Eqs.(3.20), (3.23) and (3.24) into (3.18), a cooling tower model for computing heat rejection rate is obtained as:

$$\dot{Q}_{ct} = \frac{b_1 \dot{m}_{ctw}^{e_1} \cdot b_2 \dot{m}_a^{e_1}}{b_1 \dot{m}_{ctw}^{e_1} + b_2 \dot{m}_a^{e_1}} (T_{CTWS} - T_{wb,i}) = \frac{c_1 \dot{m}_{ctw}^{c_3}}{1 + c_2 \left( \frac{\dot{m}_{ctw}}{\dot{m}_a} \right)^{c_3}} (T_{CTWS} - T_{wb,i}) \quad (3.25)$$

where  $c_1 = b_1$ ,  $c_2 = b_1/b_2$  and  $c_3 = e_1$ . These three parameters can be determined either by manufacturers' data or by real time experimental data.

Forced convection heat transfer is very complex and influenced by many factors. The approach of combining the property factors and geometric factors into the constants (characteristic parameters) was used in Eq.(3.25). Compared with the existing cooling tower model, Eq.(3.25) is characterized by fewer characteristic parameters and simplicity.

Compared with the existing models mentioned above, the proposed model releases the control variable, mass flow rate of water and air, from the lumped parameter  $Me_M$  and  $NTU$ , thus, iterative computation can be avoided when  $\dot{m}_{cw}$  and  $\dot{m}_a$  change.

By dimensional analysis, the cross-flow arrangement cooling tower can be hypothetically considered as a counter-flow arrangement with the same terminal temperatures [116, 117]. Therefore, this model can also be applied in a cross-flow cooling tower, with the equivalent water mass flow rate  $\dot{m}_{ctw, equ} = \lambda \dot{m}_{ctw}$ . For a given cooling tower, the conversion coefficient ( $\lambda$ ) is constant, thus,  $\lambda$  can be lumped in the unknown parameters  $c_1$  and  $c_2$  in Eq.(3.25).

The proposed model is deduced from the analysis of the Effective-NTU method, thus, the utilization of the proposed approaches is independent of the type of fill considered. This feature makes that it can be widely used to describe the characteristics of cooling towers with different kinds of fill arrangement.

### **3.4 Parameter Identification**

If the variables  $T_{CTWS}$ ,  $T_{wb}$ ,  $\dot{m}_{ctw}$ ,  $\dot{m}_a$  and  $\dot{Q}_{ct}$  can be obtained, manipulating the cooling tower into  $N$  states, it follows that

$$\begin{aligned}
\dot{Q}_{ct,1} &= \frac{c_1 \dot{m}_{ctw,1}^{c_3}}{1 + c_2 \left( \frac{\dot{m}_{ctw,1}}{\dot{m}_{a,1}} \right)^{c_3}} (T_{CTWS,1} - T_{wb,1}) \\
\dot{Q}_{ct,2} &= \frac{c_1 \dot{m}_{ctw,2}^{c_3}}{1 + c_2 \left( \frac{\dot{m}_{ctw,2}}{\dot{m}_{a,2}} \right)^{c_3}} (T_{CTWS,2} - T_{wb,2}) \\
&\vdots \\
\dot{Q}_{ct,N} &= \frac{c_1 \dot{m}_{ctw,N}^{c_3}}{1 + c_2 \left( \frac{\dot{m}_{ctw,N}}{\dot{m}_{a,N}} \right)^{c_3}} (T_{CTWS,N} - T_{wb,N})
\end{aligned} \tag{3.26}$$

To determine the empirical parameter  $c_1 \sim c_3$ , an objective function is defined as:

$$\mathbf{MIN} F([c_1, c_2, c_3]^T) = \mathbf{MIN} \sum_{i=1}^N \left( \frac{c_1 \dot{m}_{ctw,i}^{c_3}}{1 + c_2 \left( \frac{\dot{m}_{ctw,i}}{\dot{m}_{a,i}} \right)^{c_3}} (T_{CTWS,i} - T_{wb,i}) - \dot{Q}_{ct,i} \right)^2 \tag{3.27}$$

Since it is a non-linear unconstrained optimization problem, several existing algorithms can be used to find the solution. Here, the Levenberg-Marquardt method [118] is implemented, which uses a search direction between the Gauss-Newton and the steepest descent direction by solving the linear set of equations:

$$(J(u_k)^T J(u_k) + \lambda_k I) d_k = -J(u_k) F(u_k) \tag{3.28}$$

Where,  $u_k$  is the  $k^{th}$  iteration value of  $u = [c_1, c_2, c_3]^T$ ;

$$F_i(u_k) = F_i([c_1, c_2, c_3]^T); \tag{3.29a}$$

$$F(u_k) = [F_1(u_k), F_2(u_k) \cdots, F_N(u_k)]^T; \tag{3.29b}$$

$$J(u_k) = \begin{bmatrix} \frac{\partial F_1}{\partial c_1} & \frac{\partial F_1}{\partial c_2} & \frac{\partial F_1}{\partial c_3} \\ \frac{\partial F_2}{\partial c_1} & \frac{\partial F_2}{\partial c_2} & \frac{\partial F_2}{\partial c_3} \\ \vdots & \vdots & \vdots \\ \frac{\partial F_N}{\partial c_1} & \frac{\partial F_N}{\partial c_2} & \frac{\partial F_N}{\partial c_3} \end{bmatrix}; \quad (3.29c)$$

$$u_{k+1} = u_k + d_k \quad (3.29d)$$

In the equations,  $\lambda_k$  controls both the magnitude and direction of  $d_k$ . When  $\lambda_k$  is zero, the direction  $d_k$  is identical to that of the Gauss-Newton method. If  $\lambda_k$  tends to infinity,  $d_k$  tends towards a vector of zeros and a steepest descent direction. This makes it less effective than the Gauss-Newton search direction but more robust.

The whole procedure of model identification is given as follows:

*Step 1.* Obtain cooling tower operating points from either manufacturers' data or real time experimental data.

*Step 2.* Initialize  $u_0$  and  $\lambda_0$ , calculate  $F(u_0)$  and  $J(u_0)$  from Eqs. (3.29b) and (3.29c).

*Step 3.* Determine initial search direction  $d_0$  from Eq. (3.28).

*Step 4.* Compute the  $F(u_k)$  with Eq.(3.27) and determine the search direction of the next step from Eqs.(3.28) and (3.29).

*Step 5.* Stop the computation when  $F(u_k)$  or  $F(u_k) - F(u_{k+1})$  is less than a pre-specified small number (usually in the range of  $1 \times 10^{-6} \sim 1 \times 10^{-5}$ ). Otherwise, return to *Step 4*.

### ***3.5 Model Validation***

In order to validate the proposed model, a cooling tower operating in the Grand Hyatt Singapore hotel HVAC system with the following specifications is used:

1. Type: Induced draft, counter-flow;
2. Tower dimension: 4.94 m × 4.94 m × 3.96 m (length, width, height);
3. Nominal water circulation flow rate: 80.44 kg/s (1275 gallon/minute);
4. Designed supply water temperature: 35.00 °C (95 °F);
5. Designed return water temperature: 29.44 °C (85 °F);
6. Designed wet-bulb temperature: 26.67 °C (80 °F);
7. Heat rejection at design condition: 2461.83 kW (700 Ton);
8. Nominal fan power: 15 kW;
9. Water distribution system: low pressure down spray;
10. Fan motor location: outside air discharge steam.

Both the cooling tower fan and the water pump are equipped with Variable Speed Drive (VSD) to regulate the air and water speed during part-load condition. The air speed through the cooling tower can be estimated from the frequency of the motor driving the fan. A flow meter installed at the condenser water loop (cooling tower water is driven by the condenser water pump) shows the water flow through the cooling tower. The dry-bulb and wet-bulb temperature of the ambient environment are measured by sensors in the weather station, which has been set up near the HVAC plant. Two accurate temperature sensors are installed to monitor the water temperatures entering and leaving the cooling towers. With the temperature differences and water flow rates,

the heat rejection rate of the cooling tower can be determined as the real operating data. All these variables are recorded by EMCS in the hotel.

According to the settings of EMCS in the Grand Hyatt Singapore hotel, the sampling rate of each variable is one minute. Therefore, there are totally 1440 values for each variable in one day. In order to quantitatively show the performances of the model prediction, an error index, Root-Mean-Square of Relative Error (RMSRE), is adopted:

$$RMSRE = \sqrt{\frac{\sum_{i=1}^n \left( \frac{D_{real} - D_{calculation}}{D_{real}} \right)^2}{n}} \quad (3.30)$$

where,  $D_{real}$  denotes the real measured data, and  $D_{calculation}$  denotes the calculated data.

A whole day's data (February 03<sup>rd</sup>, 2006) is used for parameter identification of the proposed cooling tower model and the results are shown in Figure 3.4. The horizontal-axis shows the real data of heat rejection rate measured on site, while the vertical-axis shows the calculated data predicted by the cooling tower model.

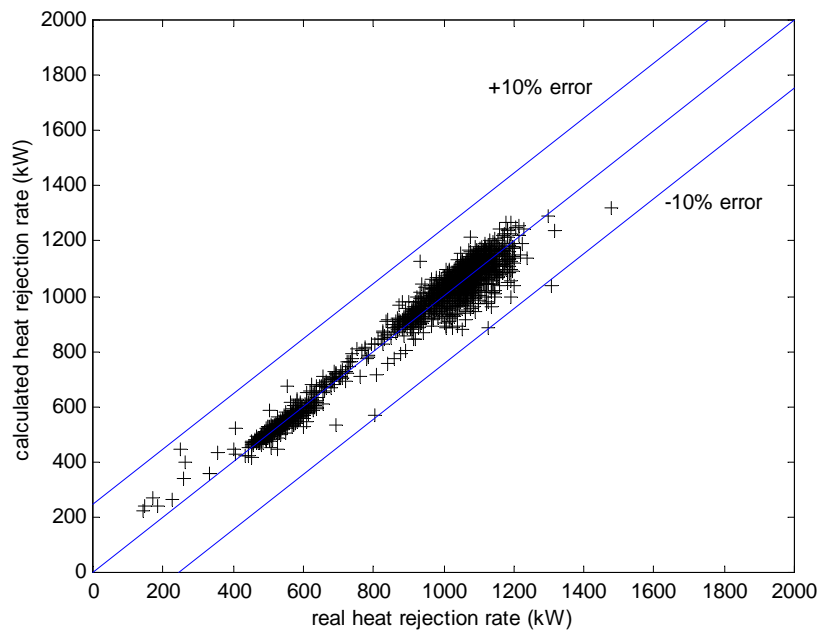


**Figure 3.4 Comparison between the calculated data and the real data on February 03<sup>rd</sup>, 2006**

There are three lines in the Figure 3.4 to indicate the performance of the cooling tower model. The line in the center indicates the ideal case, where the cooling tower model exactly predicts the heat rejection rate of the operating component. The other two lines give the boundary of  $\pm 10\%$  deviation from the ideal case. If the data points fall within a margin of  $\pm 10\%$  error, it means that the model under predicts the heat rejection rate of the cooling tower. When the data points fall in margin of  $\pm 10\%$  error, the model over-predicts the real heat rejection rate. Using the Levenberg-Marquardt method, the parameters are estimated as  $c_1=4.43$ ;  $c_2=1.12$  and  $c_3=1.11$ . The RMSRE for this model identification of 1440 data points is 0.060 and this is acceptable for control and optimization purposes.

This model is then used to predict the cooling tower performance of the very next day (February 04<sup>th</sup>, 2006). Figure 3.5 shows that the results are quite good for the model validation.

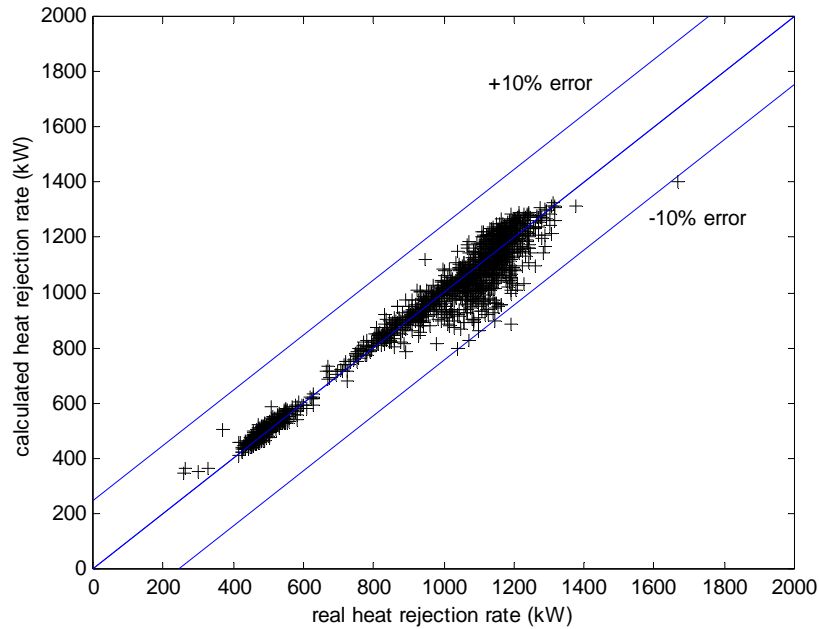


**Figure 3.5 Comparison between the calculated data and the real data on February 04<sup>th</sup>, 2006**

The RMSRE for this model validation of 1440 data points is 0.056. ( $c_1=4.43$ ;  $c_2=1.12$ ;  $c_3=1.11$ ) If all these 1440 data are used to identify the new cooling tower model, the RMSRE for the model identification is 0.054. ( $c_1=5.73$ ;  $c_2=1.61$ ;  $c_3=1.09$ ) There is no big difference between the prediction accuracies of these two models.

Secondly, the original model identified by data on February 03<sup>rd</sup>, 2006 is used to predict the cooling tower performance after seven days (February 10<sup>th</sup>, 2006). Figure 3.6 shows the results of the model validation.

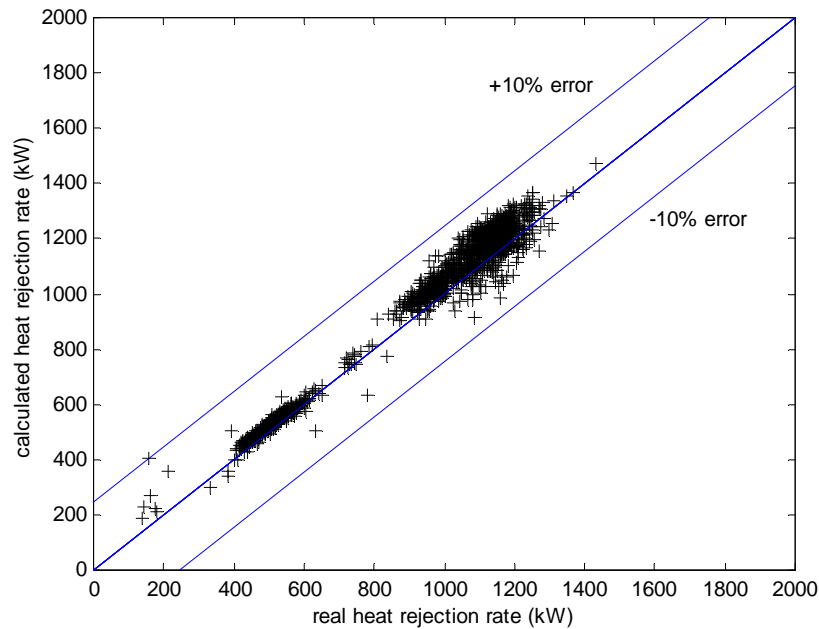


**Figure 3.6 Comparison between the calculated data and the real data on February 10<sup>th</sup>, 2006 with the model parameters identified on February 3<sup>rd</sup>, 2006**

The RMSRE for this model validation of 1440 data points is 0.082. ( $c_1=4.43$ ;  $c_2=1.12$ ;  $c_3=1.11$ ). If all these 1440 data are used to identify the new cooling tower model, the RMSRE for the model identification is 0.063. ( $c_1=4.71$ ;  $c_2=1.21$ ;  $c_3=1.09$ ) Although the results of the model validation are tolerant for engineering purposes, some avoidable errors are induced for the performance prediction by the original model.

Finally, the original model identified by data on February 03<sup>rd</sup>, 2006 is used to predict the cooling tower performance one month away (March 03<sup>rd</sup>, 2006). Figure 3.7 shows the results of the model validation.

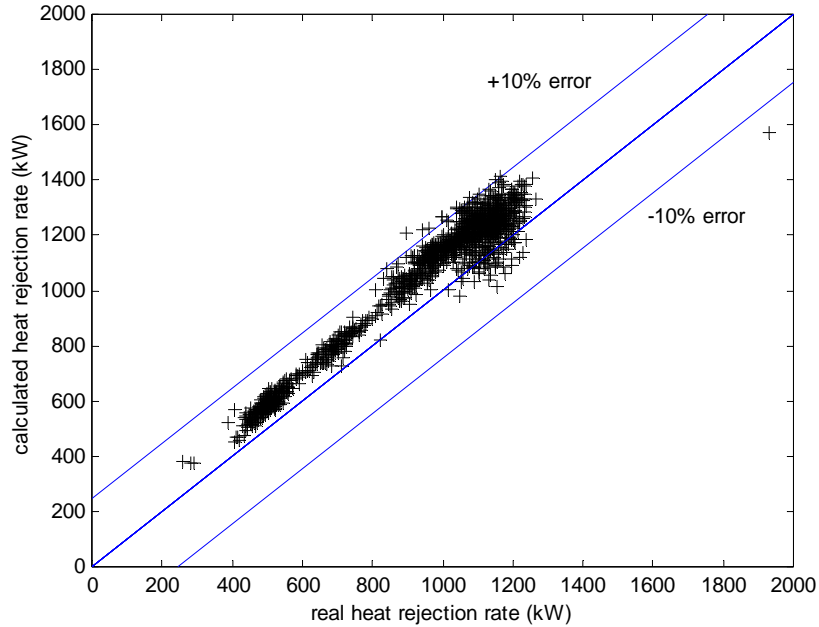


**Figure 3.7 Comparison between the calculated data and the real data on March 03<sup>rd</sup>, 2006 with the model parameters identified on February 3<sup>rd</sup>, 2006**

The RMSRE for this model validation of 1440 data points is 0.143. ( $c_1=4.43$ ;  $c_2=1.12$ ;  $c_3=1.11$ ) The results of the model may not be tolerated for accurate control and optimization. For the majority of data points, the model over-predicts the performance of the cooling tower.

For the direct contact cooling tower used for testing, the water quality and effective contact area varies in time because of the pollution from the surrounding environment. The reason why the predicted performance is not the same for different testing times is due to the decreasing effective contact area in the cooling tower. And the deterioration of water quality results in the fall of the heat exchange efficiency. As time passes, the performance of the cooling tower becomes worse. Therefore, the predicted cooling tower performance by the identified parameters on February 04<sup>th</sup>, 2006 is better than the

real performance on February 10<sup>th</sup>, 2006 and much better than the real performance on March 03<sup>rd</sup>, 2006.

Since the characteristics of the cooling tower are slow time-varying, we need to identify the characteristic parameters of the cooling tower operating on March 03, 2006. With the new parameters  $c_1=1.53$ ;  $c_2=0.62$  and  $c_3=1.29$ , we can perfectly predict the cooling tower performance with a RMSRE of 0.048, as shown in Figure 3.8.

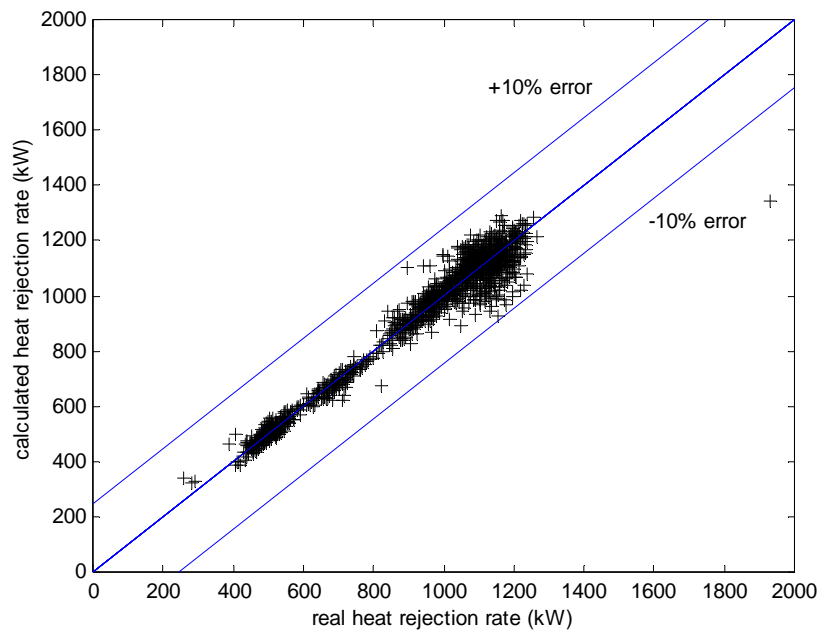


**Figure 3.8 Comparison between the calculated data and the real data on March 03<sup>rd</sup>, 2006 with new identified model parameters**

According to the validation of the proposed cooling tower model, the model with new parameters is accurate enough for process control and optimization (RMSRE<0.1). For long periods of time, e.g. a month, the characteristic parameters should be updated periodically to accurately predict the cooling tower performance since the characteristics of the cooling tower is time varying. Generally, the characteristic parameters can be used for some time interval after it is identified, and the time interval depends on the surrounding environment condition of the operating cooling tower. For example, rainfall, dust and/or pollutant deteriorate the water quality of the circulation

cooling tower water as well as the heat transfer characteristics of the fills or packings inside the cooling tower. Therefore, after a certain period of time, the cooling tower model with the original characteristic parameters might not be accurate enough and should be updated by new performance data. With this characteristic of the proposed model, the inaccuracy of the model and the requirement of updating model parameters can be used as an index for maintaining the cooling tower and replacing or purifying the circulation cooling tower water.

### ***3.6 Summary***

A simple cooling tower model has been presented in this chapter. The proposed model is based on heat resistance and energy balance principles. It introduced only three empirical parameters whose values can be determined by either manufacturers' catalog data or real operating data. Unlike other existing cooling tower models, this model captures the geometric characteristics without requiring geometric specifications and no iterative computation and initial guess are required to determine the parameters. Consequently, online determination of the model parameters becomes practical and simple. The real operating data from a HVAC system of a commercial hotel is used to identify and validate the proposed model. The slow time-varying characteristics of the cooling tower under test can be specified by altering the model parameters and accurately predict the cooling tower performance. As time evolves, the parameters of the cooling tower should be constantly updated to maintain the prediction accuracy.

The significance of the developed model is that it can be easily applied to real-time HVAC system optimization. The following is the comparison of the developed model with existing models:

*Merkel's model:*

1. The Merkel method, employing a numerical method to determine the tower characteristic  $Me_M$ , does not accurately represent the physics of the heat and mass transfer process in the cooling tower fill.
2. Iterative computation is needed.
3. Geometric specification of the cooling tower is required.

*Effectiveness-NTU model:*

1. The value of  $UA$ , which varies with the changing mass flow rate of water and air, is difficult to determine and requires geometric specification of the cooling tower.
2. An initial guess of the outlet air condition and an iterative computation are needed in order to find true outlet air conditions.

*Stoecker's method:*

1. This is an entirely empirical model and incapable of considering the variations of airflow and water flow rates. Extending this model to variable airflow rate or water flow rate requires more coefficients, which increases the complexity for model identification.
2. The model only uses a curve-fitting technique to approximate the real experimental data. It might work well under predefined conditions within the experimental data region. When the assumption is no longer true and the operating region is beyond the experimental data, the model cannot reflect the real performances of the cooling tower.

*Proposed model:*

1. The proposed model lumps the geometric information as constants and only considers the inlet and outlet conditions of the cooling tower, therefore it is incapable of providing useful information for cooling tower designs and retrofits.
2. Due to the global uniqueness of the characteristic parameters and the simple procedure to determine them, the model is more desirable for real time optimization of operating cooling towers.

In summary, the advantages of the proposed model are simple, flexible, relative accurate, and easy for engineering applications. It focuses on the characteristics of the exiting cooling tower and the relationship between heat rejection rates and mass flow rates under different circumstances. Table 3.1 summarizes the comparison of the proposed new models and existing model mentioned above.

**Table 3.1 Comparison of different cooling tower models**

Cooling tower model	Stoecker's	Merkel's	E-NTU	New model
Number of parameters	9 ( $c_1 \sim c_9$ )	1 ( $Me_M$ )	1 ( $UA$ )	3 ( $c_1 \sim c_3$ )
Variable mass flow rate	NO	YES	YES	YES
Geometric data	NO	YES	NO	NO
Iterative computation	NO	YES	YES	NO
Modeling technique	Empirical	Physical	Hybrid	Hybrid
Model application	Simulation	Simulation and design	design and control	control and optimization

According to the comparison, the main significance of the developed model is that it can be easily applied to real-time HVAC system optimization where set points of each energy consumption device in the condenser water loop are related to the model. Therefore, the cooling tower model is the constrained condition in the course of energy minimization of the loop. In Chapter 6, this hybrid model is used to analyze and

formulate the energy minimization problem of operating building HVAC system consisting of multiple cooling towers and chillers. And a model-based system optimization approach for a real HVAC system is developed and validated based on this developed hybrid cooling tower model in Chapter 7.

# **CHAPTER 4 DYNAMIC MODELS OF COOLING COILS AND COOLING TOWERS**

## ***4.1 Introduction***

The objective of this chapter is to develop dynamic models for the cooling coils and the cooling towers. The focus of this chapter will be to accurately model the transient heat and mass transfer processes taking place in the cooling coils and cooling towers. What is significant is that the modeling methodologies proposed in this chapter can be extended to model other subcategory heat exchangers of the HVAC system, e.g. condensers or evaporators.

In the sections below, we will present the simplified dynamic cooling coil and cooling tower models developed with proposed hybrid modeling methodologies. Furthermore, we will show how the model parameters are identified, and also how the models are validated through actual experiments and simulations.

## ***4.2 Hybrid Cooling Coil Model***

### **4.2.1 Modeling based on heat transfer mechanism**

A water cooling coil uses chilled water as the coolant inside the tubes. The chilled water cools and dehumidifies the moist air that flows over the external surface of the tubes and fins, as shown in Figure 4.1. To maintain a higher rate of heat transfer, the air and water normally follow a counter-flow arrangement; i.e., the low and high temperature air meets the low and high temperature water correspondingly. Through heat exchange with the air outside the cooling coil tubes, the chilled water flows from the inlet to the outlet of the cooling coil forced by the chilled water pump with inlet

temperature ( $T_{chw,i}$ ) and the mass flow rate ( $\dot{m}_{chw}$ ), the outlet temperature of the chilled water rises to  $T_{chw,o}$ . The air flows from the inlet to the outlet of the cooling coil forced by the supply air fan with the on-coil dry-bulb temperature ( $T_{a,i}$ ), wet-bulb temperature ( $T_{a,i,wb}$ ) and mass flow rate ( $\dot{m}_a$ ). Likewise, the off-coil dry-bulb and wet-bulb air temperatures descend to  $T_{a,o}$  and  $T_{a,o,wb}$ , respectively.

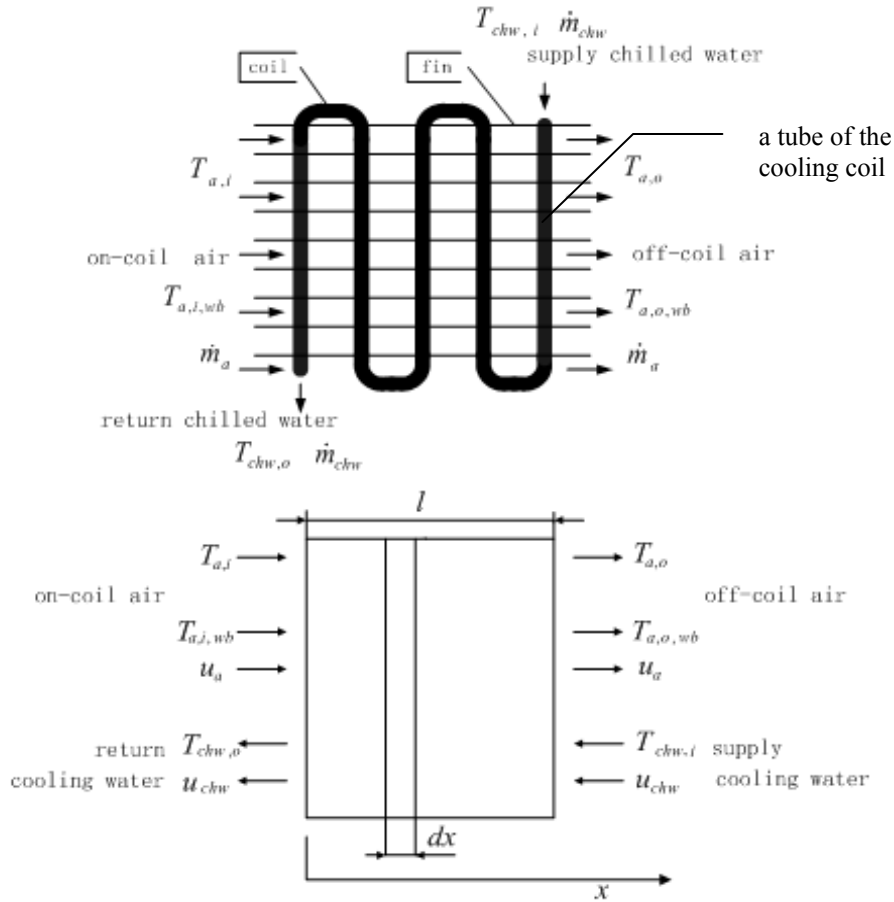


**Figure 4.1 A typical finned-tube cooling coil**

During the process of heat transfer, a quantity of heat that moves from the hot air element through the metal tube wall (usually made of copper or aluminum alloy) into the chilled water element can be given by:

$$q_{cc} = \frac{T_a - T_{chw}}{R_{total}} \quad (4.1)$$

where,  $q_{cc}$  and  $R_{total}$  denote the heat exchange quantity of the element and total heat resistance between water and air element;  $T_a$  and  $T_{chw}$  denote the temperature of air and the temperature of chilled water, respectively.

As shown in Figure 4.2, the overall heat resistance ( $R_{total}$ ) consists of three parts: heat resistance of the chilled water convection, heat resistance of the metal wall conduction and heat resistance of the air convection. However, as the materials of the metal wall used in the cooling coil are good conductors of heat and hence the resistance can be considered as a constant during the operation, the conduction effect can be lumped into the unknown coefficients and neglected in the following development.

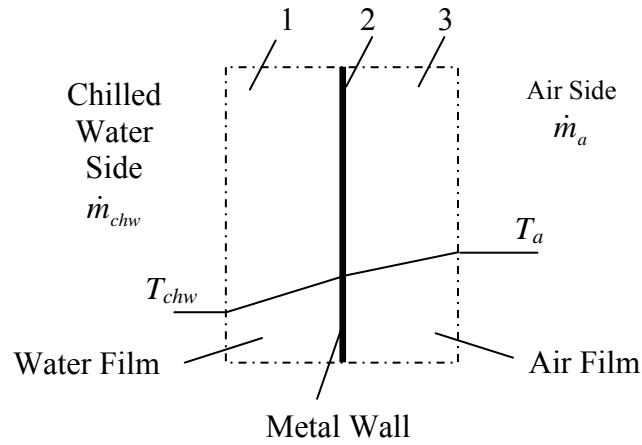


**Figure 4.2 Heat transfer mechanism of coil**

Therefore, the overall heat resistance is:

$$R_{total} = R_{chw} + R_a \quad (4.2)$$

where,  $R_{chw}$  and  $R_a$  denote the heat resistance of the chilled water convection and the heat resistance of the air convection, respectively.

The quantity of heat thus transferred depends on the nature of the surface and fluid, the geometry of the cooling coil, the velocity of the fluid over the surface as well as the

temperature differences. The overall heat resistance of a chilled-water coil can then be written as [18]:

$$R_{total} = \frac{1}{F_{chw} A_{chw}} + \frac{1}{F_a A_a} = \frac{b_{chw} A_{chw} \dot{m}_{chw}^\ell + b_a A_a \dot{m}_a^\ell}{b_{chw} A_{chw} \dot{m}_{chw}^\ell b_a A_a \dot{m}_a^\ell} \quad (4.3)$$

Where,  $F_{chw}$ ,  $F_a$ ,  $A_{chw}$ ,  $A_a$  are the film coefficient of chilled water, the film coefficient of air, the heat transfer area of the chilled water side convection and the heat transfer area of the air side convection, respectively, and  $\ell$ ,  $b_{chw}$ ,  $b_a$  are considered as constant parameters to be identified.

By combining Eqs. (4.1) and (4.3), we obtain:

$$q_{cc} = \frac{b_{chw} A_{chw} \dot{m}_{chw}^\ell b_a A_a \dot{m}_a^\ell}{b_{chw} A_{chw} \dot{m}_{chw}^\ell + b_a A_a \dot{m}_a^\ell} (T_a - T_{chw}) \quad (4.4)$$

#### 4.2.2 Modeling based on energy and mass conservation

For modeling convenience, we assume that:

1. The dry air and water vapor in the air are treated as a non-reacting mixture of ideal gases.
2. The specific heat and the density of the wet air are considered as constants in the process of heat and mass transfer.
3. Since the heat and mass exchange between moist air and the external surface of the cooling coil tubes arrives at a balance, the Lewis number (Le) is considered as a constant.
4. Both the air and the water are well mixed in the cross-section normal to its flow. Therefore, only gradients for each fluid exist in their respective flow directions [119].

5. The humidity of saturated wet air is approximately linear to its temperature when the temperature changes within a small range.

Let the total lengths of tubes and cooling coil depth be  $\xi$  and  $l$ , the velocity of the airflow ( $u_a$ ) and equivalent velocity of chilled water ( $u'_{chw}$ ) in the counter airflow direction are:

$$u'_{chw} = \frac{l}{\xi} u_{chw} = \frac{l}{\xi} \frac{\dot{m}_{chw}}{\rho_{chw} A_{tube}} \quad (4.5)$$

$$u_a = \frac{\dot{m}_a}{\rho_a A_a} \quad (4.6)$$

Using the energy and mass conservation laws, the dynamic change of chilled water temperature and air temperature in an infinitesimal volume can be expressed as:

$$\rho_{chw} V_{chw} C_{chw} \left( \frac{\partial T_{chw}}{\partial t} + u'_{chw} \frac{\partial T_{chw}}{\partial x} \right) = q_{cc} \quad (4.7)$$

$$\rho_a V_a \left( \frac{\partial h_a}{\partial t} + u_a \frac{\partial h_a}{\partial x} \right) = -q_{cc} \quad (4.8)$$

Where,  $V_{chw}$  and  $V_a$  are constants representing the volume of chilled water and air element in the mass and heat transfer process in the X direction (Figure 4.3).

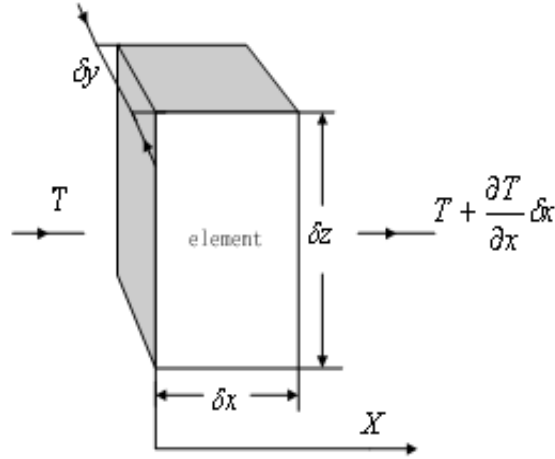


**Figure 4.3 Temperature changes in the X direction**

There is a dry-wet boundary inside the cooling coil that divides it into the sections of the dry surface and the wet surface, as show in Figure 4.4 [120].

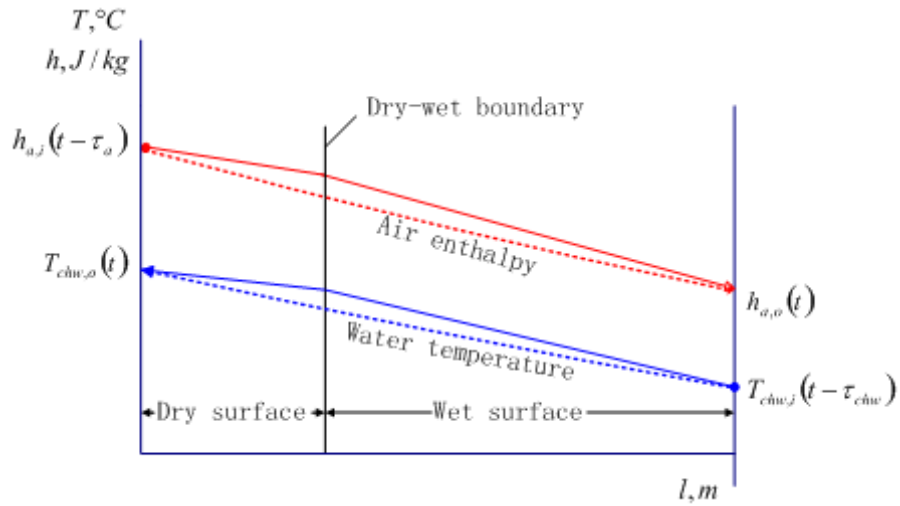


**Figure 4.4 Temperature and enthalpy profiles of cooling coil**

In this figure, the solid curves represent the true temperature and enthalpy profiles. If we approximate chilled water temperature ( $T_{chw}$ ) and air enthalpy ( $h_a$ ) variation profiles by a linear equation between the two boundaries (dotted line), then any point along the air movement direction can be expressed by:

$$T_{chw} = \frac{T_{chw,o} - T_{chw,i}}{l} x + T_{chw,i} \quad (4.9)$$

$$h_a = \frac{h_{a,o} - h_{a,i}}{l} x + h_{a,i} \quad (4.10)$$

where,  $T_{chw,o}$  and  $T_{chw,i}$  denote the chilled water temperature at the outlet and inlet of the cooling coil;  $h_{a,o}$  and  $h_{a,i}$  denote the air enthalpy at the outlet and inlet of the cooling coil, respectively.

Take the first derivative of Eqs.(4.9) and (4.10) respectively, we obtain:

$$\frac{\partial T_{chw}}{\partial x} = \frac{T_{chw,o} - T_{chw,i}}{l} \quad (4.11)$$

$$\frac{\partial h_a}{\partial x} = \frac{h_{a,o} - h_{a,i}}{l} \quad (4.12)$$

In practice, the relative humidity of the coil inlet air usually fluctuates inside a small region; therefore, the enthalpy of moist air can be approximated by the equivalent dry-bulb temperature (EDT) method [31], i.e.

$$h_a \approx C_{pa} T_a \quad (4.13)$$

$$h_{a,o} - h_{a,i} \approx C_{pa} (T_{a,o} - T_{a,i}) \quad (4.14)$$

where,  $C_{pa}$  denotes the specific heat of the moist air.

By combining Eqs. (4.7-4.14) we have:

$$\rho_{chw} V_{chw} C_{pw} \left( \frac{dT_{chw}}{dt} + u'_{chw} \frac{T_{chw,o} - T_{chw,i}}{l} \right) = q_{cc} \quad (4.15)$$

$$\rho_a V_a C_{pa} \left( \frac{dT_a}{dt} + u_a \frac{T_{a,o} - T_{a,i}}{l} \right) = -q_{cc} \quad (4.16)$$

### 4.2.3 Dynamic modeling

$q_{cc}$  is representing a heat exchange quantity of an infinitesimal volume of a cooling coil, we can replace  $q$  in Eqs. (4.15, 4.16) by Eq. (4.4) to result in:

$$\frac{dT_{chw}}{dt} + c_{cc,1} \dot{m}_{chw} (T_{chw,o} - T_{chw,i}) = \frac{c_{cc,2} \dot{m}_a^{\ell_{cc}}}{1 + c_{cc,3} \left( \frac{\dot{m}_a}{\dot{m}_{chw}} \right)^{\ell_{cc}}} (T_a - T_{chw}) \quad (4.17)$$

$$\frac{dT_a}{dt} + c_{cc,4} \dot{m}_a (T_{a,o} - T_{a,i}) = - \frac{c_{cc,5} \dot{m}_a^{\ell_{cc}}}{1 + c_{cc,3} \left( \frac{\dot{m}_a}{\dot{m}_{chw}} \right)^{\ell_{cc}}} (T_a - T_{chw}) \quad (4.18)$$

Where,  $c_{cc,1} = \frac{l}{\xi} \frac{1}{\rho_{chw} A_{tube}}$ ,  $c_{cc,2} = \frac{b_a A_a}{\rho_{chw} V_{chw} C_{pw}}$ ,  $c_{cc,3} = \frac{b_a A_a}{b_{chw} A_{chw}}$ ,  $c_{cc,4} = \frac{1}{\rho_a A_a}$ ,  
 $c_{cc,5} = \frac{b_a A_a}{\rho_a V_a C_{ma}}$ , and  $\ell_{cc}$  are constants which can be determined from the manufacturer's data or by real-time experimental data.

Notice that it will take a certain amount of time for an individual air and water fluid element at the new temperature to traverse the distance  $l$  and  $\xi$  from the inlet to the outlet of the cooling coil, any temperature changes at the air and water inlet will not be registered instantaneously at the outlet. We denote  $\tau_{chw}$  and  $\tau_a$  as the time intervals that the air and chilled water fluid element take for traversing from inlet to outlet of the cooling coil, which are defined, respectively, by:  $\tau_{chw} = \frac{\xi}{u_{chw}} = \frac{\xi \rho_{chw} A_{tube}}{\dot{m}_{chw}}$  and

$$\tau_a = \frac{l}{u_a} = \frac{l \rho_a A_a}{\dot{m}_a}.$$

Finally, the engineering dynamic model using only boundary conditions at the outlet of cooling coil package can be written as:

$$\frac{dT_{chw,o}(t)}{dt} + c_{cc,1} \dot{m}_{chw}(t) [T_{chw,o}(t) - T_{chw,i}(t - \tau_{chw})] = \frac{c_{cc,2} \dot{m}_a^{\ell_{cc}}(t)}{1 + c_{cc,3} \left( \frac{\dot{m}_a(t)}{\dot{m}_{chw}(t)} \right)^{\ell_{cc}}} [T_{a,o}(t) - T_{chw,o}(t)] \quad (4.19)$$

$$\frac{dT_{a,o}(t)}{dt} + c_{cc,4} \dot{m}_a(t) [T_{a,o}(t) - T_{a,i}(t - \tau_a)] = - \frac{c_{cc,5} \dot{m}_a^{\ell_{cc}}(t)}{1 + c_{cc,3} \left( \frac{\dot{m}_a(t)}{\dot{m}_{chw}(t)} \right)^{\ell_{cc}}} [T_{a,o}(t) - T_{chw,o}(t)] \quad (4.20)$$

In practice, the number of sensors mounted on an actual HVAC system is limited. Several variables have to be obtained by indirect methods if necessary [18].

1. The chilled water flow rate can be obtained by measuring the pressure difference across the cooling coil. From

$$\Delta p = b_0 + b_1 \dot{m}_{chw} + b_2 \dot{m}_{chw}^2 \quad (4.21)$$

where  $b_0$ ,  $b_1$ ,  $b_2$  are unknown parameters to be determined through catalog data or online testing,  $\Delta p$  is the chilled water inlet-outlet pressure difference of a coil. Therefore, the following chilled water flow rate can be derived from Eq. (4.21):

$$\dot{m}_{chw} = \frac{-b_1 + \sqrt{b_1^2 - 4b_2(b_0 - \Delta p)}}{2b_2} \quad (4.22)$$

2. By employing the method proposed in [16], the cooling load ( $\dot{Q}_{cc}$ ) can be obtained through the chilled water flow rate and the temperature difference between the cooling coil inlet and outlet, and it is given by:

$$\dot{Q}_{cc} = C_{pw} \dot{m}_{chw} (T_{chw,o} - T_{chw,i}) \quad (4.23)$$

3. According to the energy balance, the air flow rate can then be estimated by:

$$\dot{m}_a = \frac{\dot{Q}_{cc}}{h_{a,i} - h_{a,o}} \quad (4.24)$$

The coil inlet air enthalpy can also be approximated by measuring the dry-bulb temperature with an assumption of the coil inlet air relative humidity of 60% and the coil outlet air relative humidity of 95% respectively. The use of  $h_a \approx C_{pa} T_a$  eliminates

the need of separately calculating heat transfers for the dry coil and the wet coil since both dry bulb and wet bulb air temperatures are considered in calculating  $\dot{m}_a$  as:

$$\dot{m}_a = C_{pa} \frac{\dot{Q}_{cc}}{T_{a,i} - T_{a,o}} \quad (4.25)$$

Using the estimation or measurement of variables  $T_{chw,i}$ ,  $T_{a,i}$ ,  $T_{chw,o}$ ,  $T_{a,o}$ ,  $\dot{m}_{chw}$  and  $\dot{m}_a$ , the unknown model parameters  $c_{cc,1} - c_{cc,5}$  and  $\ell_{cc}$  in Eqs. (4.19) and (4.20) can be determined in the parameter identification phase (see Section 4.4). Otherwise, if  $\ell = 0.8$  (engineering rule of thumb value) is adopted, the model has only five parameters to be determined.

### 4.3 Hybrid Cooling Tower model

#### 4.3.1 Modeling based on heat transfer mechanism

To develop the cooling tower model based on the heat transfer mechanism, we adopt the following reasonable assumptions:

1. heat and mass transfer in a direction normal to the flow only;
2. the Lewis number (Le) is a constant;
3. the reduction of water flow rate by evaporation (normally 1~4%) is neglected in the energy balance;
4. the cross-sectional area of the tower and temperature distribution throughout the water stream at any cross sections is uniform;
5. the saturation enthalpy is approximately linear with respect to web-bulb temperature.

As the cooling tower can be modeled, in the steady-state regime, by an equivalent classical counter flow heat exchanger [121], heat is transferred from the water drops to the surrounding moist air by convection during the process of heat transfer.

The quantity of heat rejected from the hot cooling tower water element into an air element ( $q_{ct}$ ) can then be calculated using the overall heat resistance ( $R$ ) according to heat transfer theory and the energy balance [114].

$$q_{ct} = \frac{T_{ctw} - T_{wb}}{R} \quad (4.26)$$

where,  $T_{ctw}$  and  $T_{wb}$  denote the cooling tower water temperature and the air wet-bulb temperature, respectively.

And the overall heat resistance ( $R$ ) consists of two parts: heat resistance of the cooling tower water convection ( $R_{ctw}$ ) and heat resistance of the air convection ( $R_a$ ).

$$R = R_{ctw} + R_a \quad (4.27)$$

Convection heat transfer refers to the heat exchanged between the air-water interface and the air or water flow moving over this interface. Thus the amount of transferred heat depends on the thermo physical properties of the air and water involved in the heat and mass transfer process, the geometry of the cooling tower and the velocity of air and water flow over the interface as well as the temperature differences between air and water.

As water and air in cooling towers are driven by pumps and fans, respectively, the type of heat transfer between water and air can be equivalently considered as forced convection. Assuming the uniform cross section area of the water flow is round, with the fictitious diameter ( $D$ ), by dimensional analysis [114], the heat resistance of water convection  $R_{ctw}$  and mass flow rate  $\dot{m}_{ctw}$  can be calculated by

$$\frac{1}{R_{ctw}} = C \left( \frac{Dv\rho}{\mu} \right)^{e1} \left( \frac{C_{pw}\mu}{k} \right)^{e2} \cdot \frac{k}{D} \cdot A_{ctw} \quad (4.28)$$

$$\dot{m}_{ctw} = v \cdot \pi \cdot \frac{D^2}{4} \cdot \rho \quad (4.29)$$

where,  $v$ ,  $\rho$ ,  $\mu$  and  $k$  denote the average velocity, density, viscosity and thermal conductivity of the cooling tower water element under study. And the constant  $C$  and the exponents  $e_1$  and  $e_2$  are constant. For a uniform flow, it is reasonable to assume that the value of heat transfer area ( $A_{ctw}$ ), density ( $\rho$ ) and velocity ( $v$ ) of the cooling tower water element under study remain constant. Moreover,  $\mu$ ,  $k$  and  $C_{pw}$  are approximately constants if the temperature difference is not too big (not greater than  $6^\circ\text{C}$  for water and  $50^\circ\text{C}$  for gas). Replace  $v$  in Eq. (4.28) by Eq. (4.29), we obtain:

$$\frac{1}{R_{ctw}} = \dot{m}_{ctw}^{e_1} \left[ \frac{4^{e_1} C}{\pi^{e_1}} \cdot \frac{C_{pw}^{e_2} \cdot k^{1-e_2}}{\mu^{e_1-e_2} \cdot D^{1+e_1}} \right] A_{ctw} \quad (4.30)$$

Following the same argument, the heat resistance of air convection can be expressed as:

$$\frac{1}{R_a} = \dot{m}_a^{e_1} \left[ \frac{4^{e_1} C}{\pi^{e_1}} \cdot \frac{C_{pe}^{e_2} \cdot k^{1-e_2}}{\mu^{e_1-e_2} \cdot D^{1+e_1}} \right] A_a \quad (4.31)$$

Substitute Eqs. (4.27), (4.30) and (4.31) into (4.26), a cooling tower model for computing heat rejection rate is obtained as follows:

$$q_{ct} = \frac{b_{cw} A_{ctw} \dot{m}_{ctw}^{e_1} \cdot b_a A_a \dot{m}_a^{e_1}}{b_{cw} A_{ctw} \dot{m}_{ctw}^{e_1} + b_a A_a \dot{m}_a^{e_1}} (T_{ctw} - T_{wb}) \quad (4.32)$$

where, the parameters  $b_{ctw}$ ,  $b_a$  and  $e_1, e_2$  can be determined either by manufacturers' specification data or by real time experimental data, and

$$b_{ctw} = \dot{m}_{ctw}^{e_1} \left[ \frac{4^{e_1} C}{\pi^{e_1}} \cdot \frac{C_{pw}^{e_2} \cdot k^{1-e_2}}{\mu^{e_1-e_2} \cdot D^{1+e_1}} \right]$$

$$b_a = \dot{m}_a^{e_1} \left[ \frac{4^{e_1} C}{\pi^{e_1}} \cdot \frac{C_{pe}^{e_2} \cdot k^{1-e_2}}{\mu^{e_1-e_2} \cdot D^{1+e_1}} \right]$$

which are very complicated and influenced by many factors.

By dimensional analysis, the cross-flow arrangement cooling tower can be hypothetically considered as a counter-flow arrangement with the same terminal temperatures [114]. Therefore, this modeling procedure can also be applied in a cross flow cooling tower, with the equivalent water mass flow rate  $\dot{m}_{ctw,e} = \lambda \dot{m}_{ctw}$ . For a specific cooling tower, the conversion coefficient is constant, thus,  $\lambda$  can be lumped within the unknown parameters  $b_{ctw}$  and  $b_a$  in Eq. (4.32).

#### 4.3.2 Modeling based on energy and mass conservation

For modeling based on energy and mass conservation, without loss of generality, we assume that:

1. Dry air and water vapor in the air are treated as a non-reacting mixture of ideal gases.
2. The specific heat and the density of wet air are considered as constants in the process of heat and mass transfer.
3. Both the air and the water are well mixed in the cross-section normal to its flow. Therefore, only gradients for each fluid exist in their respective flow directions [31].
4. The humidity of saturated wet air is approximately linear to its temperature when the temperature changes.
5. The air leaving the fill is saturated with water vapor.

Using the energy and mass conservation laws, the dynamic change of cooling tower water temperature in an infinitesimal volume can be expressed as:

$$\rho_{ctw} V_{ctw} C_{pw} \left( \frac{\partial T_{ctw}}{\partial t} + u_{ctw} \frac{\partial T_{ctw}}{\partial z} \right) = -q_{ct} \quad (4.33)$$

where,  $V_{ctw}$  is a constant representing the volume of a water element in the mass and heat transfer process traveling towards the vertical (Z) direction for counter-flow type

cooling tower and towards the horizontal (X) direction for cross-flow type cooling tower (Figure 4.5).

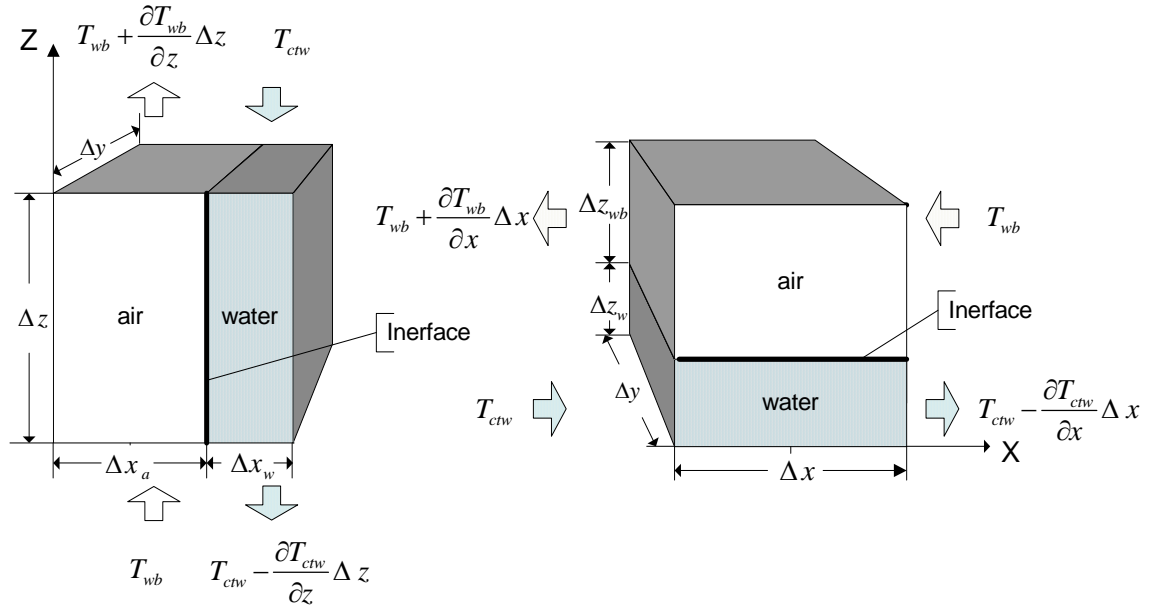


**Figure 4.5 Temperature changes towards the Z and X direction**

The simultaneous heat, mass and momentum transfer process occurring throughout the cooling tower is difficult to analyze. It would be more beneficial to subdivide the system into separate subsystem elements. For convenience, we sub-divide the system into  $0.2 \times 0.4$  m (  $\Delta Z = 0.2$  ,  $\Delta X = 0.2$  ) elements as shown in Figure 4.6. The measurement results of the temperature distribution of the cooling tower water and moist air through the cooling tower are reported in Figure 4.7 and Figure 4.8. Figure 4.7 indicates that the cooling tower water and wet bulb air temperature variations are relatively small through the width of the count-flow type cooling tower in the X direction at the same height in the Z direction, while Figure 4.8 indicates that the nonlinear process of heat transfer between water and air at Z direction can be approximated and linearized. A similar temperature variation pattern in a cross flow type cooling tower was also observed in the numerical analysis of Bourouni et al. [32]. The difference is that the air temperatures vary in the X direction. Therefore, the variation of cooling tower water and wet bulb air temperature across the cooling tower

can be linearized with the height or the width of the cooling tower in the direction of count-flow or cross-flow.

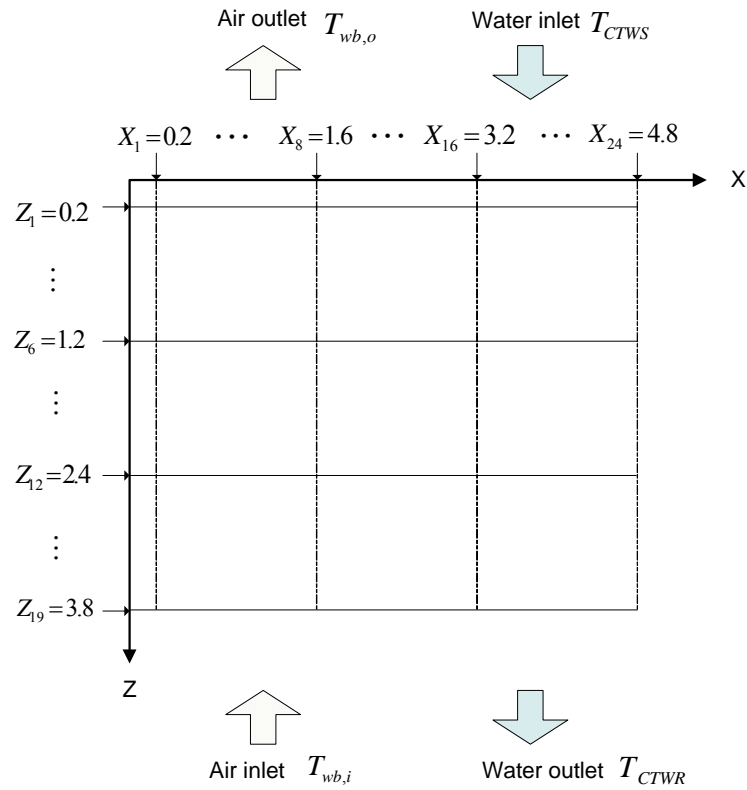


**Figure 4.6** Directions of water and air flows, levels and sections in the cooling tower

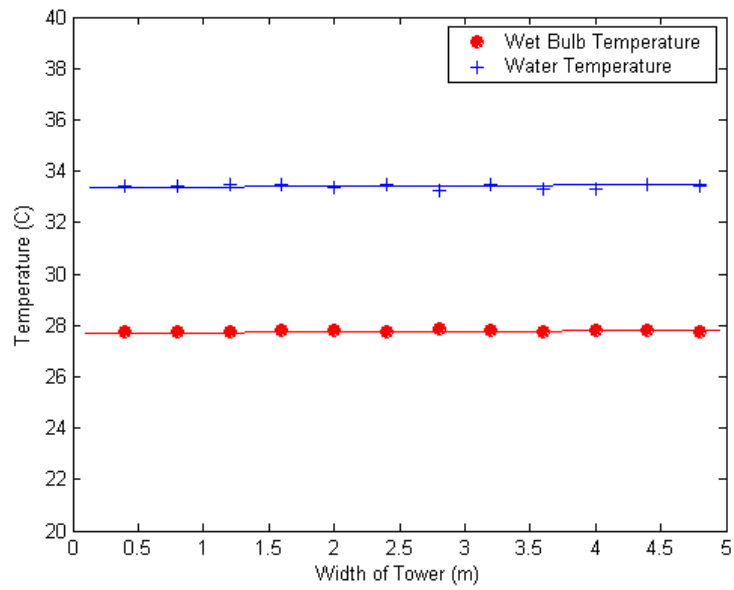


**Figure 4.7** Temperature changes in the X direction

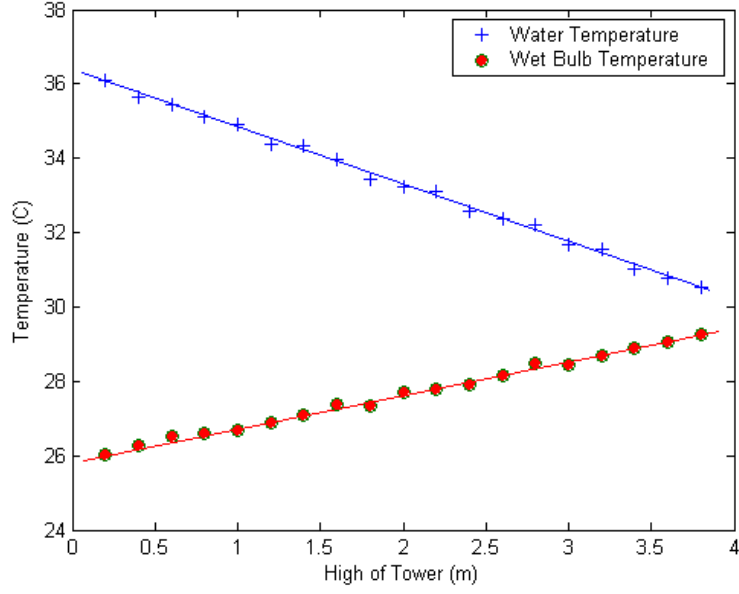


**Figure 4.8 Temperature changes in the Z direction**

In Figure 4.8, the crosses and circles represent the real measured cooling tower water temperature and air wet bulb temperature profiles respectively. Approximating  $T_{ctw}$  by a linear equation between the two boundaries, then any point along the air movement direction can be expressed by:

$$T_{ctw} = T_{CTWS} - \frac{T_{CTWS} - T_{CTWR}}{H} z \quad (4.34)$$

where,  $T_{CTWS}$ ,  $T_{CTWR}$  and  $H$  are cooling tower water supply temperature, cooling tower water return temperature and the total height of the cooling tower, respectively.

Taking the first derivative with respect to  $z$  in Eq. (4.34), we obtain:

$$\frac{\partial T_{ctw}}{\partial z} = -\frac{T_{CTWS} - T_{CTWR}}{H} \quad (4.35)$$

By combining Eqs. (4.33-4.35), the dynamic change of cooling tower water temperature can be expressed as:

$$\rho_{ctw} V_{ctw} C_{pw} \left( \frac{dT_{ctw}}{dt} - u_{ctw} \frac{T_{CTWS} - T_{CTWR}}{H} \right) = -q_{ct} \quad (4.36)$$

### 4.3.3 Dynamic modeling

We can replace  $q_{ct}$  in Eq. (4.36) by Eq. (4.32) to result in:

$$\frac{dT_{ctw}}{dt} + c_{ct,1} \dot{m}_{ctw} (T_{CTWR} - T_{CTWS}) = - \frac{c_{ct,2} \dot{m}_{ctw}^{\ell_{ct}}}{1 + c_{ct,3} \left( \frac{\dot{m}_{ctw}}{\dot{m}_a} \right)^{\ell_{ct}}} (T_{ctw} - T_{wb}) \quad (4.37)$$

where,  $c_{ct,1} = \frac{1}{H \rho_{ctw} A_{ctw}}$ ,  $c_{ct,2} = \frac{b_{ctw} A_{ctw}}{\rho_{ctw} V_{ctw} C_{pw}}$ ,  $c_{ct,3} = \frac{b_{ctw} A_{ctw}}{b_a A_a}$ , and  $\ell_{ct}$  are model parameters.

Finally, the engineering dynamic model using only boundary conditions can be written as:

$$\frac{dT_{CTWR}(t)}{dt} + c_{ct,1} \dot{m}_{ctw}(t) [T_{CTWR}(t) - T_{CTWS}(t)] = - \frac{c_{ct,2} \dot{m}_{ctw}^{\ell_{ct}}(t)}{1 + c_{ct,3} \left( \frac{\dot{m}_{ctw}(t)}{\dot{m}_a(t)} \right)^{\ell_{ct}}} [T_{CTWR}(t) - T_{wb,o}(t)] \quad (4.38)$$

In this model, the variables  $T_{CTWS}$ ,  $T_{wb,o}$ ,  $T_{CTWR}$ ,  $\dot{m}_{ctw}$  and  $\dot{m}_a$  can be estimated or measured [33], while the model parameters  $c_{ct,1-3}$  and  $\ell_{ct}$  are determined in the parameter identification phase (see the next section).

## 4.4 Parameter Identification

This section presents the method to identify the unknown parameters of the developed dynamic models from Sections 4.2 and 4.3. Since the cooling coils have a similar model as cooling towers, we only use the cooling coil model as an example to illustrate the parameter identification procedures.

For the cooling coil model, with the different model characteristic parameters of Eqs.(4.19, 4.20), the parameter identification procedure can be separated into two parts:

(1) *Steady state identification* and (2) *Dynamic identification*.

### Step 1 Steady state identification

At the steady state, the inlet air temperature ( $T_{a,i}$ ) and the inlet chilled water temperature ( $T_{chw,i}$ ) can be considered as constants, consequently  $\frac{dT_{chw,o}(t)}{dt}=0$  and  $\frac{dT_{a,o}(t)}{dt}=0$ . Then we can rewrite Eqs.(4.19) and (4.20) as:

$$\dot{m}_{chw}(T_{chw,o} - T_{chw,i}) = \frac{\frac{c_{cc,2}}{c_{cc,1}} \dot{m}_a^{\ell_{cc}}}{1 + c_{cc,3} \left( \frac{\dot{m}_a}{\dot{m}_{chw}} \right)^{\ell_{cc}}} (T_{a,o} - T_{chw,o}) \quad (4.39)$$

$$\dot{m}_a(T_{a,o} - T_{a,i}) = - \frac{\frac{c_{cc,5}}{c_{cc,4}} \dot{m}_a^{\ell_{cc}}}{1 + c_{cc,3} \left( \frac{\dot{m}_a}{\dot{m}_{chw}} \right)^{\ell_{cc}}} (T_{a,o} - T_{chw,o}) \quad (4.40)$$

By combining Eqs.(4.23) and (4.25), we have:

$$\dot{Q}_{cc} = C_{pw} \dot{m}_{chw} (T_{chw,o} - T_{chw,i}) = -C_{pa} \dot{m}_a (T_{a,o} - T_{a,i}) \quad (4.41)$$

Using Eqs.(4.39) and (4.40), we obtain the following expression:

$$\dot{Q}_{cc} = \frac{C_{pw} \frac{c_{cc,2}}{c_{cc,1}} \dot{m}_a^{\ell_{cc}}}{1 + c_{cc,3} \left( \frac{\dot{m}_a}{\dot{m}_{chw}} \right)^{\ell_{cc}}} (T_{a,o} - T_{chw,o}) = \frac{C_{pa} \frac{c_{cc,5}}{c_{cc,4}} \dot{m}_a^{\ell_{cc}}}{1 + c_{cc,3} \left( \frac{\dot{m}_a}{\dot{m}_{chw}} \right)^{\ell_{cc}}} (T_{a,o} - T_{chw,o}) \quad (4.42)$$

If we denote:

$$c_{cc,6} = C_{pw} \frac{c_{cc,2}}{c_{cc,1}} = C_{pa} \frac{c_{cc,5}}{c_{cc,4}} \quad (4.43)$$

We obtain the steady state model expression:

$$\dot{Q}_{cc} = \frac{c_{cc,6} \dot{m}_a^{\ell_{cc}}}{1 + c_{cc,3} \left( \frac{\dot{m}_a}{\dot{m}_{chw}} \right)^{\ell_{cc}}} (T_{a,o} - T_{chw,o}) \quad (4.44)$$

By employing the identification procedure used by Wang et al [18], we can obtain the parameters  $c_{cc,3}$ ,  $c_{cc,6}$  and  $\ell_{cc}$ .

## Step 2 Dynamic identification

For the dynamic identification, a simple yet robust identification method for a linear process was proposed by Bi et al. [29] which can be used to identify the model parameters.

If we denote  $c_{cc,2} = c_{cc,1} \frac{c_{cc,6}}{C_{chw}}$  and  $c_{cc,5} = c_{cc,4} \frac{c_{cc,6}}{C_{pa}}$ , then we can rewrite Eqs.(4.19)

and (4.20) as:

$$\frac{dT_{chw,o}(t)}{dt} = c_{cc,1} \phi_{chw}(t) \quad (4.45)$$

$$\frac{dT_{a,o}(t)}{dt} = -c_{cc,4} \phi_a(t) \quad (4.46)$$

$$\text{where, } \phi_{chw}(t) = \frac{\frac{c_{cc,6}}{C_{pw}} \dot{m}_a^{\ell_{cc}}(t)}{1 + c_{cc,3} \left[ \frac{\dot{m}_a(t)}{\dot{m}_{chw}(t)} \right]^{\ell_{cc}}} [T_{a,o}(t) - T_{chw,o}(t)] - \dot{m}_{chw}(t) [T_{chw,o}(t) - T_{chw,i}(t - \tau_{chw})]$$

$$\text{and } \phi_a(t) = \frac{\frac{c_{cc,6}}{C_{pa}} \dot{m}_a^{\ell_{cc}}(t)}{1 + c_{cc,3} \left[ \frac{\dot{m}_a(t)}{\dot{m}_{chw}(t)} \right]^{\ell_{cc}}} [T_{a,o}(t) - T_{chw,o}(t)] + \dot{m}_a(t) [T_{a,o}(t) - T_{a,i}(t - \tau_a)].$$

To identify the parameters  $c_{cc,1}$  and  $c_{cc,2}$ , the process has to be reset at a steady state.

Starting from this initial state, at  $t = 0$ , the step inputs of mass flow rate of water and air flow are given for testing. Assume that the interception of the tangent to the step response that has the largest slope with respect to the horizontal axis gives  $H$ , integrate the differential terms in Eqs. (4.45) and (4.46) from  $t = 0$  to  $t = \tau$  ( $\tau \geq H$ ), the

following equation comes into existence:

$$\int_0^\tau \frac{d\mathbf{T}(t)}{dt} dt = \boldsymbol{\theta} \int_0^\tau \boldsymbol{\varphi}(t) dt \quad (4.47)$$

$$\text{where } \boldsymbol{\theta} = \begin{bmatrix} c_{cc,1} & 0 \\ 0 & -c_{cc,4} \end{bmatrix}, \quad \mathbf{T}(t) = \begin{bmatrix} T_{chw,o}(t) \\ T_{a,o}(t) \end{bmatrix} \text{ and } \boldsymbol{\varphi}(t) = \begin{bmatrix} \phi_{chw}(t) \\ \phi_a(t) \end{bmatrix}.$$

With the sampling interval  $T_s$  and  $\tau = nT_s$ , we can define

$\boldsymbol{\Theta}(kT_s) = \Delta \mathbf{T}(kT_s) = \mathbf{T}(kT_s) - \mathbf{T}((k-1)T_s)$ ,  $k = 1, 2, 3 \dots n$ . When the perturbation of the input

variable is very small, we iteratively have following equations:

$$\begin{aligned} \boldsymbol{\Theta}(T_s) &= \boldsymbol{\theta} \int_0^{T_s} \boldsymbol{\varphi}(t) dt \approx \frac{T_s}{2} \boldsymbol{\theta} [\boldsymbol{\varphi}(T_s) + \boldsymbol{\varphi}(0)] \\ \boldsymbol{\Theta}(2T_s) &= \boldsymbol{\theta} \int_{T_s}^{2T_s} \boldsymbol{\varphi}(t) dt \approx \frac{T_s}{2} \boldsymbol{\theta} [\boldsymbol{\varphi}(2T_s) + \boldsymbol{\varphi}(T_s)] \\ &\vdots \\ \boldsymbol{\Theta}(nT_s) &= \boldsymbol{\theta} \int_{(n-1)T_s}^{\tau} \boldsymbol{\varphi}(t) dt \approx \frac{T_s}{2} \boldsymbol{\theta} [\boldsymbol{\varphi}(nT_s) + \boldsymbol{\varphi}((n-1)T_s)] \end{aligned} \quad (4.48)$$

By collecting Eq. (4.48) for all sampled  $T(t)$  after  $t = 0$ , a system of linear equations is obtained as:

$$\boldsymbol{\Psi} \boldsymbol{\theta} = \boldsymbol{\Gamma} + \boldsymbol{\Delta} \quad (4.49)$$

Where  $\boldsymbol{\Delta}$  is the noise or measurement error, and

$$\boldsymbol{\Psi} = \frac{T_s}{2} \begin{bmatrix} [\boldsymbol{\varphi}(T_s) + \boldsymbol{\varphi}(0)]^T \\ [\boldsymbol{\varphi}(2T_s) + \boldsymbol{\varphi}(T_s)]^T \\ \vdots \\ [\boldsymbol{\varphi}(nT_s) + \boldsymbol{\varphi}((n-1)T_s)]^T \end{bmatrix}, \quad \boldsymbol{\Gamma} = \begin{bmatrix} \boldsymbol{\Theta}(T_s) \\ \boldsymbol{\Theta}(2T_s) \\ \vdots \\ \boldsymbol{\Theta}(nT_s) \end{bmatrix}, \quad \boldsymbol{\Delta} = \begin{bmatrix} \boldsymbol{\delta}(T_s) \\ \boldsymbol{\delta}(2T_s) \\ \vdots \\ \boldsymbol{\delta}(nT_s) \end{bmatrix}$$

The best estimate of  $\hat{\boldsymbol{\theta}}$  can be found using the standard least squares method as in

Eq.(4.50), and the best estimates of  $c_{cc,1}$  and  $c_{cc,2}$  can then be obtained from  $\hat{\boldsymbol{\theta}}$ .

$$\hat{\theta} = (\Psi^T \Psi)^{-1} \Psi^T \Gamma \quad (4.50)$$

Since both cooling coil and cooling tower models are based on similar modeling methodologies and have similar model expressions, this 2-step procedure can be applied to cooling tower models as well. For a cooling tower, at the steady state, the time derivative  $\frac{dT_{CWR}(t)}{dt} = 0$ . Then we can rewrite Eq.(4.38) as:

$$\dot{m}_{ctw} (T_{CTWR} - T_{CTWS}) = - \frac{C_{ct,2} \dot{m}_{ctw}^\ell}{C_{ct,1}} (T_{CTWR} - T_{wb,o}) \quad (4.51)$$

$$1 + c_{ct,3} \left( \frac{\dot{m}_{ctw}}{\dot{m}_a} \right)^\ell$$

By employing the method proposed in [33], the heat rejection rate of the cooling tower ( $\dot{Q}_{ct}$ ) can be calculated with the cooling tower water flow rate ( $\dot{m}_{ctw}$ ) and the temperature difference between the cooling tower supply and return water, and the equation is given as:

$$\dot{Q}_{ct} = C_{pw} \dot{m}_{ctw} (T_{CTWS} - T_{CTWR}) \quad (4.52)$$

Substituted by Eq.(4.51), we have the following expression:

$$\dot{Q}_{ct} = \frac{C_{pw} \frac{C_{ct,2} \dot{m}_{ctw}^\ell}{C_{ct,1}}}{1 + c_{ct,3} \left( \frac{\dot{m}_{ctw}}{\dot{m}_a} \right)^\ell} (T_{CTWR} - T_{wb,o}) \quad (4.53)$$

If we denote:

$$c_{ct,4} = C_{pw} \frac{C_{ct,2}}{C_{ct,1}} \quad (4.54)$$

We obtain the steady state model expression:

$$\dot{Q}_{ct} = \frac{c_{ct,4} \dot{m}_{ctw}^{\ell_{ct}}}{1 + c_{ct,3} \left( \frac{\dot{m}_{ctw}}{\dot{m}_a} \right)^{\ell_{ct}}} (T_{CTWR} - T_{wb,o}) \quad (4.55)$$

Employing the identification procedure proposed in [121], we can obtain the parameters  $c_{ct,3}$ ,  $c_{ct,4}$  and  $\ell_{ct}$ .

Likewise, for a cooling tower, with the estimated  $c_{ct,4}$ , we can denote  $c_{ct,2} = c_{ct,1} \frac{c_{ct,4}}{C_{pw}}$ .

Then, Eq. (4.38) can be formulated as a nonlinear first-order model:

$$\frac{dT_{CTWR}(t)}{dt} = c_{ct,1} \phi_{ctw}(t) \quad (4.56)$$

$$\text{with } \phi_{ctw}(t) = - \frac{\frac{c_{ct,4}}{C_{pw}} \dot{m}_{ctw}^{\ell_{ct}}(t)}{1 + c_{ct,3} \left[ \frac{\dot{m}_{ctw}(t)}{\dot{m}_a(t)} \right]^{\ell_{ct}}} [T_{CTWR}(t) - T_{wb,o}(t)] - \dot{m}_{ctw}(t) [T_{CTWS}(t) - T_{CTWR}(t)] .$$

So that the dynamic identification method introduced in *Step 2* can be applied to determine the other two model parameters  $c_{ct,1}$  and  $c_{ct,2}$ .

With the parameter identification methods mentioned above, we can obtain the model parameters for the cooling coil and the cooling tower. The next section presents the model validation experiments and corresponding testing results for the cooling coil model and the cooling tower model respectively.

#### 4.5 Model Validation

A number of experimental environments were built to validate the dynamic models proposed for the cooling coil and the cooling tower individually, applying the parameter identification method described above.

#### 4.5.1 Model validation of a cooling coil

The cooling coil used in the model validations has face dimensions of 0.25 m × 0.25 m, four tube rows and 328 aluminum fins per meter, as shown in Figure 4.9. Fresh air is used to keep a relatively constant inlet air temperature.

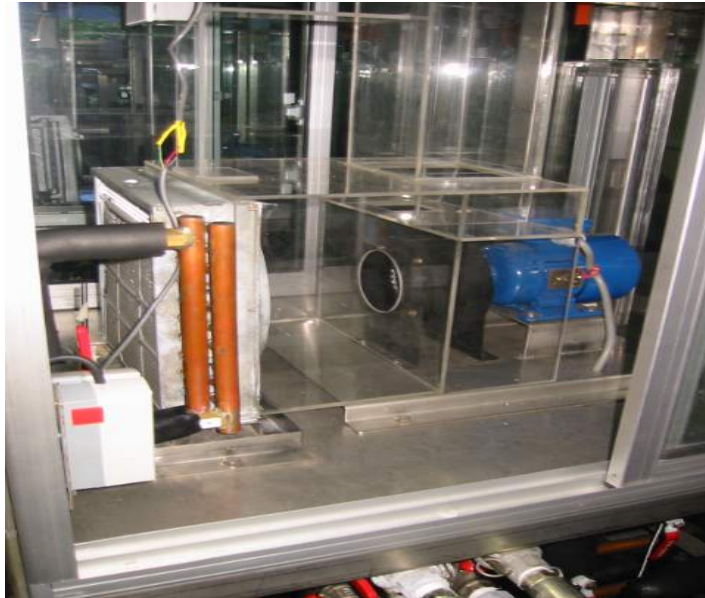


**Figure 4.9 An AHU and a cooling coil of the pilot plant**

The measurement signals for the experiment are the water and air flow rates, on-coil and off-coil air dry-bulb/web-bulb temperatures, and cooling coil inlet and outlet water temperatures. The experiment is conducted under the following conditions:

1. Fresh air is used to keep a relatively constant inlet air temperature.
2. The chilled water supply temperature is changing slowly; the cooling load variation is achieved through the air and water flow rates.

In order to study the dynamic relationships between the parameters and the cooling coil's heat exchange, real time varying conditions for testing are given (Figure 4.10).

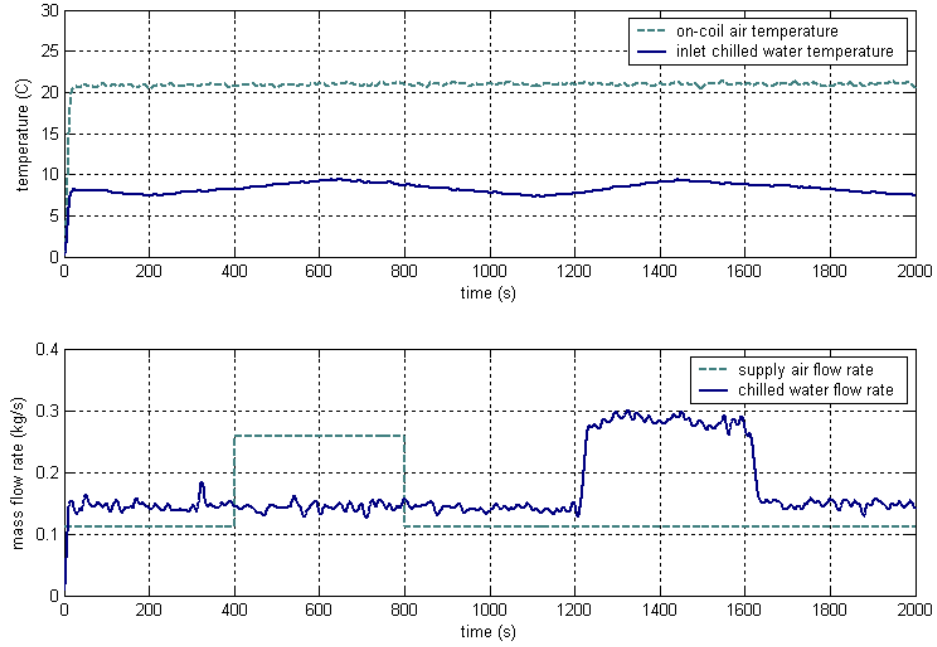


**Figure 4.10 Time varying temperature and mass flow rate of inlet air and chilled water**

Through *Step1* and *Step 2*, we can obtain the parameters  $c_{cc,1} - c_{cc,5}$ , and  $\ell_{cc}$  from experimental fitting, these are listed in Table 4.1.

**Table 4.1 Estimated parameters of the six-parameter and five-parameter model ( $\ell = 0.8$ )**

Model	Load range (kw)	$\ell_{cc}$	$c_{cc,1}$	$c_{cc,2}$	$c_{cc,3}$	$c_{cc,4}$	$c_{cc,5}$
Six-parameter	0.60-1.20	0.6078	6.7142	0.7412	0.7021	8.9936	3.9722
Five-parameter	0.60-1.20	0.8	6.9431	1.1993	0.8021	9.3274	6.4431

The results calculated from the six-parameter model and the simplified five-parameter model are compared with the measured data in Figures 4.11 and 4.12, respectively.

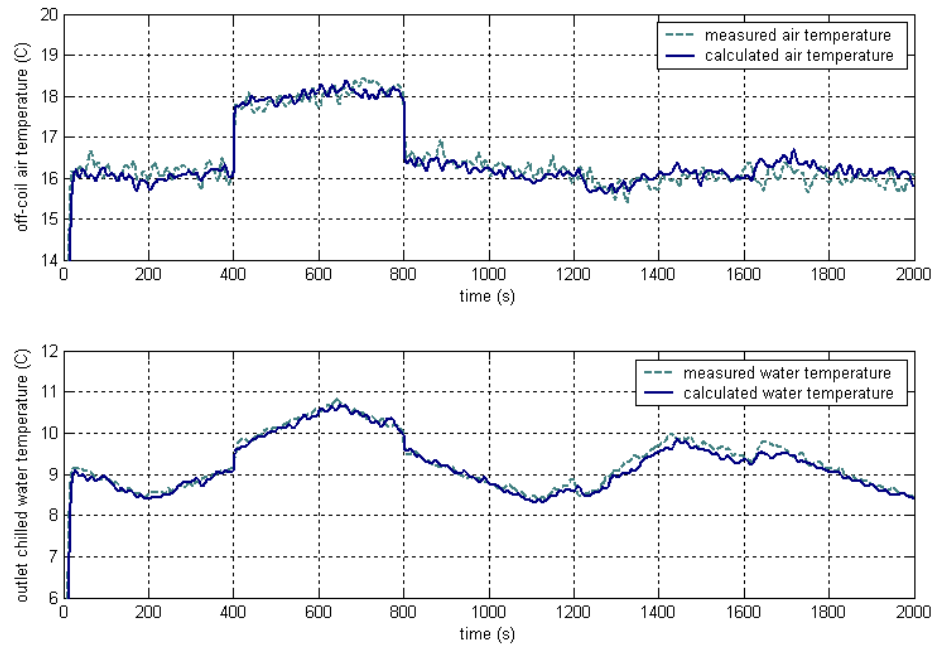


**Figure 4.11 Comparison of six-parameter model calculations with the measured data**

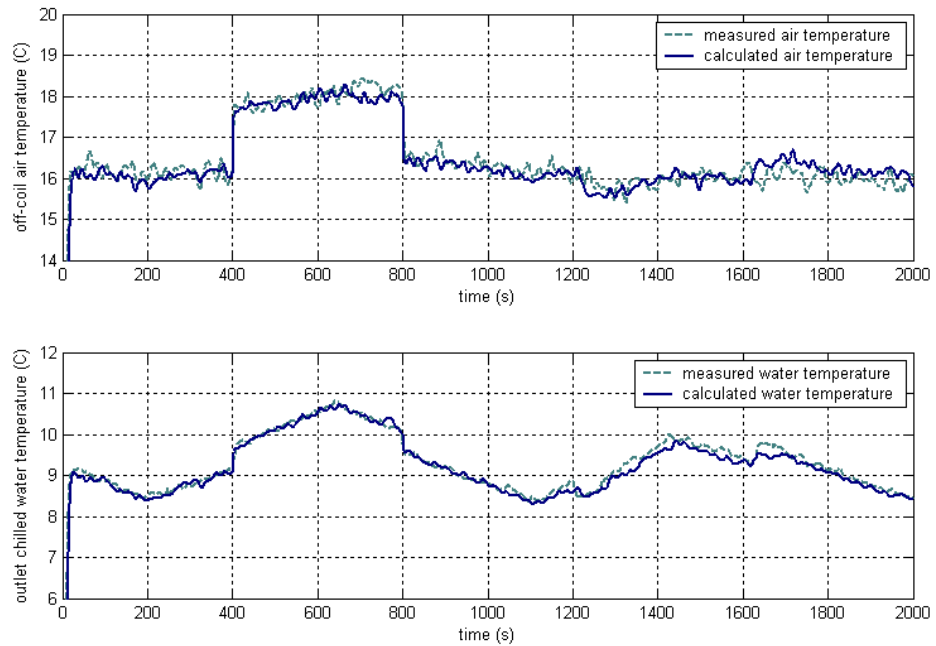


**Figure 4.12 Comparison of five-parameter model calculations with the measured data**

Finally, to quantitatively evaluate the accuracy of the model, the calculated results of the model are examined through the root mean square error (RMS) defined as:

$$\text{RMS} = \sqrt{\frac{\sum_{i=1}^N (T_{\text{calculation},i} - T_{\text{experiment},i})^2}{N}}$$

where  $N$  is the number of fitted points,  $T_{\text{calculation},i}$  is the temperature of point  $i$  predicted by the model and  $T_{\text{experiment},i}$  is the temperature of point  $i$  acquired from experimental data. The performances of the two models are given in Table 4.2.

**Table 4.2 Performances of the six-parameter model and the five-parameter model**

Model	RMS (off-coil air temperature)	RMS (chilled water temperature)
Six-parameter	0.236 °C	0.132 °C
Five-parameter	0.285 °C	0.172 °C

From the experimental results, we can conclude:

1. The proposed dynamic model accurately reflects the details of the transient performance of the cooling coil. With the constant parameters, the models work appropriately in a relatively wide operating range: both the difference of the outlet chilled water temperature and the off-coil air temperature are about 3 °C, which is the normal operating range for a cooling coil.
2. The linear approximation of the dry and wet cooling coil does not generate a significant error (RMS index) but dramatically simplifies the calculation procedure as compared to complex numerical modeling methodologies. Of course, the proposed cooling coil model may work even better in the totally dry or totally wet regime.
3. The responses of off-coil air and outlet chilled water temperature naturally have a time delay with respect to the changes of the on-coil air and inlet chilled water temperature. The testing results do not show this obviously, because the total lengths of the tubes and the cooling coil depth, i.e.  $\xi$  and  $l$ , are relatively small versus the velocity of the cooling water and airflow being  $u_{chw}$  and  $u_a$ .

4. The six-parameter model results in a little better performance over the entire operation range but with the price of more complicated calculations compared to the five-parameter model. Therefore, it may be worth sacrificing some accuracy for simplifying the parameter identification procedure in real engineering applications.

#### 4.5.2 Model validation of a cooling tower

In order to validate the proposed cooling tower model, a cooling tower operating in Grand Hyatt Singapore hotel HVAC system with the specifications as given in Section 3.5 was used.

The measurement signals for the experiments are the cooling tower water and air flow rates, ambient air dry-bulb/wet-bulb temperatures, and cooling tower water supply and return temperatures. To analyze the transient characteristic of the cooling tower, we set the sampling rate of each variable to one second, and the experiments are conducted under the following conditions:

1. Ambient air keeps a relatively constant wet bulb temperature in a short time period, e.g. 1 hour.
2. The cooling tower water supply temperature is changing slowly; the heat rejection variation is achieved only through the air and water flow rates.

By identification procedure *Step1* and *Step 2*, we can obtain the parameters  $c_{ct,1} - c_{ct,3}$ , and  $\ell_{ct}$  from an experimental fitting, and these are listed in Table 4.3.

**Table 4.3 Estimated parameters of the four-parameter model**

Load range (kW)	$\ell_{ct}$	$c_{ct,1}$	$c_{ct,2}$	$c_{ct,3}$
796.1~2290kW	1.14	2.53	13.12	20.01

A step response analysis was carried out through a change from the initial steady-state condition in each of the following inputs: water flow, air flow and cooling tower

water supply temperatures. The modeled data and measure data plots of cooling tower water return temperature ( $T_{CTWR}$ ) are compared in Figures 4.13-4.15.

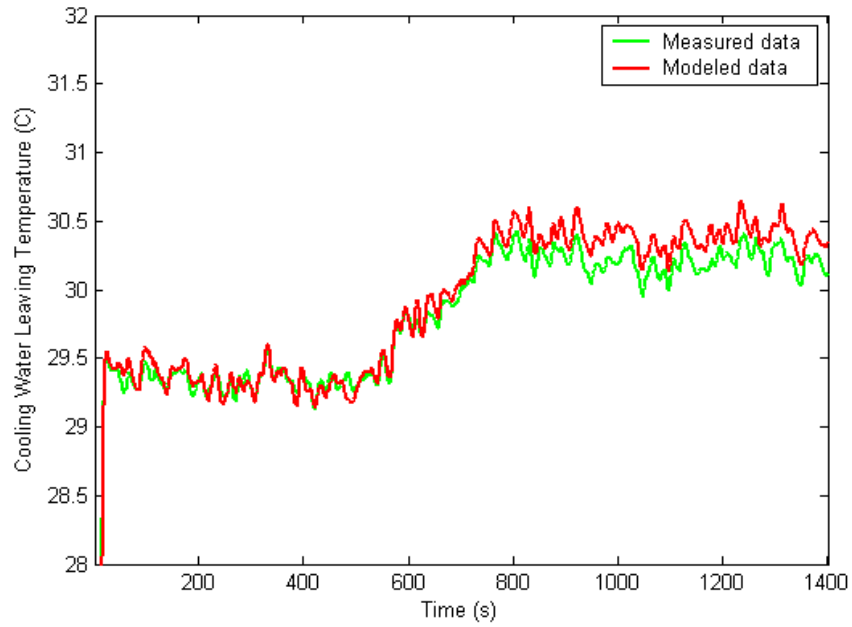


**Figure 4.13 Increase of the mass flow rate of water from 48kg/s to 80 kg/s**

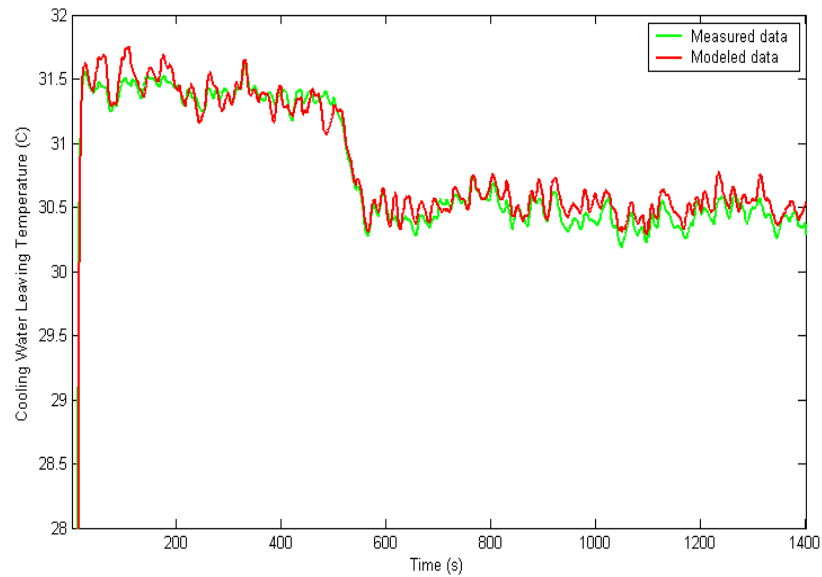


**Figure 4.14 Increase of the mass flow rate of inlet air from 175kg/s to 250 kg/s**

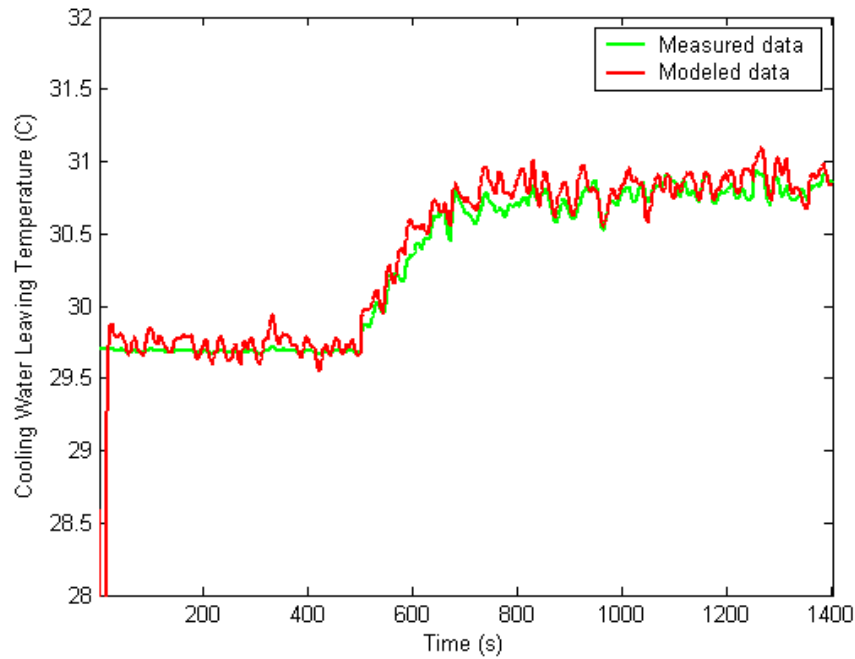


**Figure 4.15 Cooling tower water supply temperature step rise from 35.5 to 38.5 C**

To quantitatively assess the effectiveness of the model, the calculated results of the model are evaluated through the root mean square error (RMS) given in Table 4.4.

**Table 4.4 Performances of the model in different scenarios**

Scenarios	increase in $\dot{m}_{cw}$	increase in $\dot{m}_a$	$T_{cwl}$ increase (35.5 to 38.5 °C )
RMS ( $T_{CTWR}$ )	0.2867 C°	0.2436 C°	0.1972 C°

The plots illustrate that the model captures the general speed and shape of the responses of each of the outputs. Likewise, the RMS index indicates that the model is an accurate representation of the major transient dynamics of the system.

The observations from the experimental results are summarized as follows:

1. The proposed dynamic model accurately reflects the details of the transient performance of the cooling tower. With constant parameters, the models work in a relatively wide operation range: the temperature difference of supply cooling tower

water and return cooling tower water, is about 4 °C as well as the range is about 8 °C, which is the normal operating condition for the cooling towers.

2. The linear approximation of the convection and the evaporation cooling process does not generate a significant error (RMS index) but dramatically simplified the calculation procedure compared to complex numerical modeling methodologies.

#### ***4.6. Summary***

In this chapter, a simple, low order and non-linear dynamic model for a cooling coil and a cooling tower were derived based on physical analysis of the heat transfer mechanism and the energy balance with reasonable approximations. The effects of sensible and latent cooling in the heat and mass transfer behavior were also taken into consideration. Experimental results were provided to show that the models can achieve accurate transient performance prediction over a wide operating range. Since the parameters of the developed models can be obtained from the manufacturers' specifications or experimental data without going into detailed physical properties of a cooling coil and cooling tower, it can be easily applied to practical applications of a HVAC system local controls for simulation or controller design or tuning purpose.

# **CHAPTER 5 COMPOSITE MODEL OF REFRIGERATION CYCLES**

## ***5.1 Introduction***

All those physical and empirical modeling methodologies reviewed in Chapter 2 could be used to develop static models for the refrigeration cycle to simulate the steady-state performance. However, there are few composite refrigeration cycle models suitable for real-time model-based system optimization of the building HVAC system which has guaranteed reliability over a wider range of operating conditions yet requiring less computational effort.

To address this need, this chapter proposes a composite model for the refrigeration cycle of a water-cooled centrifugal chiller. The proposed model was developed on top of the hybrid component models of the refrigeration cycle. The developed composite model is validated by using the performance data of an existing chiller running under a wide range of ambient and time varying load conditions.

## 5.2 Composite Model

As shown in Figure 5.1, the refrigeration cycle in a vapor-compression water-cooled chiller consists of four major components i.e. compressor, evaporator, condenser, and expansion valve.

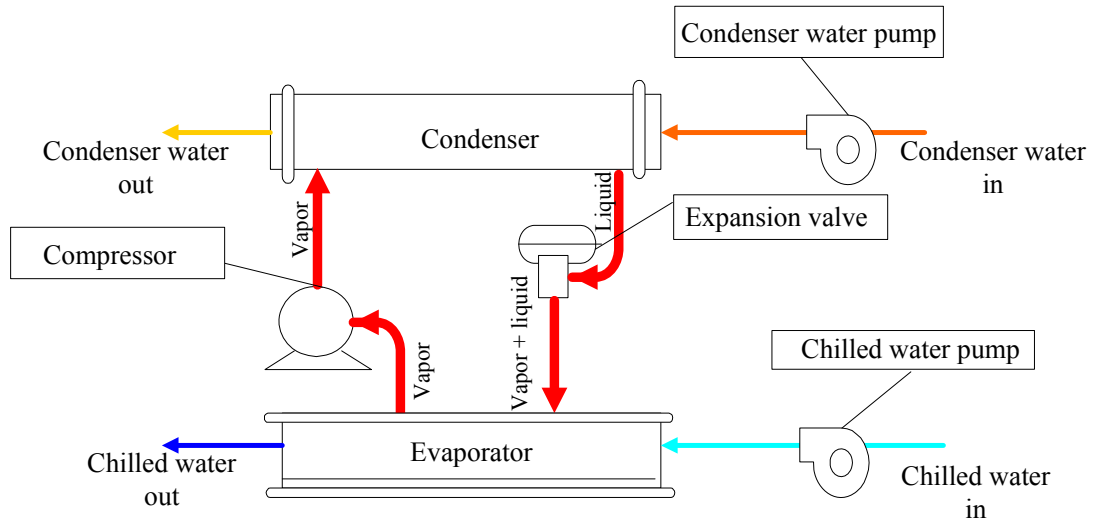


**Figure 5.1 Schematic diagram of a vapour-compression water –cooled chiller**

Figure 5.2 describes the thermodynamics of the refrigeration cycle. The saturated vapor refrigerant leaves the evaporator at point 1. From point 1 to point 1' superheating occurs both in the evaporator due to conduction through the divider plate and in the suction line to the compressor. Through polytropic compression, this process increases the refrigerant pressure to the state point 2, then the refrigerant is desuperheated in the condenser to a saturated condition at point 2'. From point 2' the refrigerant is condensed to the saturated liquid state at point 3'. From point 3' to point 3 the fluid refrigerant is further cooled to the subcooled condition. And then the subcooled liquid refrigerant expands isentropically to point 4 before entering the evaporator. If the pressure loss in the refrigerant pipelines and the compressor inlet guide vane is ignored, then  $P_1$ ,  $P_{1'}$ ,  $P_4$ ,  $P_{4'}$  can be regarded to be equal to the evaporating pressure ( $P_{ev}$ ), and  $P_2$ ,  $P_{2'}$ ,  $P_3$ ,  $P_{3'}$  can be regarded to be equal to the condensing pressure ( $P_{cd}$ ), respectively.

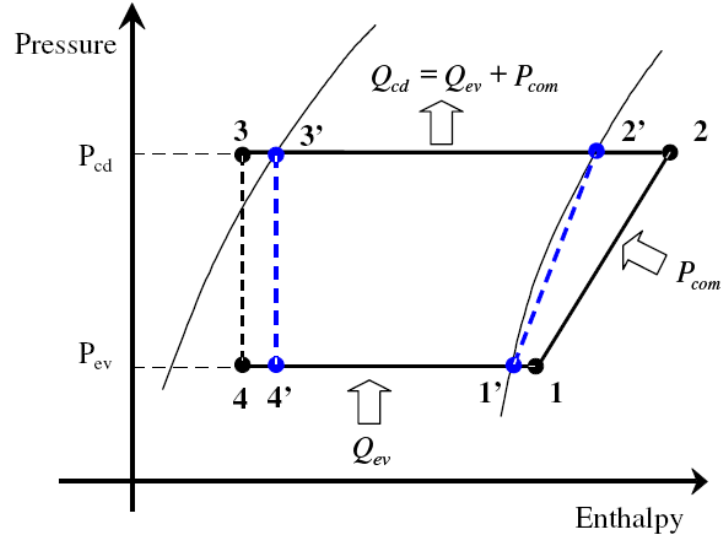


**Figure 5.2 Thermodynamics of the refrigeration cycle**

The performance of the refrigeration cycle of a chiller is determined by the performance of its components: evaporator, compressor, throttling device and condenser. Thus, it is critical to understand the processes of these components as well as to formulate the relationship between the compressor power consumption and the related operating variables of individual components, e.g., chilled water temperature entering the evaporator ( $T_{chwe}$ ), condenser water supply temperature ( $T_{CWS}$ ), part load ratio (PLR), evaporating pressure ( $P_{ev}$ ) and condensing pressure ( $P_{cd}$ ), etc. The following sections will describe the proposed refrigeration cycle model broken into individual components with their corresponding processes and adopted models.

### 5.2.1 Evaporator model

The evaporator is one of the major components of the refrigeration cycle performing as heat exchanger, and has a critical impact on the performance of the evaporation process. Inside the evaporator, the refrigerant evaporates to extract heat from the chilled water flows through the chiller. A schematic diagram of an evaporation process is shown in Figure 5.3, which consists of two loops: the refrigerant loop and the chilled water loop.

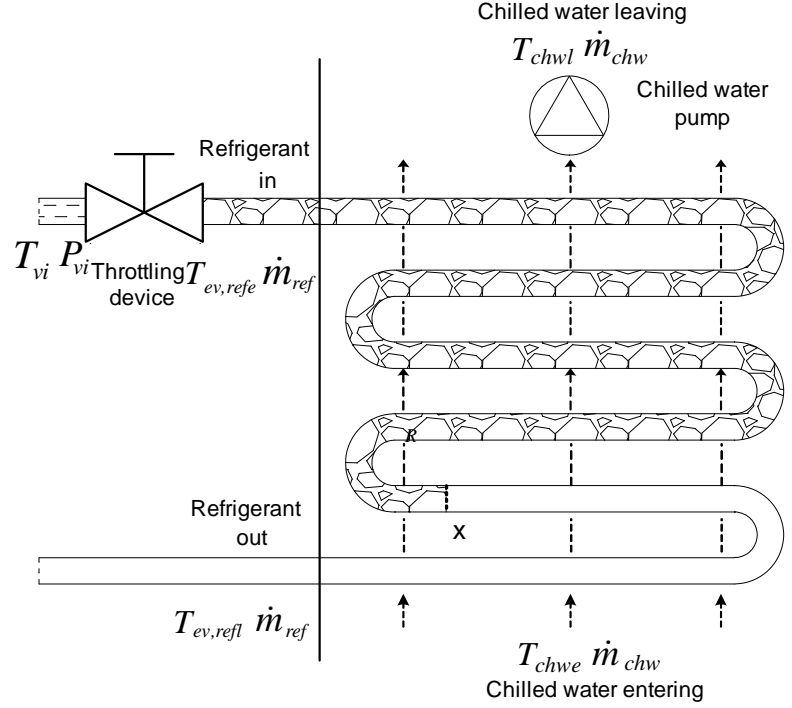


**Figure 5.3 Schematic diagram of evaporator**

In the refrigerant loop, the liquid refrigerant before entering the throttling device is of temperature ( $T_{vi}$ ), and inlet pressure ( $P_{vi}$ ), which are assumed to be equal to  $T_{ev,refe}$  and condensing pressure ( $P_{cd}$ ), respectively. After passing through the throttling device, it enters into the evaporator with reduced pressure causing it to boil and flush into vapor. Because the boiling point of the refrigerant is lower than the temperature of the chilled water surrounding the coils, heat is transferred from the chilled water to the refrigerant through the metal tube wall, and the refrigerant continues to evaporate at a low-pressure. At the position  $x$ , as shown in Figure 5.3, all the liquid has been vaporated. By the time the vapor refrigerant reaches the outlet of the evaporator, it is superheated to several degrees higher than its saturation temperature.

In the chilled water loop, the heat transfer is a single-phase forced convection process, the forced chilled water of entering temperature ( $T_{chwe}$ ), and mass flow rate ( $\dot{m}_{chw}$ ), flows through the evaporator. At the outlet of the evaporator, the temperature of the chilled water drops to  $T_{chwl}$  as a result of heat transfer with the refrigerant.

In the refrigerant loop, the heat exchange depends not only on heat convection but also phase change. The phase change from liquid to vapor makes the phenomena of heat transfer considerably more complex than those without phase change. The mass flow rate, the latent heat of vaporization, the pressure, and possibly other properties of the vapor all contribute to the effectiveness of the boiling process. According to the refrigerant physical characteristics, the evaporator can be divided into two sections, i.e., a two-phase section and a superheated vapor section, as shown in Figure 5.4.

**Figure 5.4 Heat transfer mechanism of evaporator**

A hybrid modeling approach was proposed by Cai [18, 121], to model heat exchangers with a single-phase fluid such as cooling coils and cooling towers. The

model validation showed that the modeling approach is robust and gives a better match to real performance over the entire operating range compared with other modeling methods. Based on this approach, Ding et al. [122] developed a hybrid model of an evaporator, which can correlate the heat transfer on both the refrigerant and chilled water sides, with the following expression for the heat rejection rate in the evaporator:

$$\dot{Q}_{ev} = \frac{(h_{ev,ref,sat} - h_{ev,refe})\dot{m}_{ref} + c_{ev,1}\dot{m}_{ref}^{c_{ev,3}}(T_{chwe} - T_{ev,ref,sat})}{1 + c_{ev,2}\left(\frac{\dot{m}_{ref}}{\dot{m}_{chw}}\right)^{c_{ev,3}}} \quad (5.1)$$

where  $h_{ev,ref,sat}$ ,  $h_{ev,refe}$  and  $T_{ev,ref,sat}$  are the saturation enthalpy of the refrigerant vapor, enthalpy of the entering refrigerant and the saturation temperature of the refrigerant, respectively. And  $T_{chwe}$ ,  $\dot{m}_{ref}$ ,  $\dot{m}_{chw}$ , are the entering chilled water temperature, the refrigerant mass flow rate and the chilled water mass flow rate, respectively.

In Eq. (5.1), the fluid property factors and evaporator geometric characteristics are lumped in to three characteristic constant model parameters  $c_{ev,1}$  to  $c_{ev,3}$ . Therefore, the total heat transfer rate of the evaporator can be simply and accurately described by a function of three fundamental operating variables, i.e.,  $T_{chwe}$ ,  $\dot{m}_{ref}$ ,  $\dot{m}_{chw}$  and the thermal parameters  $T_{ev,ref,sat}$ ,  $h_{ev,ref,sat}$  and  $h_{ev,refe}$ .

In practice, the refrigerant temperature entering the evaporator ( $T_{ev,refe}$ ), the chilled water temperature entering the evaporator ( $T_{chwe}$ ) and the evaporating pressure ( $P_{ev}$ ) can be measured directly using temperature or pressure sensors. For the other variables which are difficult to be measured directly, the following indirect methods are suggested in determining the model of Eq. (5.1).

1. The chilled water mass flow rate ( $\dot{m}_{chw}$ ) through the evaporator can be obtained by measuring the pressure difference across the evaporator. From

$$\Delta P_{chw} = a_0 + a_1 \dot{m}_{chw} + a_2 \dot{m}_{chw}^2 \quad (5.2)$$

where  $a_0$ ,  $a_1$ ,  $a_2$  are unknown parameters to be determined through specification data or on line testing,  $\Delta P_{chw}$  and  $\dot{m}_{chw}$  are the pressure difference and the mass flow rate of the chilled water across the evaporator, respectively. The following mass flow rate can be derived:

$$\dot{m}_{chw} = \frac{-a_1 + \sqrt{a_1^2 - 4a_2(a_0 - \Delta P_{chw})}}{2a_2} \quad (5.3)$$

2. The refrigerant mass flow rate ( $\dot{m}_{ref}$ ) can either be measured directly or indirectly. For direct measurement, a flow meter is placed before the throttle device. If an indirect method is used, the cooling load  $\dot{Q}_{ev}$  can be firstly obtained from the energy balance of the chilled water:

$$\dot{Q}_{ev} = C_{pw} \dot{m}_{chw} (T_{chwe} - T_{chwl}) \quad (5.4)$$

where  $C_{pw}$ ,  $T_{chwe}$ , and  $T_{chwl}$  are the specific heat, the chilled water temperature at evaporator inlet and outlet, respectively; and then the refrigerant mass flow rate ( $\dot{m}_{ref}$ ) can then be estimated as:

$$\dot{m}_{ref} = \frac{\dot{Q}_{ev}}{h_{ev,refl} - h_{ev,refe}} \quad (5.5)$$

where  $h_{ev,refe}$  and  $h_{ev,refl}$  are the entering and leaving refrigerant enthalpies, respectively, which can be obtained from thermodynamics tables of the refrigerant based on the entering/leaving temperature and pressure imposed on the refrigerant.

3. There are two methods to determine the saturation temperature ( $T_{ev,ref,sat}$ ), the saturation vapor enthalpy ( $h_{ev,ref,sat}$ ) and the entering enthalpy ( $h_{ev,refe}$ ) of the refrigerant:

1) Directly looking-up the fluid property database to find their values according to the measured saturated pressure and inlet pressure, which are assumed to be equal to  $P_{ev}$ , and measured inlet temperature ( $T_{vi}$ ), which is assumed to be equal to  $T_{ev,refe}$ ; 2) Using the following polynomial equations to calculate their values respectively:

$$T_{ev,ref,sat}(P_{ev}) = \sum_{i=0}^n a_i P_{ev}^i \quad (5.6a)$$

$$h_{ev,ref,sat}(P_{ev}) = \sum_{i=0}^n b_i P_{ev}^i \quad (5.6b)$$

$$h_{ev,refe}(P_{ev}, T_{ev,refe}) = \sum_{i=0}^n \sum_{j=0}^m c_{ij} P_{ev}^i T_{ev,refe}^j \quad (5.6c)$$

where the coefficients  $a_i$ ,  $b_i$  and  $c_{ij}$  can be calculated off line through curve fitting of the look-up table with the measureable  $P_{ev}$  and  $T_{ev,refe}$  respectively.

As the saturation refrigerant vapor enthalpy ( $h_{ev,ref,sat}$ ) and the inlet enthalpy of the refrigerant ( $T_{ev,ref,sat}$ ) can be uniquely determined by the evaporating pressure ( $P_{ev}$ ) and the refrigerant temperature entering the evaporator ( $T_{ev,refe}$ ), the heat transfer capacity from the model depends on five independent variables: the entering temperature of the refrigerant ( $T_{ev,refe}$ ) and chilled water ( $\dot{m}_{chwe}$ ), the mass flow rate of the refrigerant ( $\dot{m}_{ref}$ ) and the chilled water ( $\dot{m}_{chw}$ ), and the evaporating pressure ( $P_{ev}$ ). This makes the impact of each individual variable and combination of several variables on the evaporator performance to be conveniently analyzed. This hybrid evaporator model focuses on the characteristics of an existing evaporator and the relationships among heat extraction rates, refrigerant mass flow rates, chilled water mass flow rates, refrigerant entering temperature, and the chilled water temperature entering the evaporator under different

circumstances. Furthermore, as the working points of energy consumption devices for both refrigerant and chilled water are revealed in the model, it can be used as the constraint conditions in the optimization of a HVAC system operation.

### 5.2.2 Compressor model

The compressor is the heart of the refrigeration cycle. In this study, the chiller system is equipped with a hermetic variable speed centrifugal compressor. The volumetric flow rate of the refrigerant at the impeller outlet ( $V_{ref}$ ) can be evaluated from [123]:

$$V_{ref} = \frac{A_{imp}}{U_{imp}} \tan(\beta) \left[ \frac{\xi}{\xi-1} P_{ev} v_2 \left( \pi^{(\xi-1)/\xi} - 1 \right) - U_{imp}^2 \right] \quad (5.7a)$$

The angle ( $\beta$ ), outlet area ( $A_{imp}$ ) and tip speed ( $U_{imp}$ ) of the impeller can be determined from the manufacturer's product specification data or by using the parameter identification program given by Bourdouxhe et al. [123].

The system pressure ratio  $\pi$  calculated by Eq. (5.7b) accounts for the throttling rate  $\delta$  which is equal to 1 at full load. Under part load conditions,  $\delta$  is less than 1, which indicates an increase in the system pressure ratio.

$$\pi = \frac{P_{cd}}{\delta P_{ev}} \quad (5.7b)$$

Aiming to reduce the difficulty of determining the instantaneous  $\delta$  when the compressor is working at different part load ratios, it is reasonable to correlate  $\dot{m}_{ref}$  with its maximum  $\dot{m}_{ref,max}$ , at full load condition by a ratio  $\gamma$ , as shown in Eq. (5.8). The ratio  $\gamma$  is assumed to be a function of refrigeration cycle part load ratio (PLR), as shown in Eq. (5.9), where the constants  $f_1$  to  $f_3$  are identified based on the calculated  $\dot{m}_{ref}$  with

respect to various operating conditions, and the value of  $\dot{m}_{ref,max}$  can be calculated with Eq.(5.10)[123].

$$\dot{m}_{ref} = \gamma \dot{m}_{ref,max} \quad (5.8)$$

$$\gamma = f_1 \text{PLR}^2 + f_2 \text{PLR} + f_3 \quad (5.9)$$

$$\dot{m}_{ref,max} = \frac{V_{ref}}{v_2} \left[ 1 + \frac{\xi-1}{2\xi} \cdot \frac{1}{P_{ev} v_2} \cdot \left( U_{imp}^2 - \frac{V_{ref}^2}{A_{imp}^2 \sin^2(\beta)} \right) \right]^{\frac{1}{\xi-1}} \quad (5.10)$$

The actual compressor power ( $P_{com}$ ) can then be calculated from Eq.(5.11), which has three items  $W_{in}$ ,  $\eta_{pol}$  and  $\eta_m$ . The polytropic compression efficiency ( $\eta_{pol}$ ) can be expressed by Eq.(5.12a), an empirical polynomial of the part load ratio (PLR). This empirical polynomial and its parameters ( $f_{4-6}$ ) can be determined by correlating the modeled results of the mechanical work input ( $W_{in}$ ) expressed by Eq.(5.12b) to the measurable compressor performance data under part load conditions [47], while the combined motor and transmission efficiency ( $\eta_m$ ) is often considered as a constant.

$$P_{com} = \frac{W_{in}}{\eta_{pol} \eta_m} \quad (5.11)$$

Where

$$\eta_{pol} = f_4 \text{PLR}^2 + f_5 \text{PLR} + f_6 \quad (5.12a)$$

and

$$W_{in} = \dot{m}_{ref} P_{ev} v_2 \frac{\xi}{\xi-1} \left( \left( \frac{P_{cd}}{\delta P_{ev}} \right)^{\frac{\xi-1}{\xi}} - 1 \right) \quad (5.12b)$$

Therefore, the power consumption model of the compressor can be expressed as:

$$P_{com} = \frac{(f_1 \text{PLR}^2 + f_2 \text{PLR} + f_3) \dot{m}_{ref, \max} P_{ev} v_2 \frac{\xi}{\xi-1} \left( \left( \frac{P_{cd}}{\delta P_{ev}} \right)^{\frac{\xi-1}{\xi}} - 1 \right)}{(f_4 \text{PLR}^2 + f_5 \text{PLR} + f_6) \eta_m} \quad (5.13)$$

By substituting the evaporator model (Eq.(5.1)) and compressor power consumption model (Eq.(5.13)), the coefficient of performance (COP) of the refrigeration cycle can be calculated as:

$$COP = \frac{Q_{ev}}{P_{com}} = \frac{\left[ (h_{ev,ref,sat} - h_{ev,refe}) \dot{m}_{ref} + c_{ev,1} \dot{m}_{ref}^{c_{ev,3}} (T_{ev,chw} - T_{ev,ref,sat}) \right] \cdot \eta_m (f_4 \text{PLR}^2 + f_5 \text{PLR} + f_6)}{\left[ 1 + c_{ev,2} \left( \frac{\dot{m}_{ref}}{\dot{m}_{chw}} \right)^{c_{ev,3}} \right] \cdot (f_1 \text{PLR}^2 + f_2 \text{PLR} + f_3) \dot{m}_{ref, \max} P_{ev} v_2 \frac{\xi}{\xi-1} \left[ \left( \frac{P_{cd}}{\delta P_{ev}} \right)^{\frac{\xi-1}{\xi}} - 1 \right]} \quad (5.14)$$

### 5.2.3 Expansion valve model

The expansion valve is modeled as a static component while the valve is assumed to be isenthalpic. The refrigerant mass flow rate ( $\dot{m}_{ref}$ ) is calculated using the standard orifice equation in Eq.(5.15) based on the flow coefficient  $C_v$ . It is a widely used approach in expansion valve modeling. The flow coefficient curve is provided by the manufacturers and it is considered as a function of the expansion valve's steps, while the refrigerant density ( $\rho_{cd}$ ) and the exponent ( $n$ ) is considered to be a constant.

$$\dot{m}_{ref} = C_v [\rho_{cd} (P_{cd} - P_{ev})]^n \quad (5.15)$$

### 5.2.4 Condenser model

The condenser, as a key component of the condensation process where the refrigerant changes phase from vapour to liquid through rejecting heat to the surrounding media, has critical impact to the overall system operation.

A schematic diagram of a condenser is shown in Fig. 5.5, which consists of two loops: the refrigerant loop and the condenser water loop. In the refrigerant loop, imposed by the high temperature ( $T_{cd,refe}$ ), and high pressure ( $P_{cd}$ ), the refrigerant is in a vapor phase entering the condenser with a mass flow rate ( $\dot{m}_{ref}$ ). Because the refrigerant has a higher temperature than that of the condenser water, heat is transferred from the refrigerant to the condenser water through the metal tube wall between the two fluids, and the refrigerant condenses at a high pressure. At the outlet of the condenser, the refrigerant condenses to a liquid phase and its temperature drops to  $T_{cd,refl}$ . In the condenser water loop, the forced condenser water with the entering temperature ( $T_{CWS}$ ) and mass flow rate ( $\dot{m}_{cw}$ ), flows through the condenser. At the outlet of the condenser, the temperature of the leaving condenser water rises to  $T_{CWR}$  as a result of heat transfer with the refrigerant fluid.

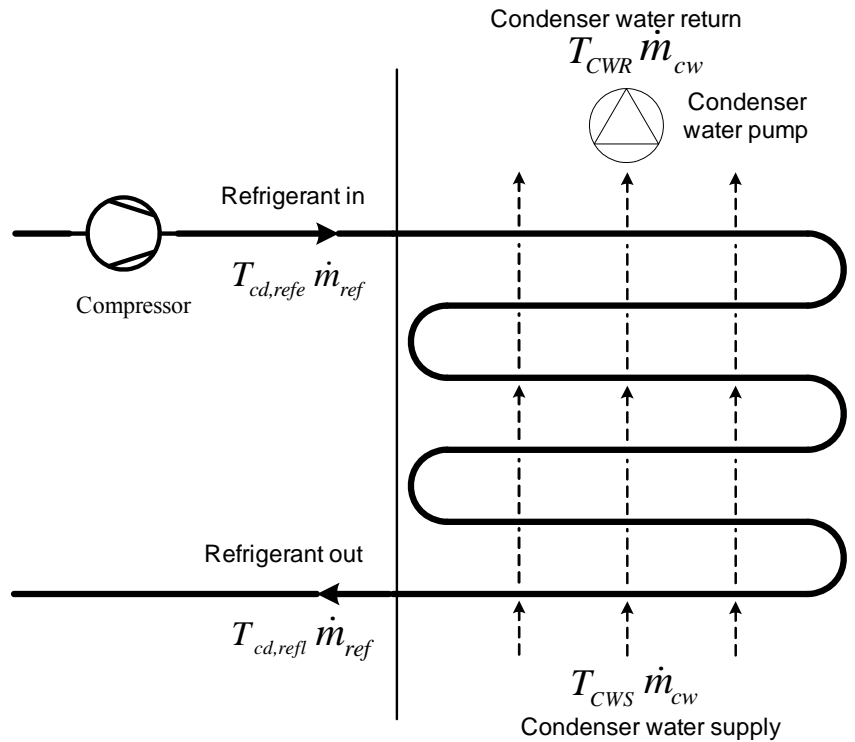


**Figure 5.5 Schematic diagram of a condenser**

In the condenser water loop, the heat transfer is a single-phase forced convection process, which is governed by the geometry of the condenser, the viscosity, the density, the thermal conductivity, the expansion coefficient, and the specific heat of the refrigerant.

In the refrigerant loop, the heat transfer is a two-phase forced convection process. The heat exchange depends not only on heat convection, but also on phase change. The phase change from vapor to liquid makes the phenomena of heat transfer considerably more complex than those without phase change. The mass flow rate, the latent heat of vaporization, the pressure, and possibly other properties of the vapor all contribute to the effectiveness of the condensation process. According to the fluid physical characteristics, the condenser can be divided into three sections, i.e., a superheated vapor section, a two-phase section, and a subcooled liquid section, as shown in Figure 5.6.

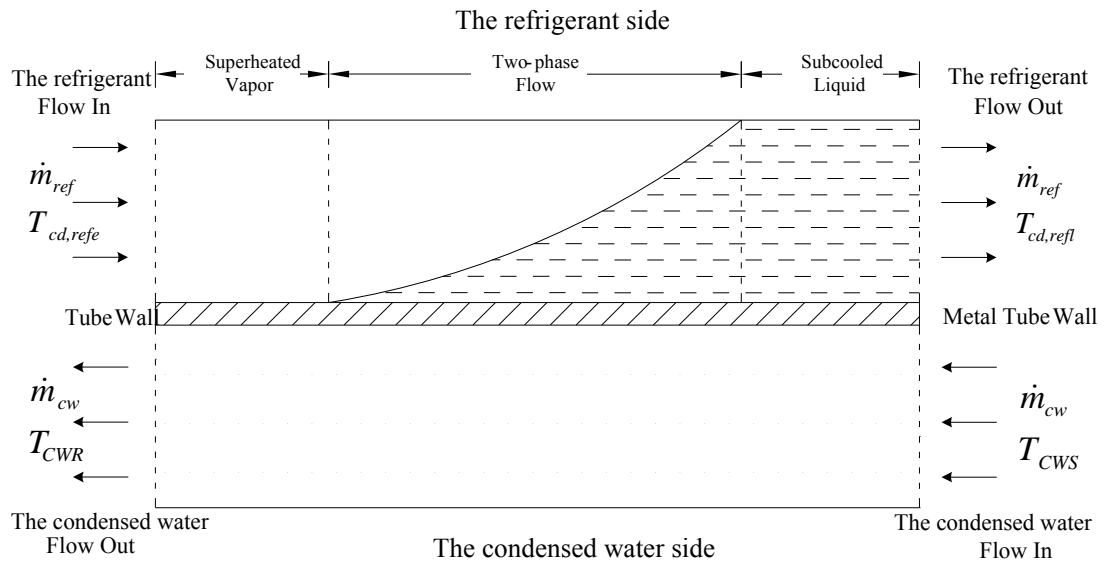


**Figure 5.6 Heat transfer mechanism of condenser**

The refrigerant entering the superheated vapor section is at a superheated status with entering temperature ( $T_{cd,refe}$ ), higher than the saturation temperature ( $T_{cd,ref,sat}$ ), and no condensation occurs. At the two-phase section, the refrigerant temperature

becomes lower and the vapor is less superheated due to heat exchange. The condensation begins, as the condenser surface temperature is below the saturation temperature of the refrigerant, and the saturation vapor becomes saturation liquid. At the subcooled liquid section, the fluid is totally condensed to the liquid phase and is further cooled to the subcooled condition. The heat transfer follows the pattern of the single-phase fluid similar to the superheated vapor section.

For applications in the areas of performance simulation, control and optimization, it is important that the model can simultaneously reflect the impact of all basic operating variables to the system output. Ding et al. [124] developed a model with no more than four key operational characteristic model parameters which can correlate the heat transfer on both the refrigerant and condenser water sides. The heat rejection  $Q_{cd}$  involves the energy and mass balance in the condenser and it is predicted by:

$$Q_{cd} = \frac{c_{cd,1} \dot{m}_{ref}^{c_{cd,4}} (T_{cd,ref,sat} - T_{CWS}) + c_{cd,2} \dot{m}_{ref} (T_{cd,refe} - T_{cd,ref,sat}) + h_{cd,ref,latent} \dot{m}_{ref}}{1 + c_{cd,3} \left( \frac{\dot{m}_{ref}}{\dot{m}_{cw}} \right)^{c_{cd,4}}} \quad (5.16)$$

where,  $T_{cd,ref,sat}$ ,  $T_{cd,refe}$  and  $h_{cd,ref,latent}$  are the saturation temperature of the refrigerant vapor, the temperature of the entering refrigerant and the latent heat of the vaporization refrigerant, respectively, while,  $T_{CWS}$ ,  $\dot{m}_{cd,ref}$  and  $\dot{m}_{cw}$  are the condenser water supply temperature, the refrigerant mass flow rate and the condenser water mass flow rate, respectively.

In Eq.(5.16), the value of the saturation temperature ( $T_{cd,ref,sat}$ ) and the latent heat of refrigerant vaporization ( $h_{cd,ref,latent}$ ) can be determined by polynomials :

$$T_{cd,ref,sat}(P_{cd}) = \sum_{i=0}^n a_i P_{cd}^i \quad (5.17a)$$

$$h_{cd,ref,latent}(P_{cd}) = \sum_{j=0}^m b_j P_{cd}^j \quad (5.17b)$$

This condenser model lumps the fluid thermal property and condenser geometric information as constant model parameters  $c_{cd,1}$  to  $c_{cd,4}$  and considers only the condenser inlet and outlet conditions. Therefore, the total heat transfer rate can be sufficiently described by a function of five basic operating variables, i.e.  $T_{cd,ref}$ ,  $\dot{m}_{ref}$ ,  $T_{CWS}$ ,  $\dot{m}_{cw}$  and  $P_{cd}$ .

In practice, the refrigerant temperature entering the condenser ( $T_{cd,ref}$ ), condenser water supply temperature ( $T_{CWS}$ ) and the condensing pressure ( $P_{cd}$ ) can be obtained by direct measurements using temperature or pressure sensors. Similar to the variables of the evaporator model, the other variables of this condenser model which are difficult to be measured directly, can be determined by indirect methods:

1. The condenser water mass flow rate ( $\dot{m}_{cw}$ ) can be obtained by measuring the pressure difference across the condenser from the empirical relation [124]

$$\Delta P_{cw} = a_0 + a_1 \dot{m}_{cw} + a_2 \dot{m}_{cw}^2 \quad (5.18)$$

where  $a_0$ ,  $a_1$ ,  $a_2$  are parameters to be determined through specification data or online testing,  $\Delta P_{cw}$  and  $\dot{m}_{cw}$  are the pressure difference and the mass flow rate of the condenser water across the condenser, respectively. Therefore, the mass flow rate can be derived from Eq. (5.19):

$$\dot{m}_{cw} = \frac{-a_1 + \sqrt{a_1^2 - 4a_2(a_0 - \Delta P)}}{2a_2} \quad (5.19)$$

2. The mass flow rate  $\dot{m}_{ref}$  of the refrigerant can either be measured directly or indirectly. If the indirect method is used, the rejected heat  $\dot{Q}_{cd}$  can be calculated from the energy balance of the condenser water

$$\dot{Q}_{cd} = C_{pw} \dot{m}_{cw} (T_{CWR} - T_{CWS}) \quad (5.20)$$

where  $C_{pw}$ ,  $T_{CWS}$ , and  $T_{CWR}$  are the specific heat, the temperature of the condenser water entering and leaving the condenser, respectively; and then the mass flow rate  $\dot{m}_{ref}$  of the refrigerant can then be estimated as:

$$\dot{m}_{ref} = \frac{\dot{Q}_{cd}}{h_{cd,refe} - h_{cd,refl}} \quad (5.21)$$

where  $h_{cd,refe}$  and  $h_{cd,refl}$  are the entering and leaving enthalpies, respectively, which can be obtained from thermodynamics tables of the refrigerant based on the entering/leaving temperature and pressure of the refrigerant.

### 5.3 Model Validation

After building up models for four key components, validation is conducted on a laboratorial HVAC pilot plant. The laboratorial system consists of a refrigeration cycle, a VSD condenser water pump and a VSD chilled water pump (see the schematic diagram in Figure 5.1). Table 5.1 summarizes the main specification parameters of the chiller system studied.

**Table 5.1 Details of the experimental chiller**

Chiller	
Nominal cooling capacity	4.8 kW
Nominal compressor power	1.5 kW
Nominal COP	3.2

Designed chilled water entering/leaving temperature	7/12 °C
Designed chilled water mass flow rate	0.23 kg/s
Designed condenser water supply/return temperature	31/37 °C
Designed condenser water mass flow rate	0.25 kg/s
Nominal condenser water pump power	0.3 kW

Since the individual models have already been validated in the previous work [122-124], in this chapter, the focus is to validate the composite refrigeration cycle model. Usually, the energy performance of refrigeration cycles is expressed as the coefficient of performance (COP), which is defined as the ratio of cooling capacity to power consumption. In this study, we will validate the composite refrigeration cycle model by comparing the measured COP with modeled COP.

For the measured COP, since the instantaneous power consumption can be obtained from the power meter (model no. Panasonic AKW1121), and the chilled water flow rate and chilled water temperature difference between the evaporator inlet and outlet can be measured in real time, it can be calculated with the real measured data. Figure 5.7 illustrates the comparison between modeled COP estimated by Eq. (5.14) and the measured COP over 7 days' chiller operation period at 1 minute's time scale.

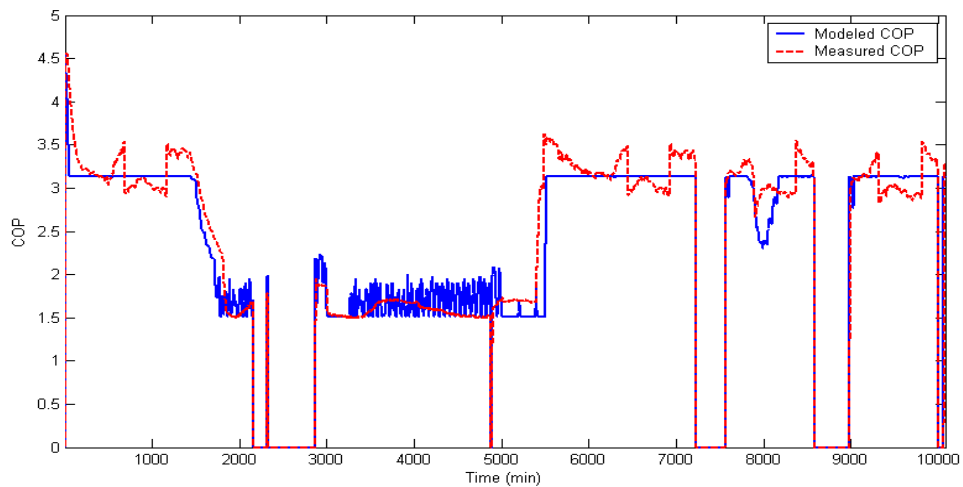


**Figure 5.7 Comparison between modeled COP and measured COP**

To further quantify the accuracy of the proposed model, the mean absolute error (MAE) and root mean square error (RMSE) of Figure 5.7 are calculated in Table 5.2. The figures below indicate that the proposed model achieves an accurate prediction of the COP.

**Table 5.2 Model accuracy**

	<i>Mean absolute error</i>	<i>Root mean square error</i>
COP	0.1638	0.2531

## 5.4 Summary

This chapter presented a component-based refrigeration cycle model developed specifically to investigate the factors affecting the refrigeration cycle performance. The model considers physical and thermal characteristics such as the heat-transfer rate estimation of the evaporator and condenser. Experimental results show that the developed model is sophisticated enough to determine the steady-state COP under various operating conditions over a long operating period, as well as to estimate the power consumption with respect to the varying operating conditions.

Moreover, this model does not require an iteration procedure to figure out the model parameters, thus can be easily used in model based optimization. In the next chapter, this refrigeration cycle model will be used to develop a practical model based supervisory and optimal control strategy to systematically optimize the operating set points to achieve the maximum energy saving for a real operating HVAC plant.

# CHAPTER 6 HVAC SYSTEM OPTIMIZATION

## – OUT-BUILDING SECTION

### **6.1 Introduction**

As introduced in Chapter 1, the centralized HVAC process consists of five loops, which can be further grouped into two sections geographically: the in-building section and the out-building section. Because the configuration of a real building HVAC system is very complex, the online optimization of a building HVAC system are often separated into the optimization of the in-building section and the optimization of the out-building section.

The in-building section consists of an indoor air loop and part of the chilled water loop. The indoor air loop includes terminal units, cooling coils, dampers, fans, ducts, and controls. The chilled water loop includes cooling coils, evaporators, pumps, pipes, valves, and controls [1]. The evaporator prepares the supply chilled water through the heat exchange between the water and the refrigerant. To satisfy the indoor cooling loads, this chilled water with controlled temperature and flow rate is distributed to each AHU cooling coil through a chilled water distribution system of the HVAC in-building section. Lu et al. [107] presented a practical method to optimize the in-building section. Their method considered the variation of the cooling load of each end user and employed an adaptive neuro-fuzzy inference system (ANFIS) to model duct and pipe networks and obtains optimal differential pressure (DP) set points based on limited sensor information. A mix-integer nonlinear constraint optimization of the system energy was formulated and solved by a modified GA approach.

The out-building section, as schematically shown in Figure 6.1, consists of three other loops: the refrigerant cycle, the condenser water loop and the ambient air loop

[120]. The condenser transfers cooling loads and the heat generated by compressors to the condenser water loop. Pumps provide the energy to circulate the condenser water between the condensers and the cooling towers. The heat is then rejected to the ambient air through heat transfer and evaporation by cooling towers.

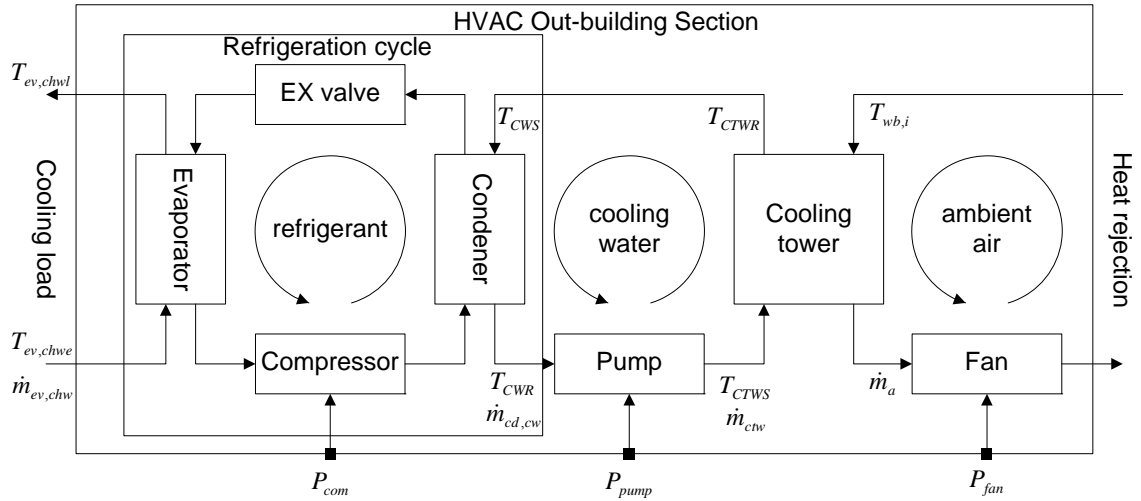


**Figure 6.1 Block diagram of HVAC out building section**

The out-building section is a main power consumer in a HVAC system and its energy consumption contributes to the majority of the overall operating cost. Many studies introduced in Chapter 2 centered on optimizing the chillers and cooling towers to enhance their performance and energy efficiency [70, 88, 92-99, 106, 108-109, 125-128].

To perform system optimization for a HVAC outbuilding section, accurate and reliable system component models and associated optimization algorithms are essential. The models are used to predict the system energy performances, as well as the system response to the changes of the control settings, weather conditions and cooling loads. However, so far, most of the model-based system optimization approaches introduced in Chapter 2 utilize either pure empirical data driven component models [88, 92-99] or traditional physical component models [125-128]. The drawbacks of both types of the models examined in Chapter 2 may limit their real-time online application in building

HVAC system optimization when the processes are nonlinear and have wide operating ranges.

Comparing with the models presented in literature, the models proposed or adopted in the thesis have the advantages of:

- 1) simple model structure without cumbersome iterative computation
- 2) high accuracy with physical significances

Moreover, without the proposed models, it is difficult to identify the interactions among HVAC components, derive the constraints, and formulate the complex optimization problem in the HVAC system. Consequently, using simplified hybrid models becomes a more promising choice.

With all these advantages of hybrid models, we adopt this modeling approach for HVAC system out-building section optimization in our study. In Chapter 3 and 5, we have proposed simple yet accurate component models for the cooling towers and the refrigeration cycle of the HVAC systems. Based on these models, this chapter will extend the work of Lu et al. [106, 108-109] to simultaneously optimize the overall performance of the HVAC out-building section.

For the chosen of optimization algorithm, because the HVAC optimization problem is a combinational optimization problem with nonlinear constraints and contains both continuous and discrete variables, conventional gradient-based optimization methods cannot be applied directly. Although an exhaustive search method or a combined exhaustive search with conventional gradient-based methods can be applied to find the optimal solutions, it is impractical in the real time applications for such a complicated problem due to its time consuming nature. Thus, according the literature review of Chapter 2, we chose evolutionary algorithms, PSO algorithm and GA to determine the control settings which minimize the system power consumption.

## 6.2 Formulation of Model-Based Optimization

### 6.2.1 Objective function

In the out-building section of a centralized HVAC system, there are three types of devices which consume energy, namely compressors, condenser water pumps and cooling tower fans. Therefore, the objective function for optimization is to minimize the total energy consumption of these devices.

$$J = \min_{T_{w,cd,in}} P_{total} = \sum_{k=1}^{N_{ch}} P_{com,k} + \sum_{k=1}^{N_{ch}} P_{pump,k} + \sum_{j=1}^{N_{ct}} P_{fan,j} \quad (6.1)$$

where the power consumption model of compressors have been discussed in Chapter 5.

For large-scaled HVAC systems with multiple compressors, the operating power consumption models of the compressors are adjusted as:

$$P_{com,k} = \frac{\left( f_{1,k} \text{PLR}_k^2 + f_{2,k} \text{PLR}_k + f_{3,k} \right) \dot{m}_{ref,max,k} P_{ev,k} V_{2,k} \frac{\xi_k}{\xi_k - 1} \left[ \left( \frac{P_{cd,k}}{\delta_k P_{ev,k}} \right)^{\frac{\xi_k - 1}{\xi_k}} - 1 \right]}{\eta_{m,k} \left( f_{4,k} \text{PLR}_k^2 + f_{5,k} \text{PLR}_k + f_{6,k} \right)} \quad (6.2)$$

The operating power consumption of associated condenser water pumps and cooling tower fans can then be given by

$$\sum_{k=1}^{N_{ch}} P_{pump,k} = \sum_{k=1}^{N_{ch}} P_{pump,nom,k} \left( d_0 + d_1 \left( \frac{\dot{m}_{cd,cw,k}}{\dot{m}_{cw,nom,k}} \right) + d_2 \left( \frac{\dot{m}_{cd,cw,k}}{\dot{m}_{cw,nom,k}} \right)^2 + d_3 \left( \frac{\dot{m}_{cd,cw,k}}{\dot{m}_{cw,nom,k}} \right)^3 \right) \quad (6.3)$$

and

$$\sum_{j=1}^{N_{ct}} P_{fan,j} = \sum_{j=1}^{N_{ct}} P_{fan,nom,j} \left( e_0 + e_1 \left( \frac{\dot{m}_{a,j}}{\dot{m}_{a,nom,j}} \right) + e_2 \left( \frac{\dot{m}_{a,j}}{\dot{m}_{a,nom,j}} \right)^2 + e_3 \left( \frac{\dot{m}_{a,j}}{\dot{m}_{a,nom,j}} \right)^3 \right) \quad (6.4)$$

where  $N_{ch}$  and  $N_{ct}$  are the total numbers of chillers and cooling towers in a HVAC out-building section, respectively. And  $k$  denotes the number of a operating chiller (condenser water pump is regarded as a part of a chiller) in the total  $N_{ch}$  chillers while  $j$  denotes the number of a operating cooling tower in the total  $N_{ct}$  cooling towers. The subscript “ $nom$ ” stands for the nominal values of variables.

In Eq.(6.2), the device operating variables  $\dot{m}_{ref,max,k}$ ,  $v_{2,k}$ ,  $\xi_k$ ,  $\delta_k$  can be determined with the manufacturer's specification data and the compressor model parameters  $f_{1-6,k}$  can be determined at the system modeling phase, thus the power consumption model of the refrigeration cycle can be regarded to be a function of the independent variables, namely the evaporating pressure ( $P_{ev,k}$ ), the condensing pressure ( $P_{cd,k}$ ) and the part load ratio control ( $PLR_k$ ).

In Eqs. (6.3) and (6.4),  $\dot{m}_{cd,cw,k}$  and  $\dot{m}_{a,j}$  denote the mass flow rate of condenser water and air, respectively, which are the only independent variables of power consumption models for condenser water pumps and cooling tower fans.

Therefore, the independent variables in the objective function are listed as follows:

$PLR_k$  part load ratio of the  $k^{th}$  refrigeration cycle

$\dot{m}_{cd,cw,k}$  water flow rate of the  $k^{th}$  condenser water pump

$\dot{m}_{a,j}$  air flow rate of the  $j^{th}$  cooling tower fan

$P_{ev,k}$  evaporating pressure of the  $k^{th}$  evaporator

$P_{cd,k}$  condensing pressure of the  $k^{th}$  condenser

With these independent variables, the model parameters and the manufacturers' specification data, the total power consumption of the HVAC system out-building section can be determined uniquely for the given cooling load. Any change of these independent variables will impact the efficiency of the whole HVAC system. However, the operation of the out-building section has to obey a number of constraints, i.e. mechanical limitations, basic energy and mass balances and interaction of individual components etc. These constraints have to be considered in solving the optimization problem. In general, these constraints can be categorized into two types: physical

limitations of components and interaction between components. In this study, nine constraints are identified as elaborated below.

### 6.2.2 Physical limitation constraints of components

*Constraint (1)* The physical limitations for  $\dot{m}_{cd,cw,k}$  and  $\dot{m}_{a,j}$  are:

$$\dot{m}_{cd,cw,k,\min} \leq \dot{m}_{cd,cw,k} \leq \dot{m}_{cd,cw,k,\max} \quad (6.5)$$

$$\dot{m}_{a,j,\min} \leq \dot{m}_{a,j} \leq \dot{m}_{a,j,\max} \quad (6.6)$$

If the condenser water mass flow rate ( $\dot{m}_{cd,cw,k}$ ) through the condenser is too small, the condenser water temperature may increase above the safety limit for a big cooling load. Therefore, the minimal condenser water flow rate ( $\dot{m}_{cd,cw,k,\min}$ ) of the  $k^{\text{th}}$  condenser water pump is to keep the condenser water temperature within normal operation range. At the same time, the maximum condenser water flow rate ( $\dot{m}_{cd,cw,k,\max}$ ) of the  $k^{\text{th}}$  condenser water pump is limited by the capability of the motor driving the pump. Similarly, the minimal and maximum air flow rates ( $\dot{m}_{a,j,\min}, \dot{m}_{a,j,\max}$ ) of the  $j^{\text{th}}$  cooling tower fan are also limited.

*Constraint (2)* To ensure the occurring of superheating and subcooling in the refrigeration cycle, the evaporating and condensing pressures ( $P_{cd,k}, P_{ev,k}$ ) should be restricted by boundaries provided by the manufacturers:

$$P_{ev,k,\min} \leq P_{ev,k} \leq P_{ev,k,\max} \quad (6.7)$$

$$P_{cd,k,\min} \leq P_{cd,k} \leq P_{cd,k,\max} \quad (6.8)$$

*Constraint (3)* the condenser water supply temperature ( $T_{CWS}$ ) at the condenser inlet is limited by

$$T_{CWS,\min} \leq T_{CWS} \leq T_{CWS,\max} \quad (6.9)$$

Assuming the mixed cooling tower water return temperature equals to the condenser water supply temperature ( $T_{CWS}$ ), the lower bound of the condenser water supply temperature ( $T_{CWS,min}$ ) is the ambient wet bulb temperature ( $T_{wb,i}$ ), which is the theoretical lower limit of the heat transfer process in the mechanical draft cooling tower. Its upper bound ( $T_{CWS,max}$ ) is a safety requirement from chiller manufacturers to keep the pressure in the condensers at an acceptable level.

*Constraint (4)* The  $PLR_k$  of the  $k^{th}$  operating refrigeration cycle is given by

$$PLR_{k,min} \leq PLR_k \leq PLR_{k,max} \quad (6.10)$$

where  $PLR_{k,min}$  and  $PLR_{k,max}$  are the minimal and maximal operating part load ratios of the  $k^{th}$  refrigeration cycle which are specified by the manufacturer's catalog.

### 6.2.3 Interaction constraints between components

Besides the physical limitations of components themselves, the interactions among components also place restrictions on the feasible solution of the optimization problem. This section identifies these interactions based on the component models of the evaporator, the condenser and the cooling tower described in Chapter 3 and Chapter 5. For large-scale HVAC systems with multiple refrigeration cycles and cooling towers, the models of evaporators, condensers and cooling towers are rewritten as follows:

Evaporator model of the  $k^{th}$  refrigeration cycle:

$$\dot{Q}_{ev,k} = \frac{(h_{ev,ref,sat,k} - h_{ev,refe,k})\dot{m}_{ref,k} + c_{ev,1,k}\dot{m}_{ref,k}^{c_{ev,3,k}}(T_{ev,chw,k} - T_{ev,ref,sat,k})}{1 + c_{ev,2,k}\left(\frac{\dot{m}_{ref,k}}{\dot{m}_{chw,k}}\right)^{c_{ev,3,k}}} \quad (6.11)$$

Condenser model of the  $k^{\text{th}}$  refrigeration cycle:

$$\dot{Q}_{cd,k} = \frac{c_{cd,1,k} \dot{m}_{ref,k}^{c_{cd,4,k}} (T_{cd,ref,sat,k} - T_{cwe}) + c_{cd,2,k} \dot{m}_{ref,k} (T_{cd,refe,k} - T_{cd,ref,sat,k}) + h_{cd,ref,latent,k} \dot{m}_{ref,k}}{1 + c_{cd,3} \left( \frac{\dot{m}_{ref,k}}{\dot{m}_{cd,cw,k}} \right)^{c_{cd,4,k}}} \quad (6.12)$$

Cooling tower model of the  $j^{\text{th}}$  cooling tower:

$$\dot{Q}_{ct,j} = \frac{c_{ct,1,j} \dot{m}_{ctw}^{c_{ct,3,j}}}{1 + c_{ct,2} \left( \frac{\dot{m}_{ctw}}{\dot{m}_{a,j}} \right)^{c_{ct,3,j}}} (T_{CTWS} - T_{wb,i}) \quad (6.13)$$

Without loss of generality, for a cooling tower, it is assumed that the distributed cooling tower water mass flow rates follows:

$$\dot{m}_{ctw} = \frac{\sum_{k=1}^{N_{ch,op}} \dot{m}_{cd,cw,k}}{N_{ct,op}} \quad (6.14)$$

where  $N_{ch,op}$  denotes the number of chiller (the associated condenser water pump is regarded as a part of chiller) in operation and  $N_{ct,op}$  denotes the number of cooling towers in operation. Take note that not all chillers or cooling towers will be in operation, especially at part load ratio conditions, the number of operating chillers and cooling towers should be decided by the optimizer.

If we assume that the condenser water flows from each condenser are ideally mixed before being supplied to the cooling towers, then the cooling tower water supply temperature can be determined by:

$$T_{CTWS} = \frac{\sum_{k=1}^{N_{ch,op}} (T_{CWR,k} \dot{m}_{cd,cw,k})}{N_{ct,op} \dot{m}_{ctw}} \quad (6.15)$$

Likewise, the mixed condenser water supply temperature follows:

$$T_{CWS} = \frac{\sum_{j=1}^{N_{ct,op}} (T_{CTWR,j} \cdot \dot{m}_{ctw})}{\sum_{k=1}^{N_{ch,op}} \dot{m}_{cd,cw,k}} \quad (6.16)$$

*Constraint (5)* Based on the first law of thermodynamics, the rejected heat rate of the  $j$ th cooling tower follows:

$$\dot{Q}_{ct,j} = \dot{m}_{ctw} C_{pw} (T_{CTWS} - T_{CTWR,j}) \quad (6.17)$$

Replacing  $\dot{Q}_{ct,j}$  with the hybrid cooling tower model of Eq.(6.13), we obtain:

$$\frac{c_{ct,1,j} \dot{m}_{ctw}^{c_{ct,3,j}}}{1 + c_{ct,2} \left( \frac{\dot{m}_{ctw}}{\dot{m}_{a,j}} \right)^{c_{ct,3,j}}} (T_{CTWS} - T_{wb,i}) = \dot{m}_{ctw} C_{pw} (T_{CTWS} - T_{CTWR,j}) \quad (6.18)$$

According to Eq.(6.18), there are two factors affecting cooling tower performance, one is  $\dot{m}_{ctw}$  vs.  $\dot{m}_{a,j}$  and the other is  $T_{CTWS}$  vs.  $T_{wb,i}$ . To simplify the analysis, it is assumed that  $T_{CTWS}$  and  $T_{wb,i}$  are constants when the effect of  $\dot{m}_{ctw}$  vs.  $\dot{m}_{a,j}$  is discussed. The performance of a cooling tower is simulated by the model provided by Braun et al. [10]. Figure 6.2 shows five curves of equal heat rejection rate, where the horizontal-axis represents the percentage of water flow rate and the vertical-axis represents the percentage of airflow rate. These curves of equal heat rejection rate are divided into three regions.

- Region (1): The airflow rate is very small and the water flow rate must be very large in order to achieve a given heat rejection rate. In this case, the airflow rate is too small to exchange heat efficiently with the cooling tower water. The outlet airflow wet-bulb temperature is almost the same as that of the inlet water.

- Region (2): The airflow rate is very large while the water flow rate is very small, the heat exchange is saturated and the outlet water temperature is nearly equal to the ambient air wet-bulb temperature.
- Region (3): The heat rejection rate of the cooling tower increases with either the increased airflow rate or the increased water flow rate, and vice versa.

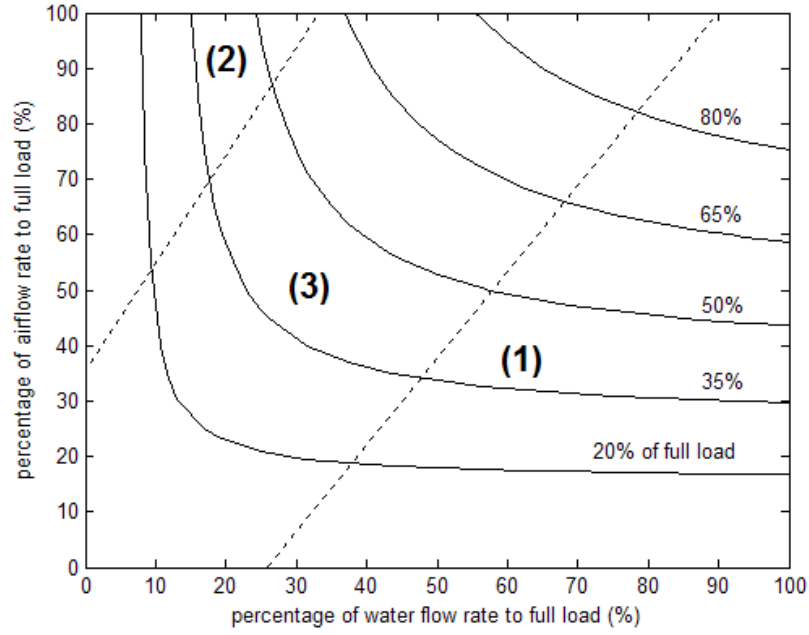


**Figure 6.2 Performance of a cooling tower**

Apparently, the energy-efficient operating range must drop inside Region (3). In this region, the reduced airflow rate leads to lower fan power consumption, yet the water flow rate has to be increased, resulting in the increased pump power consumption. Similarly, the reduced water flow rate lowers the pump power consumption but results in increased fan power consumption. Constraint (1) limits the value of  $\dot{m}_{ctw}$  and  $\dot{m}_{a,j}$  due to the cooling tower characteristics.

The term  $(T_{CTWS} - T_{wb,i})$  in Constraint (5) (Eq.(6.18)) reflects the effect of  $T_{wb,i}$  on the cooling tower performance. Assuming the cooling tower heat rejection rate and cooling tower water supply temperature are fixed for the given cooling demand, the

optimal operating point of the cooling towers changes when the ambient wet-bulb temperature ( $T_{wb,i}$ ) changes. Figure 6.3 gives an example where the cooling tower heat rejection rate is assumed to be a fixed value for two wet-bulb temperatures of the ambient air, 20 °C and 25 °C, respectively. The optimal operating points are labeled as large stars to indicate the corresponding power consumption of fans and pumps. While the curves of fan power consumption are the same for different wet-bulb temperatures, the cooling tower water flow rate changes with changing airflow and outdoor environment for a constant cooling tower heat rejection rate.

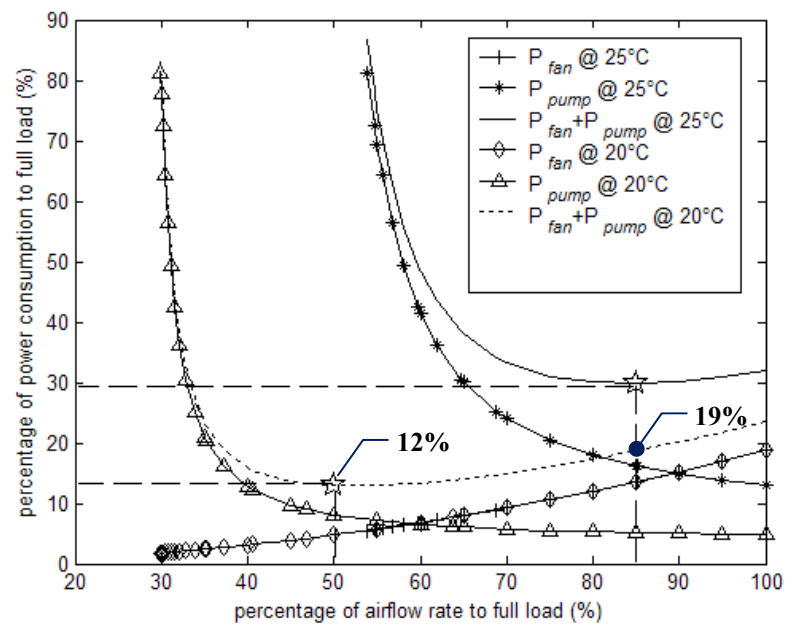


**Figure 6.3 Optimal operating points at different wet-bulb temperatures**

The optimal airflow rate is 85% of the full-load at 25 °C and 50% at 20 °C. For an optimal operating point, the power consumption is 12% of the full-load at 20 °C wet-bulb temperature. If the airflow rate is kept at 85% of the full-load at 20 °C instead of 50%, the combined power consumption of fan and pump is 19% of the full-load. Compared with 12% of the full-load at the optimal point, almost 7% energy of the full-load savings could be achieved with the varying mass flow rate of water and air when the ambient wet-bulb temperature is at 20 °C.

*Constraint (6)* In the refrigeration cycle, base on the second law of thermodynamics, the heat exchange rate in the  $k^{\text{th}}$  evaporator, i.e., the cooling load can be expressed as

$$\dot{Q}_{ev,k} = \dot{m}_{chw,k} C_{pw} (T_{ev,chw,k} - T_{ev,chwI,k}) \quad (6.19)$$

*Constraint (7)* Likewise, the heat rejection rate in the  $k^{\text{th}}$  condenser can be calculated by

$$\dot{Q}_{cd,k} = \dot{m}_{cd,cw,k} C_{pw} (T_{CWR,k} - T_{CWS}) \quad (6.20)$$

*Constraint (8)* The interactions between the  $k^{\text{th}}$  compressor mechanical work and the heat exchange rate in the associated condenser and evaporator is expressed as:

$$W_{in,k} = P_{com,k} \eta_{pol,k} \eta_{m,k} = \dot{Q}_{cd,k} - \dot{Q}_{ev,k} \quad (6.21)$$

Replacing  $W_{in,k}$  and  $\dot{Q}_{cd,k}$  with Eqs. (5.7b) and (6.20), respectively, we obtain:

$$\dot{m}_{ref,k} P_{ev,k} v_2 \frac{\xi}{\xi-1} \left( \left( \frac{P_{cd,k}}{\delta P_{ev,k}} \right)^{\frac{\xi-1}{\xi}} - 1 \right) = \dot{m}_{cd,cw,k} C_{pw} (T_{CWR,k} - T_{CWS}) - \dot{Q}_{ev,k} \quad (6.22)$$

Based on Eq. (6.22), the interactions between the compressor power consumption and condenser water pump power consumption can be identified. Assuming the cooling load ( $\dot{Q}_{ev,k}$ ) remains unchanged, an increase of the compressor frequency consumes more electric power and leads to an increase of the evaporating pressure ( $P_{ev,k}$ ) as well as the condensing pressure ( $P_{cd,k}$ ) if the compressor and throttling devices are controlled for maintaining a constant refrigerant mass flow rate ( $\dot{m}_{ref,k}$ ). This increase of evaporating pressure ( $P_{ev,k}$ ) and condensing pressure ( $P_{cd,k}$ ) will result in the increase of evaporating temperature and condensing temperature, respectively. If the condenser water supply temperature ( $T_{CWS}$ ) remained constant through the cooling tower fan control, with an increased condensing temperature, the condenser is able to generate a

higher condenser water return temperature ( $T_{CWR,k}$ ) which results in a larger temperature range of condenser water ( $T_{CWR,k} - T_{CWS}$ ). With this larger temperature range, the condenser water mass flow rate ( $\dot{m}_{cd,cw,k}$ ) can be reduced for power savings of the condenser water pump. On the contrary, an increased condenser water mass flow rate requires a potential smaller ( $T_{CWR,k} - T_{CWS}$ ), which leads to the power savings of the compressor by reducing the  $P_{ev,k}$  and  $P_{cd,k}$ . Therefore, the evaporating pressure ( $P_{ev,k}$ ) and condensing pressure ( $P_{cd,k}$ ) are important variables which need to be optimized. Figures 6.4 and 6.5 show the test results of the condensing pressures, evaporating pressures, superheat and refrigerant flow rate at the same ambient wet-bulb temperature and decreasing cooling load conditions (100 to 40%, 15kW to 6kW) for the cases of constant condensing pressure and optimal condensing pressure control. We can observe how the condensing pressure and the evaporating pressure vary with respect to the decreasing cooling load (four pressure transducers for each side, compressor outlet, condenser inlet and outlet, valve inlet for the condensing pressure side, valve outlet, evaporator inlet and outlet, compressor inlet for the evaporating pressure side). We can also see how the refrigerant flow rates ( $\dot{m}_{ref,k}$ ) (denoted by “REFR flow” in the Figures) drop in both cases with the cooling load demand.

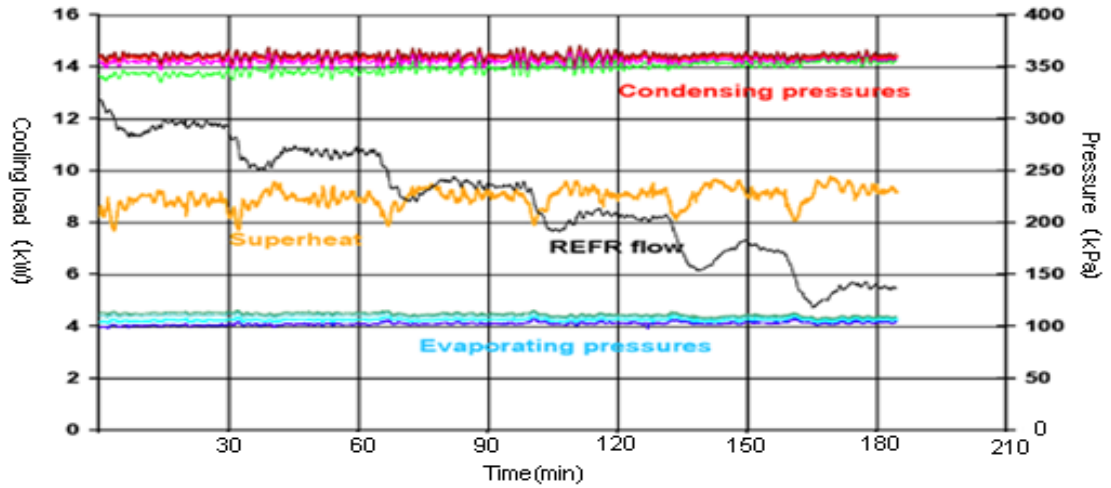


**Figure 6.4 Pressures & refrigerant flow for decreasing cooling load with constant condensing pressure control**

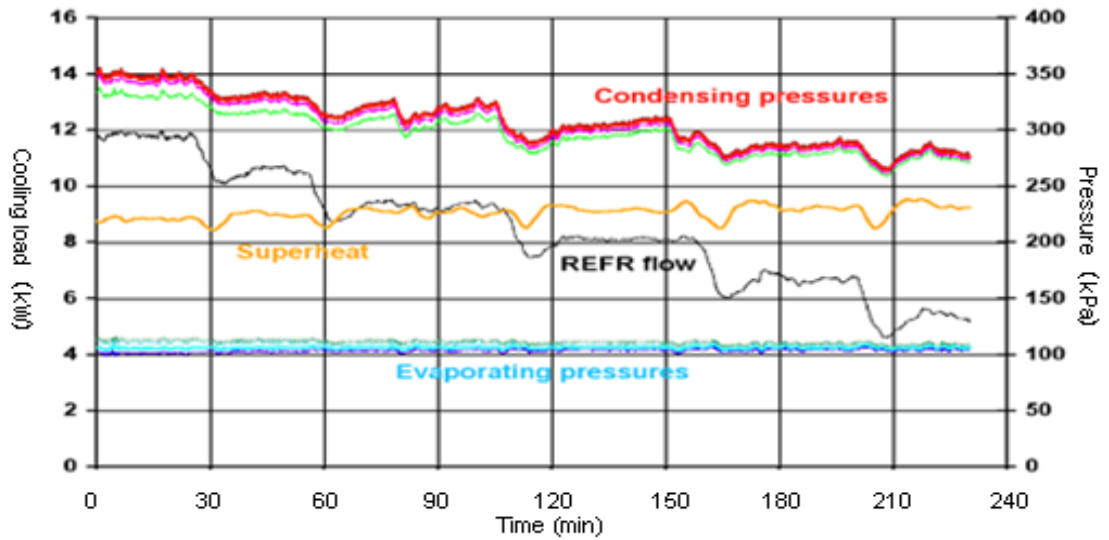


**Figure 6.5 Pressures and refrigerant flow for decreasing cooling load with optimal condensing pressure control**

Figures 6.6 and 6.7 show the different power consumptions and COPs corresponding to Figures 6.4 and 6.5, respectively. As the cooling load decreases, the cooling capacity and power consumption also decreases. We can observe that the optimal condensing pressure control (Figure 6.5) leads to a power consumption reduction (Figure 6.7 vs. Figure 6.6) when compared to the constant condensing pressure control (Figure 6.4) and consequently results in a higher COP as well as a lower power consumption at light-load conditions.

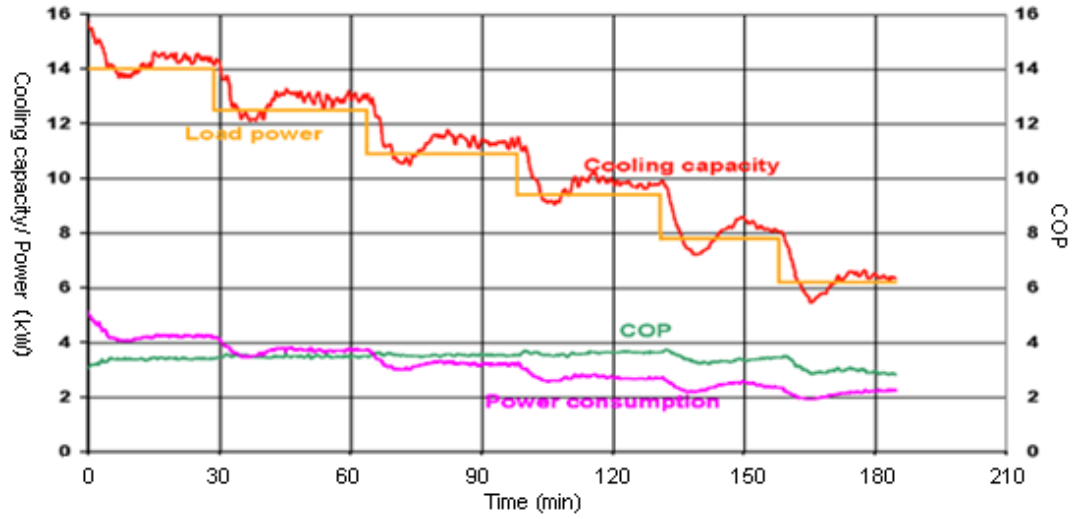


Figure 6.6 Power consumption and COP for decreasing cooling load with constant condensing pressure control

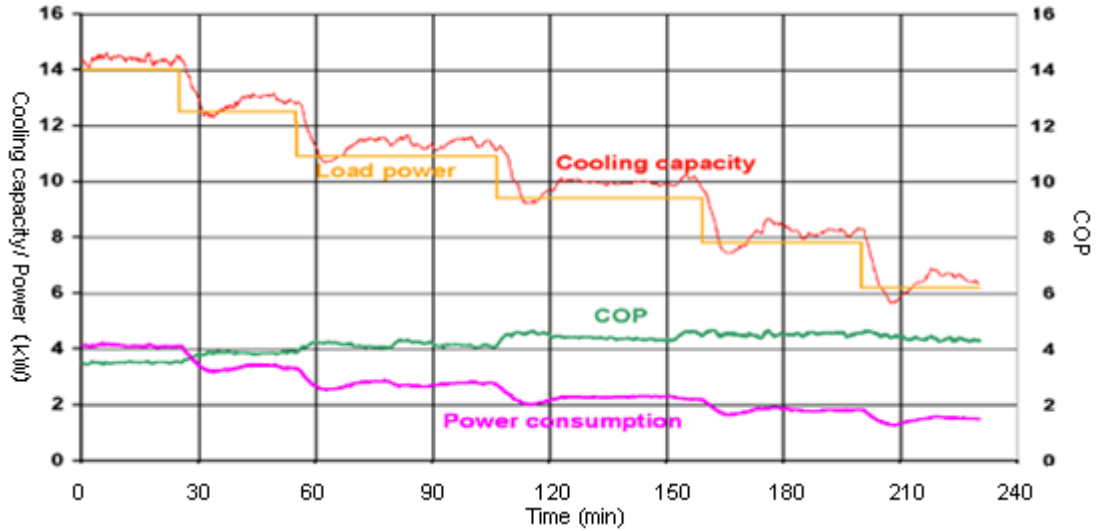


Figure 6.7 Power consumption and COP for decreasing cooling load with optimal condensing pressure control

On the other hand, if the condenser water mass flow rate ( $\dot{m}_{cd,cw,k}$ ) remains constant, with the increased condensing temperature, the condenser can accept a higher condenser water supply temperature ( $T_{CWS}$ ) and consequently results in a higher condenser water return temperature ( $T_{CWR,k}$ ) for the same heat rejection rate of a condenser. This improves the cooling tower efficiency with the same ambient wet bulb temperature, because of the larger enthalpy difference between the ambient air and the condenser water return temperature ( $T_{CWR,k}$ ) for the cooling tower inlet, which results in less

electricity consumption of the cooling tower fan for the same heat rejection rate of the cooling tower. Therefore, the condenser water supply temperature ( $T_{CWS}$ ), i.e., the mixed cooling tower water return temperature is also an important independent variable which needs to be optimized.

*Constraint (9)* For a multi-chiller system, the total heat rejection rate in the cooling towers equals the heat absorbed by the condenser water from the chiller condensers:

$$\sum_{j=1}^{N_{ct}} \dot{Q}_{ct,j} = \sum_{k=1}^{N_{ch}} \dot{Q}_{cd,k} \quad (6.23)$$

By adopting the cooling tower model and by rearranging Eq. (6.21) to substitute  $\dot{Q}_{cd,k}$ , we can rewrite Eq.(6.23) as:

$$\sum_{j=1}^{N_{ct}} \frac{c_{1,j} \dot{m}_{ctw}^{c_{ct,3,j}}}{1 + c_{2,j} \left( \frac{\dot{m}_{ctw}}{\dot{m}_{a,j}} \right)^{c_{ct,3,j}}} (T_{CTWS} - T_{wb,i}) = \sum_{k=1}^{N_{ch}} (P_{com,k} \eta_{pol,k} \eta_{m,k} + \dot{Q}_{ev,k}) \quad (6.24)$$

Then, based on Eq.(6.24), the interactions between the compressor power consumption and cooling tower fan power consumption can be identified. Figure 6.8 illustrates the trade-off between the chiller power and corresponding cooling tower fan power with respect to the increasing tower airflow [96]. Here, a fixed cooling tower water mass flow rate ( $\dot{m}_{ctw}$ ) and cooling tower water supply temperature ( $T_{CTWS}$ ) are assumed. As the airflow increases, the fan power increases. At the same time, there is a reduction in the mixed cooling tower water return temperature, i.e. condenser water supply temperature ( $T_{CWS}$ ) (refer to Eq.(6.16)), resulting in a lower compressor power consumption according the analysis in *Constraint (8)*.

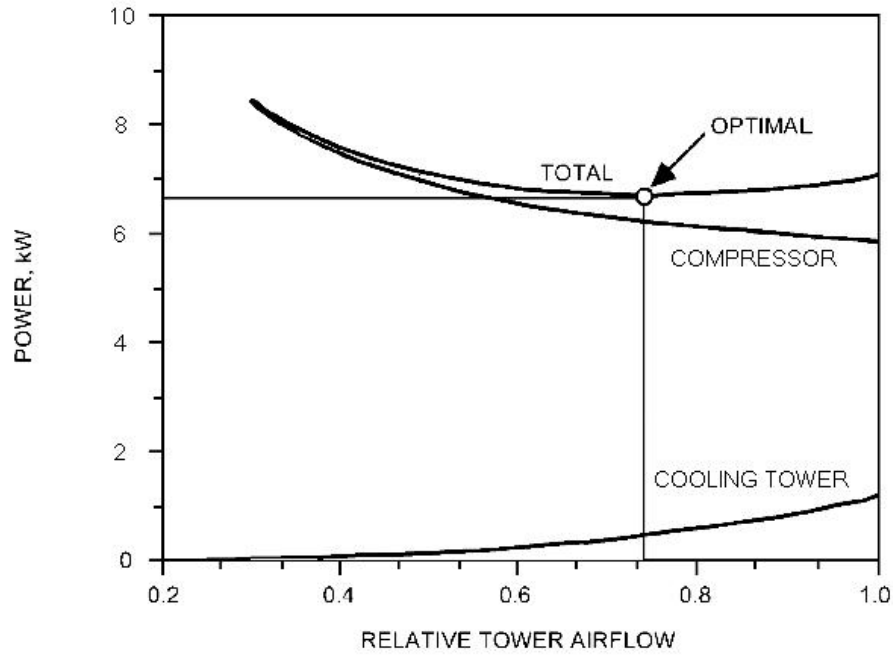


**Figure 6.8 Trade-offs between compressor power and fan power [96]**

On the other hand, the condenser water return temperature ( $T_{CWR,k}$ ) affects the heat exchange efficiencies of cooling towers. Because for the same heat rejection rate of the cooling tower, a lower mixed condenser water return temperature, i.e. cooling tower water supply temperature ( $T_{CTWS}$ ) (refer to Eq.(6.15)), results in lower efficiencies of the cooling towers under the same ambient wet-bulb temperature as the enthalpy difference between ambient air and cooling tower supply water becomes smaller. Consequently, if the power consumption of compressor and condenser water pump remains unchanged, more power will be consumed by the cooling tower fan according the cooling tower model expressed by Eq.(6.13). Thus, the optimal operating point occurs at a point where the rate of power increment in the fans is equal to the rate of power reduction in the chillers.

With the expressions of the component models, the objective function, and the constraints, it is easy to conclude that the optimal control of the HVAC out-building section results from an optimum trade-off in the power consumption of the compressors,

condenser water pumps and cooling tower fans with the optimum combination settings of the independent variables of part load ratio ( $PLR_k$ ) of the  $k^{\text{th}}$  refrigeration cycle, evaporating pressure ( $P_{ev,k}$ ) of the  $k^{\text{th}}$  evaporator, condensing pressure ( $P_{cd,k}$ ) of the  $k^{\text{th}}$  condenser, water flow rate ( $\dot{m}_{cd,cw,k}$ ) of the  $k^{\text{th}}$  condenser water pump, condenser water supply temperature ( $T_{CWS}$ ) and air flow rate ( $\dot{m}_{a,j}$ ) of the  $j^{\text{th}}$  cooling tower fan.

### 6.3 Optimization Based on PSO Algorithms

PSO, developed by Eberhart and Kennedy [129], is a population based stochastic optimization technique promising in solving nonlinear optimization problems of building HVAC system with its features of easy-to-implement, low memory requirement and faster calculation speed. The algorithm is divided into four parts: initialization, construction of the fitness function, update of velocity and position, and termination.

#### 6.3.1 Initialization

In PSO, each particle represents a potential solution. In simple terms, each particle flows through a multidimensional search space, where the position of each particle is adjusted according to its own experience and that of its neighbors.

As the search space is multidimensional, the particle  $i$  of the swarm can be represented by an  $n$ -dimensional vector  $\mathbf{X}_i = (x_{i1}, x_{i2}, \dots, x_{in})$ , which also denotes the position of the particle  $i$ , and  $n$  denotes the number of variables of the optimization problem. For this particular problem,  $\mathbf{X}_i = (P_{ev,1}, P_{ev,2}, \dots, P_{ev,k}, P_{cd,1}, P_{cd,2}, \dots, P_{cd,k}, PLR_1, PLR_2, \dots, PLR_k, \dot{m}_{cd,cw,1}, \dot{m}_{cd,cw,2}, \dots, \dot{m}_{cd,cw,k}, T_{CWS}, \dot{m}_{a,1}, \dot{m}_{a,2}, \dots, \dot{m}_{a,j})$ , therefore,  $n = 4k + j + 1$ . The

velocity of this particle can be represented by another  $n$ -dimensional vector  $\mathbf{V}_i = (v_{i1}, v_{i2}, \dots, v_{in})$ .

In the initialization step, the particles with random positions and velocities are uniformly distributed over the search space.

### 6.3.2 Construction of the fitness function

Since the objective of this optimization problem is to minimize  $P_{total}$ , the fitness function should be constructed to give the maximum value for the smallest  $P_{total}$ . In addition, in order to fulfill the constraints described by Eqs.(6.5-6.24), penalty functions are commonly used to penalize an unfeasible solution. In this step, a penalty function is added if any constraint cannot be fulfilled. Therefore, the fitness function is expressed in the following equation.

$$fitness = \frac{1}{P_{total} + \sum_k^{N_{ch}} (P_{1,k} + P_{2,k} + P_{3,k} + P_{6,k} + P_{7,k} + P_{8,k} + P_{9,k} + P_{11,k}) + \sum_j^{N_{ct}} (P_{4,j} + P_{7,j}) + P_5 + P_{10}} \quad (6.25)$$

With the constraints written as:

$$P_{1,k} = \theta_{1,k} \cdot [\dot{Q}_{ev,k} - \dot{m}_{ev,chw,k} C_{pw} (T_{ev,chw,e,k} - T_{ev,chw,l,k})]^2 \quad (6.26a)$$

$$P_{2,k} = \theta_{2,k} \cdot [\dot{Q}_{cd,k} - \dot{m}_{cd,cw,k} C_{pw} (T_{CWR,k} - T_{CWS})]^2 \quad (6.26b)$$

$$P_{3,k} = \theta_{3,k} \cdot (P_{com,k} \eta_{pol,k} \eta_{m,k} + \dot{Q}_{ev,k} - \dot{Q}_{cd,k})^2 \quad (6.26c)$$

$$P_{4,j} = \theta_{4,j} \cdot [\dot{Q}_{ct,j} - \dot{m}_{ctw,j} C_{pw} (T_{CTWR,j} - T_{CTWS})]^2 \quad (6.26d)$$

$$P_5 = \theta_5 \cdot \left( \sum_{j=1}^{N_{ct}} \dot{Q}_{ct,j} - \sum_{k=1}^{N_{ch}} \dot{Q}_{cd,k} \right)^2 \quad (6.26e)$$

$$P_{6,k} = \begin{cases} 0 & \text{if } \dot{m}_{cd,cw,k,\min} \leq \dot{m}_{cd,cw,k} \leq \dot{m}_{cd,cw,k,\max} \\ \theta_{6,k} \cdot (\dot{m}_{cd,cw,k} - \dot{m}_{cd,cw,k,\min})^2 & \text{if } \dot{m}_{cd,cw,k} < \dot{m}_{cd,cw,k,\min} \\ \theta_{6,k} \cdot (\dot{m}_{cd,cw,k} - \dot{m}_{cd,cw,k,\max})^2 & \text{if } \dot{m}_{cd,cw,k} > \dot{m}_{cd,cw,k,\max} \end{cases} \quad (6.26f)$$

$$P_{7,j} = \begin{cases} 0 & \text{if } \dot{m}_{a,j,\min} \leq \dot{m}_{a,j} \leq \dot{m}_{a,j,\max} \\ \theta_{7,j} \cdot (\dot{m}_{a,j} - \dot{m}_{a,j,\min})^2 & \text{if } \dot{m}_{a,j} < \dot{m}_{a,j,\min} \\ \theta_{7,j} \cdot (\dot{m}_{a,j} - \dot{m}_{a,j,\max})^2 & \text{if } \dot{m}_{a,j} > \dot{m}_{a,j,\max} \end{cases} \quad (6.26g)$$

$$P_{8,k} = \begin{cases} 0 & \text{if } P_{ev,k,\min} \leq P_{ev,k} \leq P_{ev,k,\max} \\ \theta_{8,k} \cdot (P_{ev,k} - P_{ev,k,\min})^2 & \text{if } P_{ev,k} < P_{ev,k,\min} \\ \theta_{8,k} \cdot (P_{ev,k} - P_{ev,k,\max})^2 & \text{if } P_{ev,k} > P_{ev,k,\max} \end{cases} \quad (6.26h)$$

$$P_{9,k} = \begin{cases} 0 & \text{if } P_{cd,k,\min} \leq P_{cd,k} \leq P_{cd,k,\max} \\ \theta_{9,k} \cdot (P_{cd,k} - P_{cd,k,\min})^2 & \text{if } P_{cd,k} < P_{cd,k,\min} \\ \theta_{9,k} \cdot (P_{cd,k} - P_{cd,k,\max})^2 & \text{if } P_{cd,k} > P_{cd,k,\max} \end{cases} \quad (6.26i)$$

$$P_{10} = \begin{cases} 0 & \text{if } T_{CWS,\min} \leq T_{CWS} \leq T_{CWS,\max} \\ \theta_{10} \cdot (T_{CWS} - T_{CWS,\min})^2 & \text{if } T_{CWS} < T_{CWS,\min} \\ \theta_{10} \cdot (T_{CWS} - T_{CWS,\max})^2 & \text{if } T_{CWS} > T_{CWS,\max} \end{cases} \quad (6.26j)$$

$$P_{11,k} = \begin{cases} 0 & \text{if } 0.1 \leq \text{PLR}_k \leq 1, \text{PLR}_{\min} = 0.1 \\ \theta_{11,k} \cdot (\text{PLR}_k - 0.1)^2 & \text{if } \text{PLR}_k < 0.1, \text{PLR}_{\min} = 0.1 \\ \theta_{11,k} \cdot (\text{PLR}_k - 1)^2 & \text{if } \text{PLR}_k > 1, \text{PLR}_{\min} = 0.1 \end{cases} \quad (6.26k)$$

where  $\theta_1 \sim \theta_{11}$  are the penalty multipliers, which should be large positive numbers. With this fitness function, the minimal system power consumption without violating any constraints has the maximal fitness value.

### 6.3.3 Updating velocity and position

The fitness of each particle with associated unique position and velocity can be evaluated according to the fitness function of the optimization problem defined by Eq. (6.25). The best previously visited position of the particle  $i$  is noted as its individual best position  $\mathbf{P}_i = (p_{i1}, p_{i2}, \dots, p_{in})$ . The position of the best individual of the whole swarm is noted as the global best position  $\mathbf{G}_i = (g_1, g_2, \dots, g_n)$ . At each iteration step, the velocity of the particle and its new position will be assigned according to

$$\mathbf{V}_i = \omega \cdot \mathbf{V}_i + c_1 \cdot r_1 \cdot (\mathbf{P}_i - \mathbf{X}_i) + c_2 \cdot r_2 \cdot (\mathbf{G}_i - \mathbf{X}_i) \quad (6.27)$$

$$\mathbf{X}_i = \mathbf{X}_i + \mathbf{V}_i \quad (6.28)$$

where  $\omega$  is the inertia weight that controls the impact of the previous velocity of the particle on its current one;  $r_1$ ,  $r_2$  are independently uniformly distributed random variables with range  $(0, 1)$ ;  $c_1$ ,  $c_2$  are positive constant acceleration coefficients which control the maximum step size. Eq. (6.24) is used to calculate the new velocity according to its previous velocity and according to the distance of its current position from both its own best historical position and the best position of the entire population or its neighborhood. Generally, the value of each component in  $\mathbf{V}_i$  can be clamped to the range  $[-v_{\max}, v_{\max}]$  to control excessive roaming of particles outside the search space. Then the particle flies toward a new position according to Eq. (6.28). This process is repeated until user-defined termination criteria are reached, which are defined in the next section.

#### 6.3.4 Termination

The computation of the PSO is terminated when one of the following termination criteria is reached:

- when a maximum number of iterations has been exceeded.
- when an acceptable solution has been found.
- when no improvement is observed over a number of iterations.
- when the objective function slope is approximately zero.

#### 6.3.5 PSO implementation

The PSO can be implemented by the following steps:

**Step I:** Initialize a swarm of particles with random positions and velocities. These random particles must be formed at allowed ranges for each variable. These ranges are determined by the optimization problem formulated in Section 6.2.2.

**Step II:** Calculate the fitness values of all particles. Set the individual best position  $\mathbf{P}_{best}$  and its corresponding fitness for each particle equal to the current position and fitness value of the particle. Set the global best position  $\mathbf{G}_{best}$  and its corresponding fitness value equal to the best position and fitness value attained by the swarm.

**Step III:** Update the velocity and position of each particle according to Eqs. (6.27) and (6.28).

**Step IV:** Update  $\mathbf{P}_{best}$  and  $\mathbf{G}_{best}$ . Evaluate the fitness values of all particles. For each particle, compare its current fitness value with the best fitness value it attained so far ( $\mathbf{P}_{best}$ ). If the current value is better, then update  $\mathbf{P}_{best}$  and its fitness value with the current position and fitness value. Determine the best particle of the current population with the best fitness value. If the fitness value is better than the fitness value of  $\mathbf{G}_{best}$ , then update  $\mathbf{G}_{best}$  and its fitness value with the position and fitness value of the current best particle.

**Step V:** Check termination criteria. If a stopping criterion is met, then output  $\mathbf{G}_{best}$  and its fitness value; otherwise go to step III.

The flowchart of optimization procedure of the PSO based optimizer is shown as in Figure 6.9 [130].

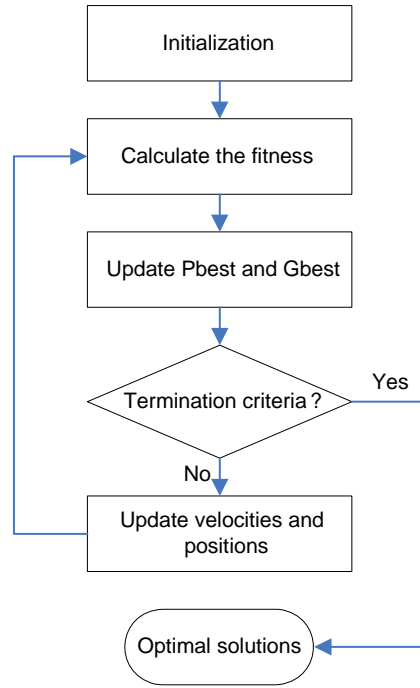


**Figure 6.9 Optimization procedure of PSO based optimizer**

The optimization algorithm can be easily implemented without encoding variables and changing optimal settings' units. A reasonable number of commonly used sensors is required to monitor the overall system, and the optimal settings can be calculated based on mathematical models and the PSO algorithm. Of course, this standard PSO can be further improved to reduce the risk of convergence to a suboptimal solution. But, in consequence, an improved PSO will increase the computational cost and memory requirement. However, this study will not discuss further on this point because the effectiveness of optimization techniques is very case specific.

#### ***6.4 Optimization Based on Genetic Algorithms (GA)***

To compare the control accuracy and application feasibility in practice, genetic algorithms (GA) is also employed to resolve the formulated system optimization problem for HVAC out-building section.

Similar to PSO, genetic algorithms (GA) are stochastic global search methods, which are based on principles of nature biological evolution. The basic principles of

genetic algorithms were first proposed by Holland [131], and the consolidation of their theories was later developed by Goldberg in 1989 [132]. It has been recognized as a powerful tool for solving many complex problems, such as combinatorial optimization, planning, symbolic regression and automatic programming.

Generally, four steps are required to complete a simple genetic algorithm procedure: encoding, construction of a fitness function, execution of the evolutionary operation, and finding termination criteria. These steps are briefly introduced in the following sections.

### 6.4.1 Encoding

In genetic algorithms, it is presumed that the potential solution of a problem is an individual and can be represented by a set of variables. These variables are regarded as the genes of a chromosome and can be structured by a string of values in binary form. The procedure to convert a set of variables into a string is called encoding.

Binary string encoding [133] is the most classical approach used by researchers because of its simplicity. Here, each variable in an individual is encoded as a binary string and these strings are concatenated to form a chromosome. The use of Gray coding has been advocated as a method of overcoming the hidden representational bias in conventional binary representation as the Hamming distance between adjacent values is constant [134]. The following shows the contrast between binary string and Gray code:

Real value:	0	1	2	3	4	5	6	7
Binary string:	000	001	010	011	100	101	110	111
Gray code:	000	001	011	010	110	111	101	100

The above example shows that a Gray code represents each number in the sequence of an integer as a binary string in an order such that adjacent integers have Gray code representations that differ in only one bit position.

Whilst binary string encoding is most commonly used, there are some alternative encoding strategies, such as integer and real-valued representations [134]. However, there is no general consensus on which encoding strategy is superior for a given problem.

For this particular problem, according to Eqs. (6.1-6.4), each independent variable ( $P_{ev,k}$ ,  $P_{cd,k}$ ,  $PLR_k$ ,  $\dot{m}_{cd,cw,k}$ ,  $T_{CWS}$  and  $\dot{m}_{a,j}$ ) in Equation (6.15) is converted into a binary string. And all of these strings are combined together to form a chromosome. For the independent variables ( $P_{ev,k}$ ,  $P_{cd,k}$ ,  $PLR_k$ ,  $\dot{m}_{cd,cw,k}$ ,  $T_{CWS}$  and  $\dot{m}_{a,j}$ ), the upper and lower bounds of their binary strings stand for minimum and maximum values in Constraint (1), (2), (3) and (4). The lengths of the binary strings are determined by the control precision of the corresponding variables: the more precise set point requires the longer binary string.

#### 6.4.2 Construction of the fitness function

Similar to that of PSO, the fitness function of GA is used to provide a measure of how individuals have performed in the whole population. It is an important link between genetic algorithms and the practical optimization problems. In the case of a minimization problem, the fittest individual should have the lowest numerical value of the associated objective function and have the highest numerical value of the associated fitness function. In other words, the fitness function is normally used to transform the objective function value into a measure of relative fitness, thus:

$$F(x) = g(f(x)) \quad (6.29)$$

where  $f(.)$  is the objective function,  $g(.)$  transforms the value of the objective function into a non-negative number and  $F(.)$  is the resulting relative fitness.

A simple way to transform a minimization problem into a maximization problem is using a large positive constant to minus the objective function. This large positive constant should guarantee that all the fitness values incurred are positive numbers. For a maximization problem with the negative object values, a large positive constant should be chosen to add to the objective function. Similarly, the constant should be large enough to guarantee all positive fitness results. A linear transformation which offsets the objective function is often used prior to fitness assignment as:

$$F(x) = a f(x) + b \quad (6.30)$$

where  $a$  is a positive scaling factor if the optimization is to maximize and negative if it is to minimize. The offset  $b$  is used to ensure that the resulting fitness values are non-negative.

The linear scaling and offsetting outlined above are, however, susceptible to premature convergence. The evolutionary operators select individuals for reproduction on the basis of their relative fitness. Using linear scaling, the expected value of the offspring is approximately proportional to the individual's performance. As there is no constraint on an individual's performance in a given generation, highly fit individuals in the early generation can dominate the reproduction causing premature convergence to possibly sub-optimal solutions. Similarly, if there is little deviation in the population, then scaling provides only a small bias towards the fittest individuals [135].

Here, the GA based optimizer shares the same fitness function as the PSO based optimizer which is constructed in section 6.3.3.

### 6.4.3 Evolutionary operation

The typical evolutionary operation of GA consists of selection, crossover, mutation, and reinsertion.

Selection is the process of determining the number of times that a particular individual is chosen for reproduction and, thus, the number of offspring that an individual will produce. The roulette wheel selection method is generally adopted in most genetic algorithms due to its characteristics of zero bias and unlimited spread. The probability to select an individual as one of the parents for the next generation is proportional to the fitness value of the associated individual. It is stochastic sampling with replacement. The selection operation is repeated until the mating pool for reproduction is full of individuals.

Crossover is the basic operation for producing new chromosomes of the next generation. It produces new individuals who have some parts of both parents' genetic information. Normally, there are three types of crossover: one-point crossover, multi-point crossover, and uniform crossover. Although the preference of which crossover techniques to use is arguable [131], one-point crossover is the simplest and most likely to be adopted. An example of a one-point crossover operation for binary coded chromosomes is shown as follows:

Parent 1: 1 1 1 1 1 1	“crossover at the 2nd bit”	New individual 1: 1 1 0 0 0 0
Parent 2: 0 0 0 0 0 0	⇒	New individual 2: 0 0 1 1 1 1

The crossover point is usually selected randomly throughout the chromosomes. The probability of crossover is a user-controlled option and the determination of this parameter is briefly discussed in [132].

Mutation plays a secondary role in an evolutionary operation [132]. It makes alternations to the values of one or more genes in a chromosome with low probability. The function of mutation is to give new information to the population and to prevent the population from becoming saturated or premature convergent. Single-bit mutation is commonly used and is shown in the following example.

Original individual: 1 1 1 1 1 1 “mutation at the 5th bit” New individual: 1 1 1 1 0 1

Like in crossover, the mutation bit is also selected randomly throughout the chromosomes. Large mutation rates increase the probability of destroying good individuals, but increase population diversity. In contrast, small mutation rates intend to keep the good individual and decrease population diversity. The determination of this parameter is also discussed in [132].

Reinsertion is the last step to complete a generation. New individuals produced by crossover and mutation are selected on the basis of fitness to replace some or all the individuals in old population to form a new population. Usually, the worst chromosomes are replaced when new chromosomes are inserted into the population and the best chromosomes are kept to the succeeding generation.

For this particular problem, elitist roulette wheel selection [136], single-point crossover, and single-bit mutation operators are adopted. The crossover and mutation points are all selected randomly in each generation. Fitness-based reinsertion is adopted to operate according to the predetermined generation gap.

#### **6.4.4 Termination**

Because genetic algorithms are a stochastic search method, it is difficult to formally specify convergence criteria. Here, the computation of genetic algorithms is terminated when any of the following criteria is satisfied.

- The maximum number of generations is reached;
- The fitness value of the best chromosome converges to some asymptote.

Once the algorithm is terminated, a set of optimal set points of independent variables ( $P_{ev,k}$ ,  $P_{cd,k}$ ,  $PLR_k$ ,  $\dot{m}_{cd,cw,k}$ ,  $T_{CWS}$  and  $\dot{m}_{a,j}$ ) are achieved corresponding to the certain outdoor environment and cooling load.

### 6.4.5 GA implementation

The optimization procedure can be implemented by the following algorithm and visualized in Figure 6.10.

- Step 1:* Predetermine the parameters of component models based specification data or on-site testing data (refer to Chapter 3 and 5) and input the measurement variables;
- Step 2:* Initialize parameters of the genetic algorithm: population size, maximum number of generations, precision of each variables, generation gap, and probabilities of crossover and mutation;
- Step 3:* Perform the evolutionary operations as illustrated in Figure 6.10;
- Step 4:* Repeat *Step 3* until the genetic algorithm is terminated;
- Step 5:* Verify the optimal values of the independent variables to avoid the uncertainties of the genetic algorithm caused by insufficient computation. If the results are not reasonable, maintain the set points unchanged for the current sampling period;
- Step 6:* Calculate the optimal set points of each component based on the optimization results in *Step 5*;
- Step 7:* Pass the optimal set points to supervisory control strategy for the final decision for each local control unit.

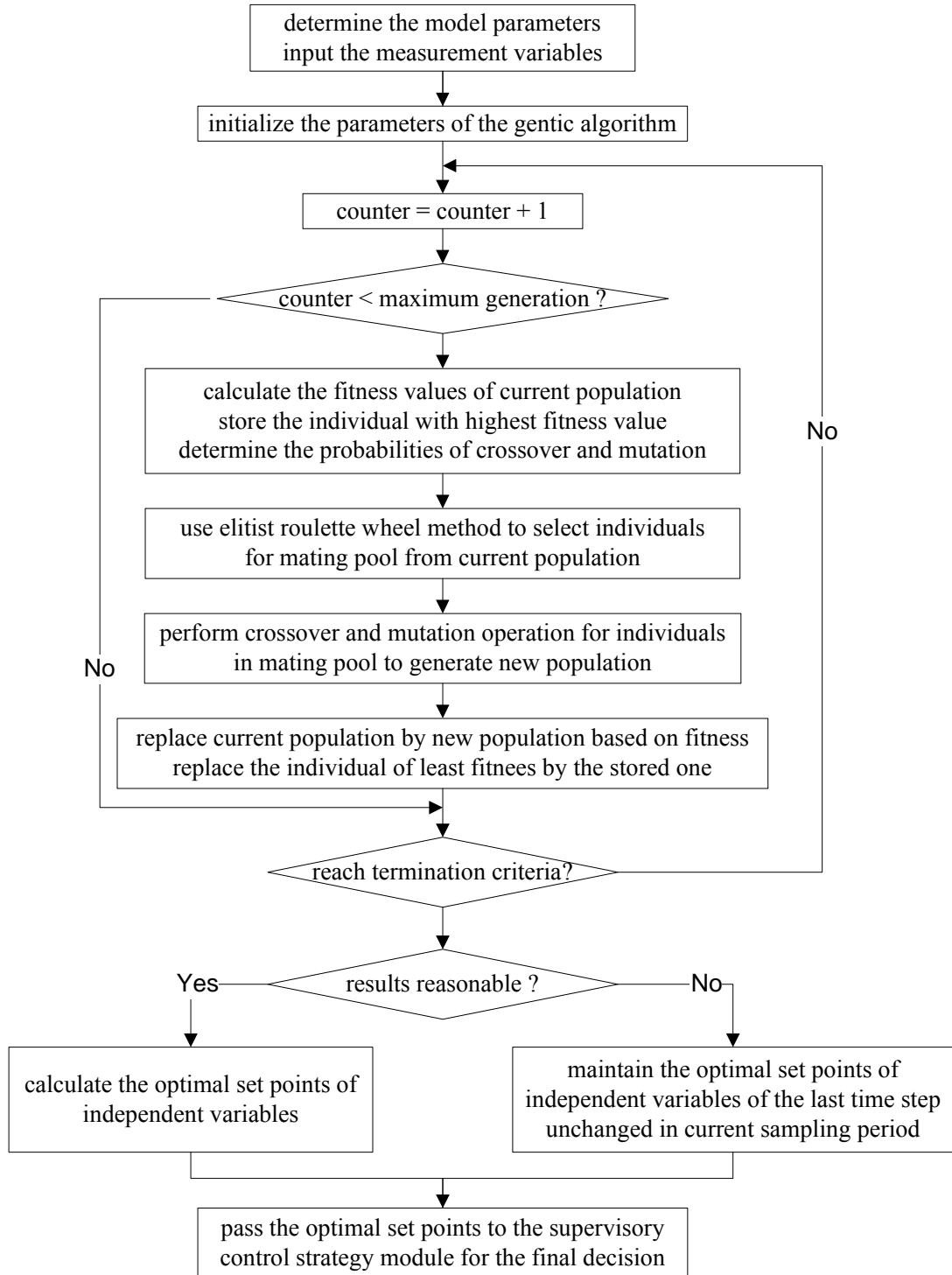


Figure 6. 10 Optimization procedure of GA based optimizer

### 6.5 Comparison Study of Two Optimization Methods

In this section, with the given environment and cooling load conditions, the control accuracy, computation time and the size of memory requirement are evaluated by

comparing the simulation results of the PSO based optimizer with that of the GA based optimizer.

The simulation studies are based on a laboratory HVAC system consist of three identical refrigeration cycles and three identical cooling towers (see the schematic diagram in Figure 6.11).

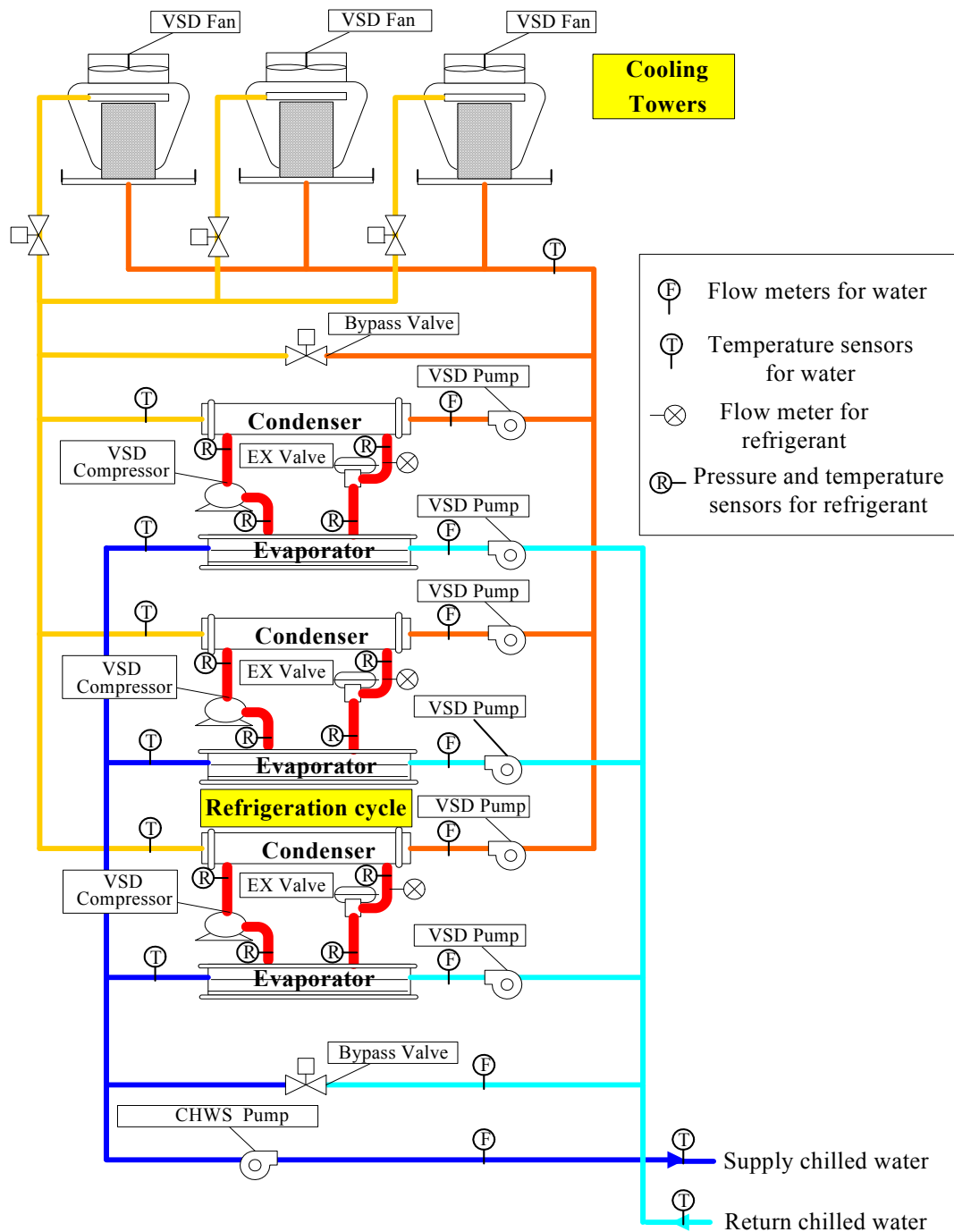


Figure 6.11 Schematic of the laboratorial HVAC out-building section

The parameters of the cooling towers and chillers are listed in Table 6.1.

**Table 6.1 Parameters of the pilot HVAC system under study**

<i>Total cooling capacity (kW)</i>	<i>14.4 kW</i>
<i>(Three identical sets of chillers, pumps and cooling towers)</i>	
Chiller	
Nominal cooling capacity	4.8 kW
Nominal compressor power	1.5 kW
Nominal COP	3.2
Designed chilled water entering/leaving temperature	7/12 °C
Designed chilled water mass flow rate	0.23 kg/s
Designed condenser water supply/return temperature	31/37 °C
Designed condenser water mass flow rate	0.25 kg/s
Nominal condenser water pump power	0.3 kW
Cooling tower	
Nominal heat rejection capacity	8 kW
Designed entering/leaving temperature	38/31 °C
Designed water circulation mass flow rate	0.25 kg/s
Designed air mass flow rate	0.5kg/s
Nominal fan motor power	0.45 kW

Three typical cases, which represent the typical operation conditions of the HVAC system in the light-load, medium-load and heavy-load, respectively, were selected to simulate and evaluate the performance of the proposed hybrid model-based system optimization approaches as presented in Table 6.2. The properties of the computer used for simulating these cases are presented in this table as well.

**Table 6.2 Typical test conditions, and optimization results using different optimization techniques**

Items	Load conditions					
	Light-load		Medium-load		Heavy-Load	
Working conditions						
$Q_{load}$ (kW)	4.26		8.44		13.87	
$T_{ev,chw_e}$ (°C)	11.7		11.5		11.2	
$T_{ev,chw_l}$ (°C)	7		7		7	
$T_{wb,i}$ (°C)	21.56		23.77		25.45	
Items	Tools					
	PSO	GA	PSO	GA	PSO	GA
Optimization results						
$P_{total}$ (kW)	1.39	1.38	2.88	2.88	4.33	4.34
$N_{ch}$	1	1	2	2	3	3
$N_{ct}$	2	2	3	3	3	3
$T_{CWS}$ (°C)	27.34	27.39	29.81	29.83	31.64	31.62
Computation time (s)	9.42	35.22	9.54	36.06	8.88	36.72
Memory requirement (MB)	72	348	72	348	72	348
Computer properties						
Operating system	Microsoft windows XP professional					
Processor	Intel(R) Core(TM) 2 Quad CPU @ 2.33 GHz					
Memory	2.00 GB of RAM					

These simulation results show that the model-based system optimization approach using PSO can accurately find the one-point global optimal solutions for all three typical cases with significant reduced computation times; from around 36 s for the GA based optimizer to around 9 s for the PSO based optimizer. Moreover, the memory requirements are reduced greatly, from 348 MB for the GA based optimizer to 72 MB for the PSO based optimizer. The reduction of the average computation time and the reduction of memory requirement of the system optimization approach using PSO as the optimization technique are about 70% and 80% respectively, compared with the system optimization approach using the same models but using the GA as the optimization technique.

## **6.5 Summary**

This chapter formulated and resolved the global optimization problem of the HVAC out-building section based on the simplified hybrid models developed in Chapter 3 and Chapter 5. These proposed component models have high predictive accuracy as well as the physical significance of the model parameters which have been verified by experimental tests. Based on these component models, the interactions among these components are examined, and then the nonlinear, highly-constrained optimization problem of the HVAC out-building section for energy minimization is formulated. Finally, easy-to-implement nonlinear optimization tools, PSO as well as GA are employed to resolve this optimization problem. The performance comparison between PSO based optimizer and GA based optimizer in terms of the control accuracy, computation time and memory requirement are also given. The simulation results demonstrate that the system optimization approach using the PSO optimization technique has the same control accuracy as the system optimization approach using GA as the optimization technique, but the required memory is reduced by around 4 times in the tests. And the average computation time reduction when applying the proposed model-based system optimization approach using the PSO based technique was 80% compared to that using the GA as the optimization technique.

Comparing with GA, the PSO algorithm does not require coding and decoding the individual solutions and converges much faster. These features lead to the significant reduction of computation time and memory requirement as what have been approved through comparison studies. Hence, the hybrid model-based system optimization approach using PSO based optimizer becomes our proposed method for implementation. In Chapter 7, real applications of the proposed method to a HVAC system will be examined and validated by experimental studies.

# CHAPTER 7 REAL SYSTEM IMPLEMENTATION

## ***7.1 Introduction***

The ultimate objective of any technique development is its application. Engineers are always trading off among cost, energy efficiency, and ease of implementation etc. Through experiment studies, this chapter will validate and evaluate the application of the HVAC EMCS, integrated with the proposed model-based system optimization approach using PSO as the optimization technique, for which details can be found in Chapter 6.

The studies designed to validate and evaluate the EMCS control strategies are divided into two categories: energy performances of the control strategies, and realistic control performances of control strategies. When the realistic performances of the control strategies are of concern, the dynamics of the system include not only the building thermal dynamics but also the controllers, coils, cooling towers etc. which affect the local loop control activities and should be properly modeled and evaluated in the application.

When only the energy performances of the strategies are of concern, the dynamics of the process, such as the HVAC components thermal dynamics etc., which noticeably affect the energy performance of the system, are investigated. The dynamics of the components such as sensors, actuators, and coils only affect the control performance but do not affect the energy performance and thus are not investigated in the application of optimizing energy savings. For practical applications, control and optimization strategies are expected to be simple and easy-to-implement while still providing satisfactory performance with high control reliability and stability. The computation time and memory requirement are generally manageable and can meet the requirements

of online control applications. When the optimal set points are downloaded to the local loop, the local loop controls should ensure stable and reliable transient performance of the HVAC system. The following sections will use on-site experiments to validate and evaluate the energy performance of the proposed hybrid model-based system optimization approach.

## ***7.2 Description of Experimental HVAC System***

Experiments are conducted on a laboratorial HVAC pilot plant (see the schematic diagram in Figure 6.11 and the real system in Figure 7.1) to validate and evaluate the proposed system optimization approach. The laboratory scale HVAC system consists of three identical refrigeration cycles in parallel, each of which is associated with one VSD condenser water pump and one VSD chilled water pump. The three refrigeration cycles are connected by one constant primary chilled water pump. The multiple VSD pumps are connected by a bypass pipe that connects the return and supply headers. Each set consisting of a refrigeration cycle and pump (as can be seen in Figure 6.11) operates independently. And three identical cooling towers equipped with the dedicate VSD fans are installed as a group. The electric valves mounted on the condenser water return pipes are used to select the operating cooling tower. To make the system operate to serve a designed cooling demand/load, the supply chilled water head and return chilled water headers can be connected to an electrical water heater (the electrical water heater is not illustrated in Figure 6.11), which can heat up the supply chilled water and give it back to the system as the return chilled water.

For the measurement part, resistance temperature detectors (RTDs) PT100  $\Omega$  with an accuracy of  $\pm 0.05^\circ\text{C}$  are installed to measure the chilled water temperature and condenser water temperature. And the mass flow rate of chilled water and condenser water are measured from a flow meter. As the mass flow rate of the refrigerant flows

through the evaporator is the same mass flow rate of the refrigerant flows through the condenser, it is measured through a flow meter with an accuracy of  $\pm 0.5\%$  of full scale. The pressure transducers with a measurement pressure range of 0–1600 kPa and an accuracy of  $\pm 0.5\%$  of full scale are used to measure the evaporating pressure and condensing pressure. The refrigerant temperatures at the inlet and outlet of the evaporator and condenser are measured with T-type thermal couples with a measurement range of  $-40$  to  $150\text{ }^{\circ}\text{C}$  with an accuracy of  $\pm 0.1\text{ }^{\circ}\text{C}$  (the measurement points of temperature, pressure and mass flow rate are illustrated in Figure 7.1). The ambient air temperature and relative humidity (RH) is measured using an EE21 transmitter with an accuracy of  $\pm 0.2\text{ }^{\circ}\text{C}$  for temperature and  $\pm 2\%$  RH for relative humidity. Thus the wet-bulb temperature can be calculated from the measured dry-bulb temperature and relative humidity with a psychometrics-subroutine. The power meters (model no.: Panasonic AKW1121) with an accuracy of  $\pm 0.01\text{ kW}$  and  $\pm 0.01\text{ kWh}$  are installed in the power distribution box to record the instantaneous power consumption and accumulated energy consumption of the chillers and cooling towers. All the measured data were controlled and recorded automatically by a computer through a National Instrument data acquisition interface. The experimental data were recorded continuously with 1-minute time intervals. And the accumulated energy consumption data were calculated hourly-based.

Commissioning tests were conducted to analyze the steady state performance of the experimental HVAC system. The uncertainties of the cooling capacity and COP estimated by the composite system model for the real laboratorial HVAC system were approximately 4.5% and 5%, respectively. The maximum difference between the chilled water-side and the refrigerant-side capacity was also less than 5%. The maximum difference between the condenser water-side and the refrigerant-side capacity was less

than 3%. The maximum difference between condenser capacity and cooling tower capacity was less than 6%. These uncertainties are acceptable in the real application. For the local control, the DDC controllers are installed to control the frequency of the VSD pump and fan ( $Freq_{pump}$  and  $Freq_{fan}$ ), the opening ratio of the expansion valve ( $\mu_{valve}$ ) and the frequency of the VSD compressor ( $Freq_{com}$ ) to the set points.

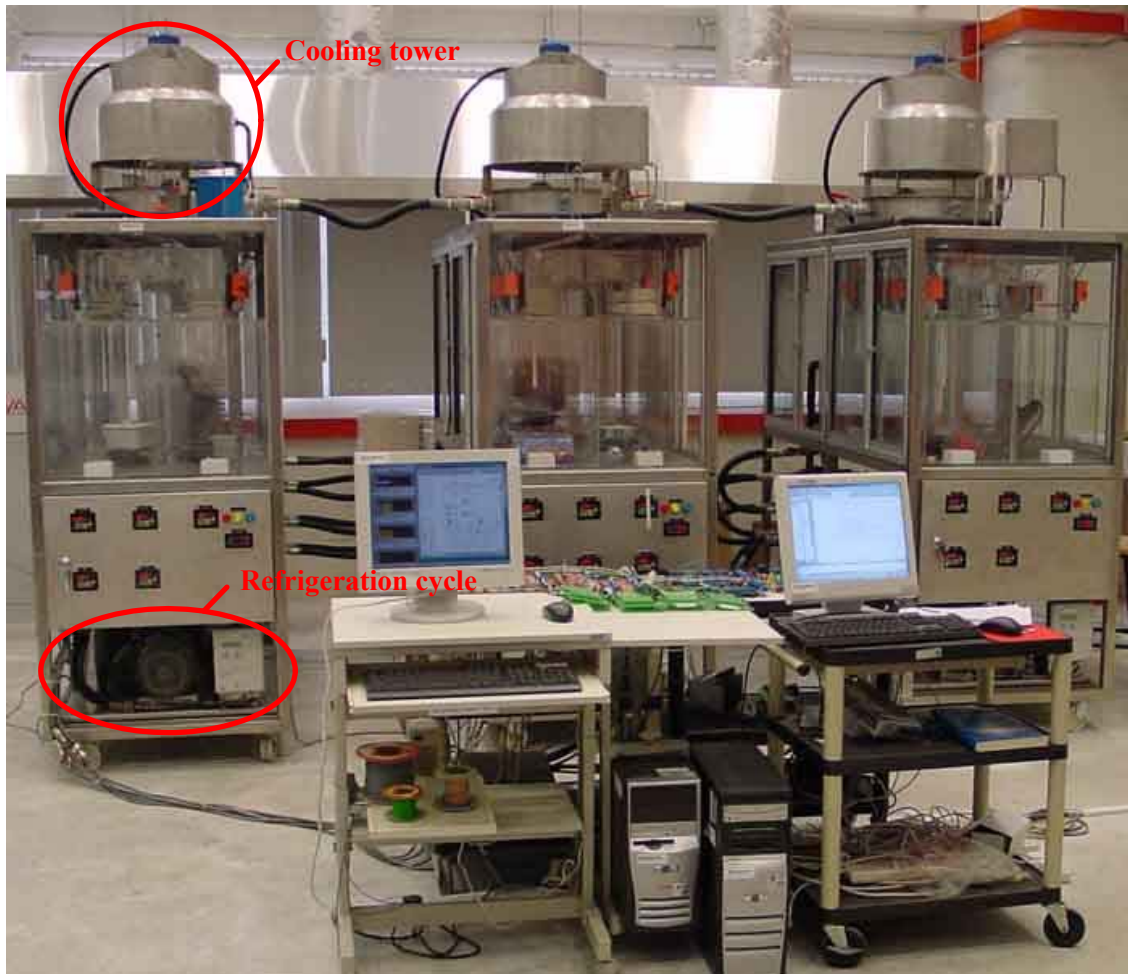


**Figure 7.1 Experimental setup**

The main parameters of the components of the pilot HVAC out-building section are already given in Table 6.1.

### ***7.3 Implementation of System Optimization Approach***

The hybrid model-based optimization approach presented in this thesis is developed as part of EMCS implemented in the laboratory scale HVAC system located in Singapore.

Based on the optimization problem formulation in Chapter 6, the hybrid model-based system optimization approach for the HVAC system outbuilding section should include two main functions for energy efficiency optimization: one is to seek the optimal set points of the condenser water temperature entering the condenser, and the other is to determine the best combination of control settings of the chillers (the condenser water pump is regarded as a part of the chiller system) and the cooling towers that can control the system of HVAC out-building section to satisfy the ever-changing cooling load requirement with the minimal instantaneous power input in each sampling period, e.g., one hour, and thus the minimal energy consumption in a certain period of time, e.g., one hour. In this study, the HVAC component models developed in the previous chapters are used to predict the system's energy performances of the HVAC out-building section with respect to the changes of the cooling load and ambient conditions. All of the component models are connected together according to their interactional thermal and power consumption relationships to form a system thermal performance and power consumption model.

The detailed online implementation procedures of this hybrid model-based system optimization approach using PSO are illustrated in Figure 7.2. Online measurements collected from the sensors and transmitters are sent to a measurement filter to remove the noisy or bad readings. These validated measurements and pre-defined initial settings, i.e., the initialization values of the independent variables for performing PSO are the inputs to the HVAC component models. The HVAC component models used for

optimization, including the cooling tower model and the refrigeration cycle model, are already parameterized in the model parameter identification phase, the method for model parameter identification have been introduced in Chapter 3, 4 and 5, respectively. For online applications, the parameters of the HVAC component models are required to be updated periodically to ensure the prediction accuracy.

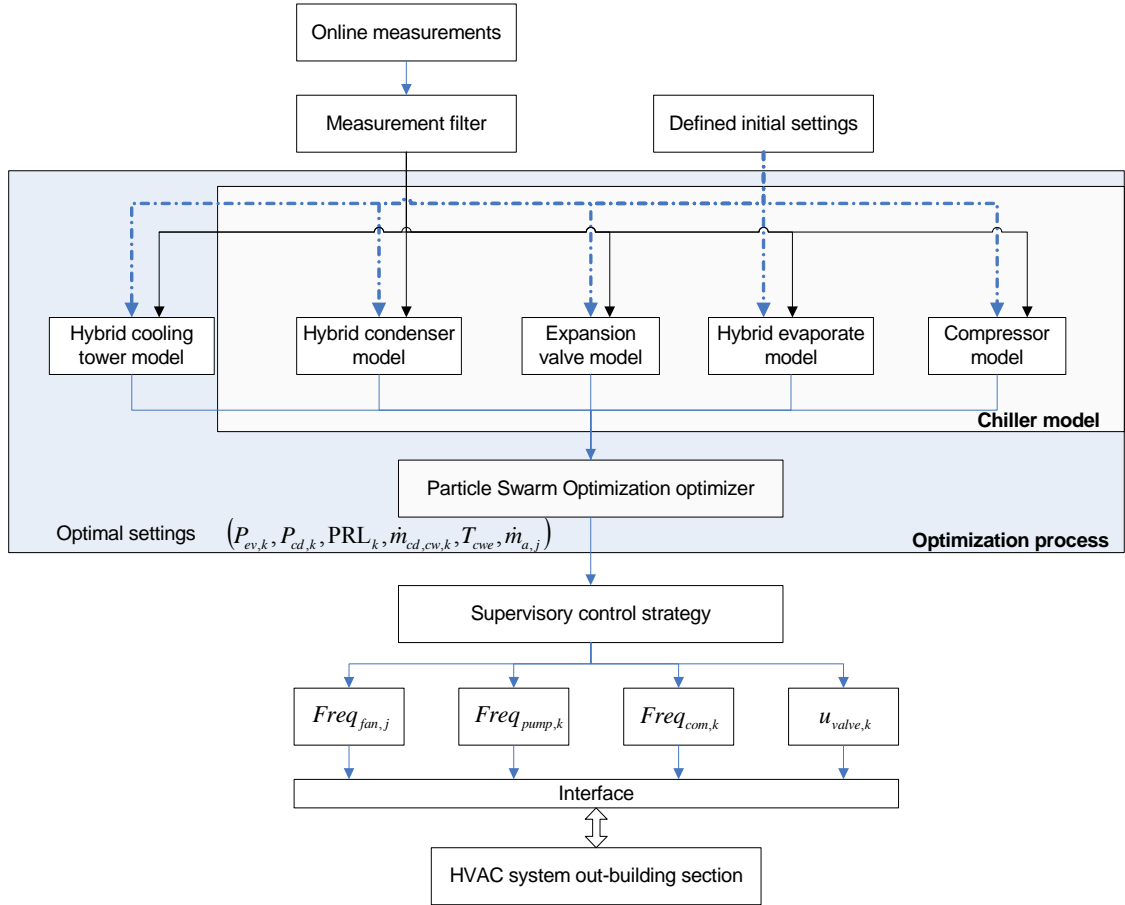


**Figure 7.2 Implementation procedures of the proposed system optimization approach**

Table 7.1 lists the measurements and initial settings of each component model.

**Table 7.1 Measurements and defined initial settings for system component models**

Component	Measurement/pre-identified data	Pre-defined initial settings
Cooling tower	$T_{wb,i}, T_{CTWS}$	$\dot{m}_{ctw}, \dot{m}_{a,j}$
Condenser	$\dot{m}_{ref,k}, \delta_k, \dot{m}_{chw,k}, T_{cd,refe,k}$	$PLR_k, P_{ev,k}, P_{cd,k}, T_{CWS}, \dot{m}_{cd,cw,k}$
Expansion valve	$\dot{m}_{ref,k}$	$P_{ev,k}, P_{cd,k}, PLR_k$
Compressor	$\dot{m}_{ref,k}, \delta_k$	$PLR_k, P_{ev,k}, P_{cd,k}$
Evaporator	$\dot{m}_{ref,k}, \delta_k, \dot{m}_{chw,k}, T_{ev,chw,k}, T_{ev,refe,k}$	$PLR_k, P_{ev,k}, P_{cd,k}$

Based on those component models, the optimizer using the PSO algorithm is then applied to determine the optimal set points for the independent variables of the overall system, i.e.,  $P_{ev,k}$ ,  $P_{cd,k}$ ,  $PLR_k$ ,  $\dot{m}_{cd,cw,k}$ ,  $T_{CWS}$  and  $\dot{m}_{a,j}$ . The relationships between these optimal set points and the corresponding actual system components control settings, i.e., compressor frequency ( $Freq_{com,k}$ ), valve setting ( $u_{valve,k}$ ), pump frequency ( $Freq_{pump,k}$ ) and fan frequency ( $Freq_{fan,k}$ ) can be determined by a look-up subroutine based on the manufacturers' specifications data or factory test data. And the supervisory control strategy of the EMCS will provide the final decision, i.e. control settings, for the EMCS taking into account the real time dynamic operating constraints for a practical application, e.g., the time interval between changes of two sets of control settings should avoid an alternating ON/OFF of the corresponding components etc. Then those final control settings are downloaded into the local DDC controllers to operate the corresponding components to achieve the minimal overall system energy consumption.

This hybrid model-based system optimization approach can be easily implemented without changing local controllers or HVAC system structures. Only a reasonable number of commonly used sensors are required to monitor the overall system, and the optimal operating set points can be provided based on the proposed hybrid models and the PSO optimization technique. The comparison between traditional control strategies and the proposed method are given as follows:

- $N_{ct,op}$ ,  $N_{ch,op}$ : In traditional methods, they are controlled by the scheduler of the EMCS. In the model-based system optimization approach, they are determined by the PSO based optimizer. For the experimental HVAC system tested in this thesis, an solution has following structure:

$$( P_{ev,1}, P_{cd,1}, PLR_1, \dot{m}_{cd,cw,1}, P_{ev,2}, P_{cd,2}, PLR_2, \dot{m}_{cd,cw,2}, P_{ev,3}, P_{cd,3}, PLR_3, \dot{m}_{cd,cw,3}, \dot{m}_{a,1}, \dot{m}_{a,2}, \dot{m}_{a,3}, T_{CWS} )$$

According to the constraint 4 of section 6.2.2, when  $PLR_k \leq PLR_{k,min}$ ,  $k = 1, 2, 3$ ;

$PLR_{k,min} = 0.1$ , that means the  $k^{th}$  chiller is not selected, and  $P_{ev,k}, P_{cd,k}, PLR_k$  and  $\dot{m}_{cd,cw,k}$  are set to be zero by the optimizer. Similarly, according to Constraint 1 of section 6.2.2, when  $\dot{m}_{a,j} \leq \dot{m}_{a,j,min}$ ,  $j = 1, 2, 3$ , that means the  $j^{th}$  cooling tower is not selected by the optimizer.

- $P_{ev,k}, P_{cd,k}$  : In traditional methods, they are controlled by an inverter driven compressor motor as well as expansion valves, and considered as a constant. In the model-based system optimization approach, they are computed as independent variables.
- $PLR_k$  : As a multiple chiller system consists of two or more refrigeration cycles, traditional optimization methods such as mixed integer linear and non-linear programming can be used to determine the PLR of each connected chiller; however, difficulties arise due to multiple local minima and the overwhelming computational effort. In the model-based system optimization approach, it is determined by the PSO based optimizer.
- $\dot{m}_{cd,cw,k}$  : In traditional methods, the mass flow rate of condenser water of  $k^{th}$  chiller condenser ( $\dot{m}_{cd,cw,k}$ ) is unchangeable for the majority of building HVAC systems. In the model-based system optimization approach, it is controlled by VSD pumps and the value is given by optimal independent variables directly.

- $T_{CWS}$ : In traditional methods, it is controlled by adjusting the frequency of the cooling towers VSD fans. The value of this variable is usually a constant or changes gradually with the cooling rejection rate as well as ambient condition. In the model-based system optimization approach, it is computed as one of the independent variables.
- $\dot{m}_{a,j}$ : In traditional methods, they are directly controlled by cooling tower VSD fans. The values of those variables are usually changed gradually to keep a set point value of condenser water temperature entering the condenser ( $T_{cwe}$ ) with the cooling rejection rate as well as ambient condition. In the model-based system optimization approach, it is also computed as the independent variables.

#### ***7.4 Experimental Study of Energy Performances***

In this study, the energy performance of the proposed hybrid model-based system optimization approach subject to the time varying loads and weather conditions is evaluated by comparing it with that of the conventional control strategy. Among the existing conventional control strategies, the fixed approach (the temperature difference between the condenser water supply temperature and ambient wet-bulb temperature remains constant) control method is one of the simplest strategies from an implementation point of view. The fixed approach control method varies the cooling tower air flow rate to maintain a constant temperature difference between the condenser water supply temperature and the ambient air wet bulb temperature.

In this study, the performance of the fixed approach control method (approach temperature is 6 °C) is used as the benchmark. And the comparison was in terms of the set points of the condenser water supply temperature and the total power consumption of the HVAC out-building section including chillers and cooling towers. Three typical

days, which represent the three typical operation conditions of the air conditioning system in the three different weather seasons of Singapore are selected to test and evaluate the energy performance of the proposed hybrid model-based system optimization approach.

#### **7.4.1 Building cooling load calculation**

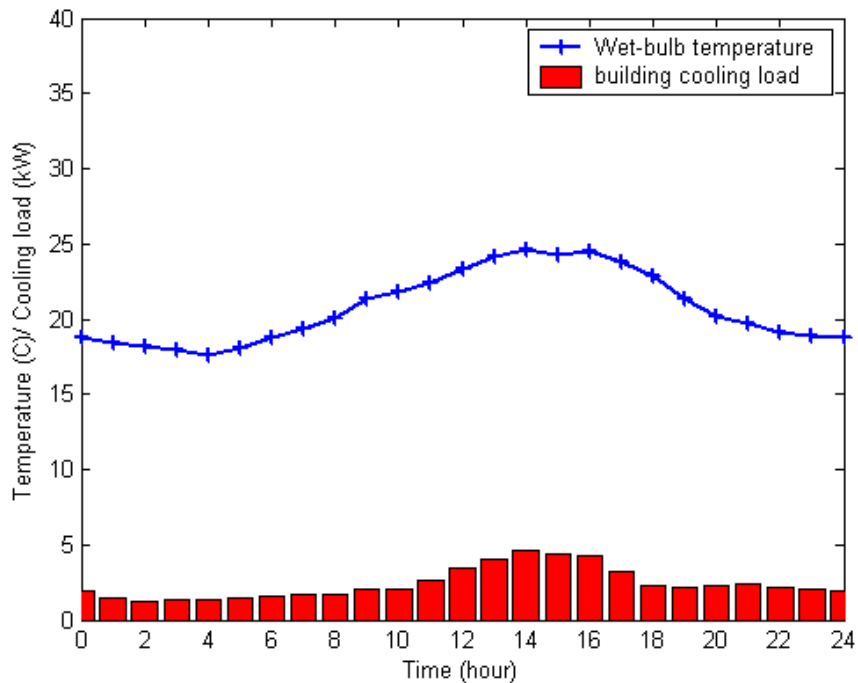
Because of its Southeast Asian location, Singapore is characterized by a hot and humid climate. Located just one degree north of the equator, Singapore quite naturally enjoys a tropical/equatorial climate. There is no clear-cut wet or dry season and rain is experienced every single day, usually in the afternoons and early evenings. However, there are two main monsoon seasons in Singapore: the Northeast Monsoon Season (December-March) and the Southwest Monsoon Season (June-September). Separating these two seasons is the inter-monsoon period (April-May and October-November), also named as non-monsoon season. To investigate the operation characteristics of a HVAC system under different weather conditions, we do the experiments with the HVAC system on each typical day of the three seasons (December 12th 2008, June 15th 2009, October 6th 2009) and the recorded daily weather data of these three typical days' are also used for simulations. Moreover, to also take into consideration the impact of weather condition on the cooling load of the building, we use TRNSYS 17 [137] multi-zone building model (Type 56) to build a one-floor empty building model to calculate the hourly based 24-hour cooling load profiles of the building under the weather conditions of the three seasons. TRNSYS standard model Type 56 is a complete, modular, and expansible simulation model for the transient simulation of multi-zone buildings.

This building under study is 10 meters in length, 8 meters in width and 3 meters in height, the thermal information of the building envelope are summarized in Table 7.2.

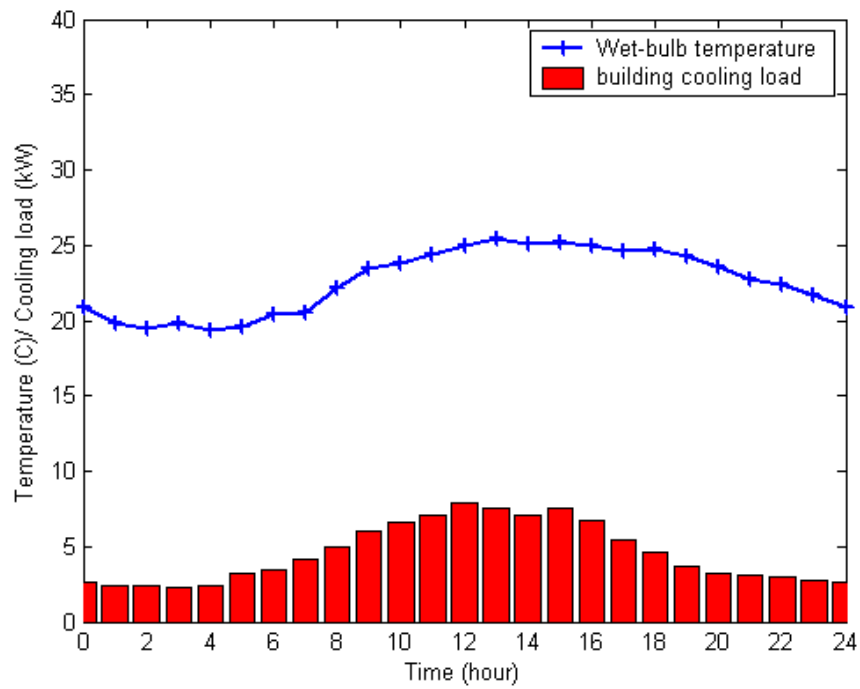
**Table 7.2 Building envelop parameters of the studied building**

Building envelop		Heat transfer coefficient [ $\text{W}/\text{m}^2\cdot\text{K}$ ]	
External wall		0.44	
External roof		0.29	
Ceiling	External ceiling	0.29	
	Adjacent ceiling	0.49	
Door		1.5	
Adjacent wall		0.93	
Window		Design value	
Window orientation	Window-wall ratio	Heat transfer coefficient [ $\text{W}/\text{m}^2\cdot\text{K}$ ]	shading
east	0.04	2	0.7
south	0.35	2	0.7
west	0.04	2	0.7
north	0.22	2	0.7

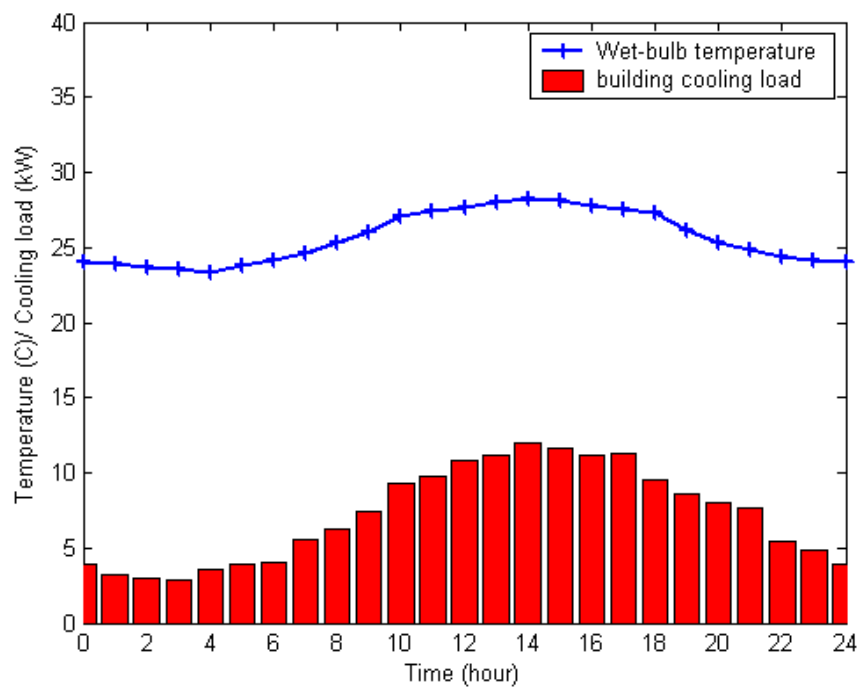
The profiles of daily building cooling load under the three typical days of three season, including (a) Northeast Monsoon Season, (b) Southwest Monsoon Season, and (c) Non-monsoon Season, are presented in Figures 7.3 (a) ~7.3 (c), respectively.



**(a) Northeast Monsoon Season**



(b) Southwest Monsoon Season



(c) Non-monsoon Season

**Figure 7.3 Wet-bulb temperature and building cooling load profile for a typical day**

Through Figure 7.3(a) ~ 7.3(c), we can observe that the cooling loads of an empty building without any internal thermal gain are dramatically impacted by the ambient

wet-bulb temperature. The building cooling load increases/decreases with respect to the increase/decrease of the ambient wet-bulb temperature. And we also can notice that the cooling load at different times of the day may be different even for the same wet-bulb temperature. This is because the building cooling load is also affected by other weather factors, e.g., sun irradiation and wind speed etc. To simulate exactly the same cooling loads in the experiments, we can just change the temperature set point of the return chilled water through controlling the power input of the auxiliary electrical water heat. The control strategy is then implemented into the EMCS for the laboratorial HVAC system to optimize the energy performance under the weather conditions of the three typical days. The condenser water supply temperature can be directly measured from the temperature transmitter; and the corresponding instantaneous power consumptions as well as the accumulated energy consumption of the system are recorded by the power meter.

#### **7.4.2 Fixed approach control method simulation and implementation**

Since different models may result in different calculation deviations, the fixed approach control method utilizes the same refrigeration cycle and cooling tower models as that of the proposed system optimization approach used to predict the system performance in the following comparison studies. For the fixed approach method, it is impossible to achieve identical operating weather conditions under which the proposed method is tested on the experimental HVAC system. Alternatively, with the recorded weather data of these three typical days, only simulation data of the fixed approach method based on the real HVAC system are used to compare with the experiment data of the proposed method. For the fixed approach method, a traditional sequencing control algorithm for the chillers and cooling towers is adopted, which is an increment/decrement sequencing, where the additional chiller is staged on when the

cooling load is above a certain value, for example, 90% of chiller capacities, and the extra chiller is staged off in the same manner. For the sequencing of chilled water pumps, condenser water pumps, and cooling tower fans, they are switched on or off with the dedicated chillers. The implementation procedures of the fixed approach method based supervisory control are illustrated in Figure 7.4.

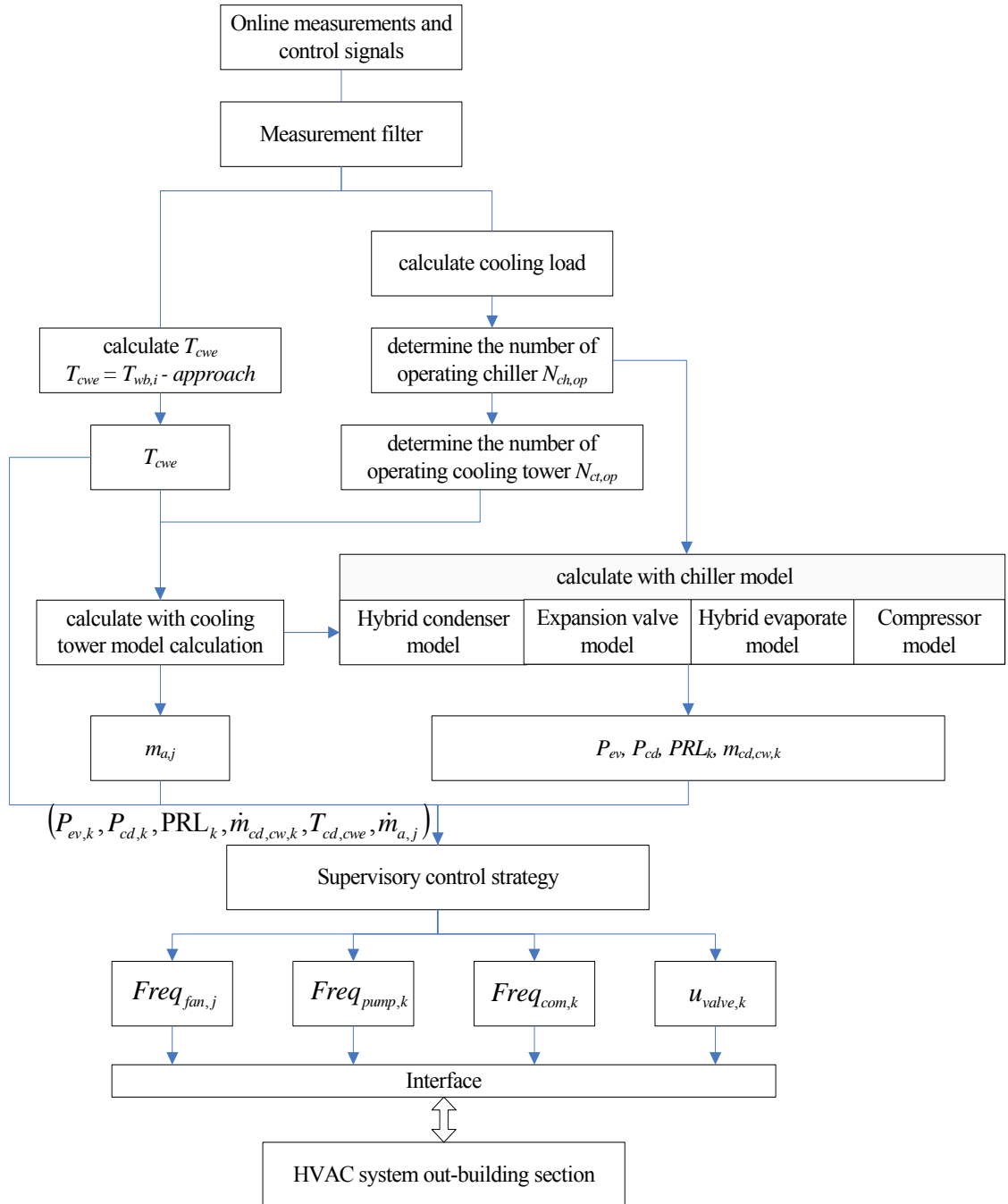
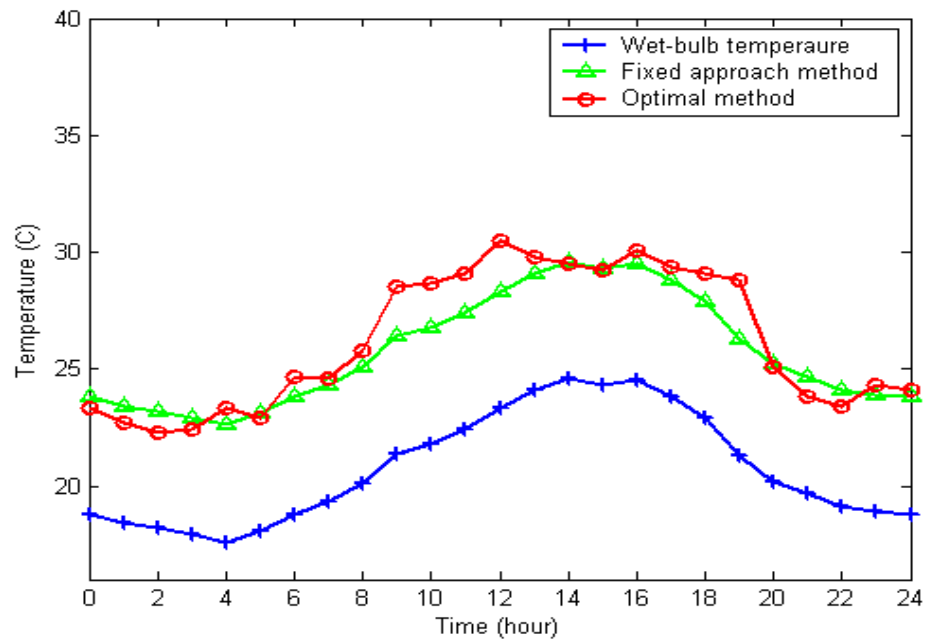


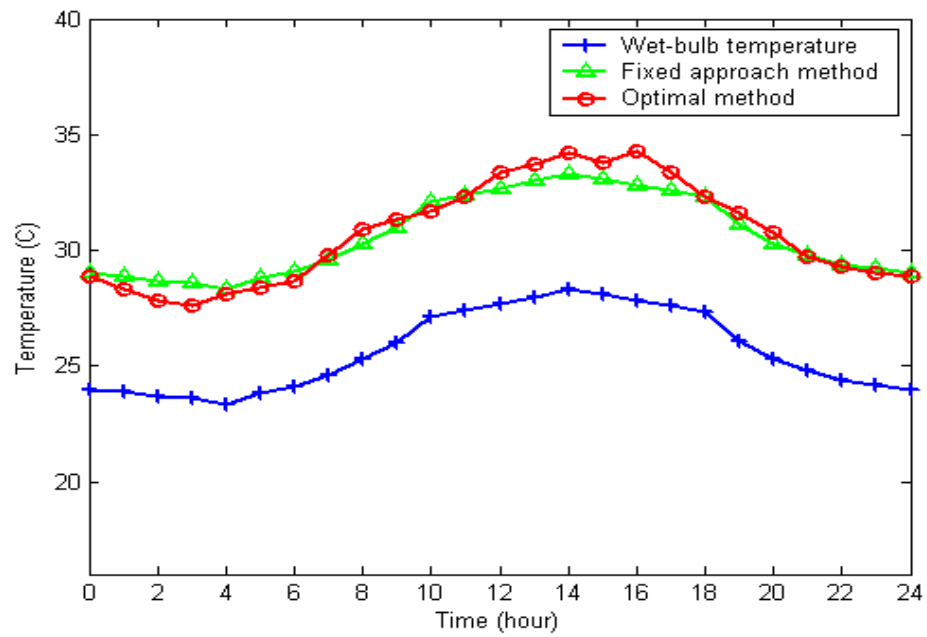
**Figure 7.4 Implementation procedures of the fixed approach method**

### 7.4.3 Evaluation of energy performance

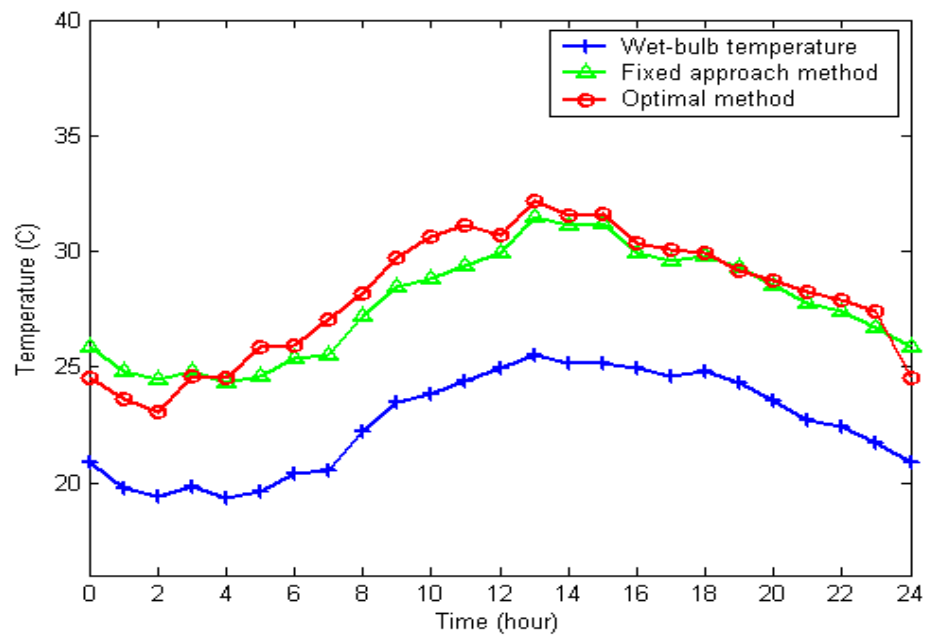
Figures 7.5(a) ~ 7.5(c) present the profiles of the hourly set points of the condenser water supply temperature obtained by using the proposed hybrid model-based system optimization method (indicated as optimal method in the figures), the fixed approach method along with the hourly wet-bulb temperature of the typical day in (a) the Northeast Monsoon Season, (b) the Southwest Season and (c) the Non-monsoon Season, respectively. These figures reveal that the optimal set points of the condenser water supply temperature by using the proposed hybrid model-based system optimization method deviate from the values determined by using the fixed approach control method.



(a) Northeast Monsoon Season



**(b) Southwest Monsoon Season**



**(c) Non-monsoon Season**

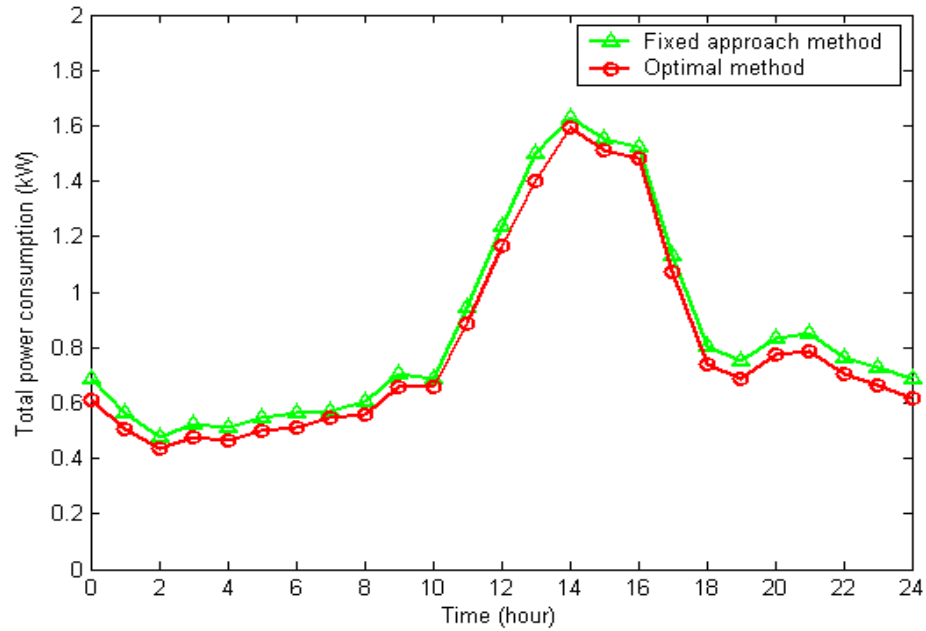
**Figure 7.5 Condenser water supply temperatures and wet-bulb temperatures for a typical day**

And considering the weather characteristic of Singapore, the search range of the set points of the condenser water supply temperature is pre-constrained between 20 °C and 36 °C. Figures 7.5(a) ~ 7.5(c) illustrate that the optimal set points of the condenser

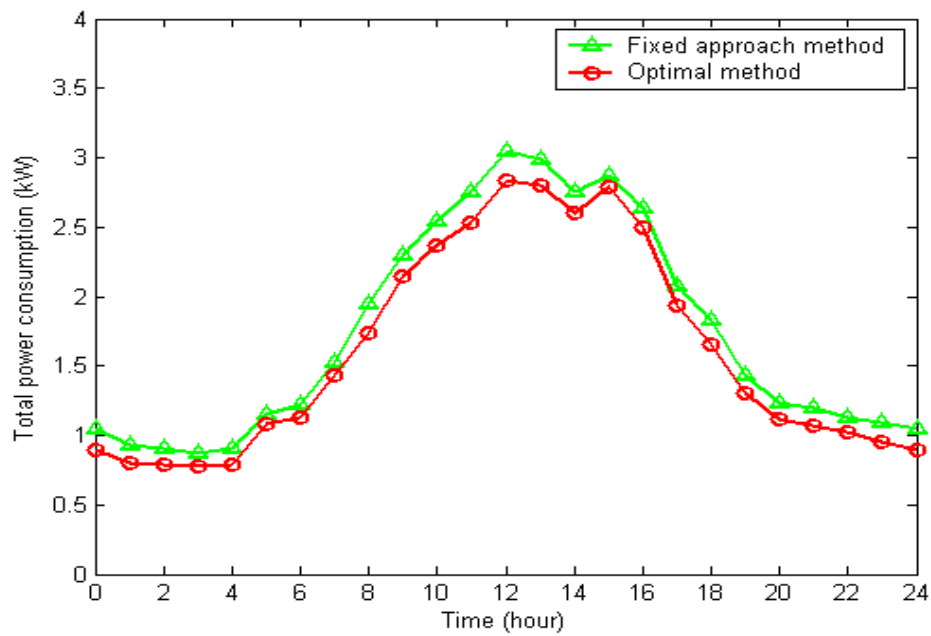
water supply temperature searched by using the proposed hybrid model-based system optimization approach are all within the defined search ranges for the three typical days, which can further verify the effectiveness of the proposed method. It is worth pointing out that the search range for each sampling period can be further narrowed down, as the set points of the condenser water supply temperature decided by the fixed approach method can be a good reference of the search range of the optimal set points of the condenser water supply temperature. From Figures 7.5(a) ~ 7.5(c), we can observe that optimal set points of the condenser water supply temperature at each sampling period may occur near to those set points decided by the fixed approach method. The reason is that besides the characteristics of the cooling towers and chiller systems in a HVAC system out-building section, the optimal set points of the condenser water supply temperature are partly impacted by the outdoor wet-bulb temperature; the detailed analysis of this point was examined in section 6.2.3. Therefore, the future work of fine tuning the search range may help to reduce the computational cost of proposed hybrid model-based system optimization approach using PSO based optimizer.

The performance of this hybrid model-based system optimization approach is further validated in terms of system power consumptions. Figures 7.6(a) ~ 7.6(c) present the differences between the hourly averaged power consumptions using the fixed approach control method and the proposed hybrid model-based system optimization approach (indicated as optimal method in the figures) in the typical days in the Northeast Monsoon season, Southwest Monsoon season and Non-monsoon season, respectively. From figures 7.6(a) ~ 7.6(c), it is obvious that the hourly averaged power consumption of the HVAC system outbuilding section controlled by the proposed method is less than that of the fixed approach method in each time interval, which means substantial energy can be saved when this hybrid model-based system

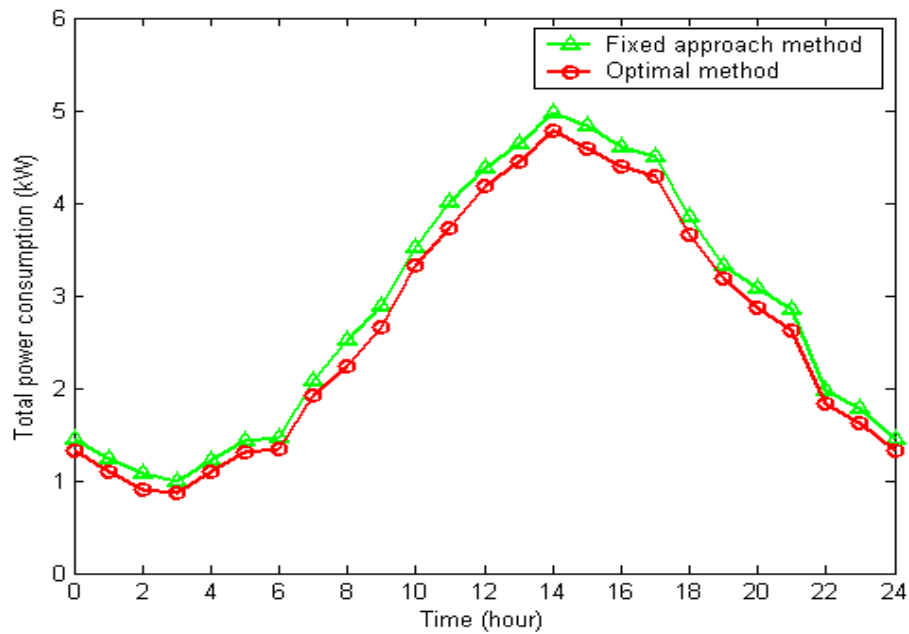
optimization approach is used. These comparisons reveal that the proposed method can provide much more energy efficient control than the fixed approach control method.



**(a) Northeast Monsoon Season**



**(b) Southwest Monsoon Season**



(c) No-monsoon Season

Figure 7.6 Total power consumptions for a typical day

Table 7.3 presents the accumulated energy consumptions of the HVAC out-building section (chillers + cooling towers) for three typical days when using different control methods. Compared with the fixed approach control method, the energy consumption saved by applying the proposed system optimization approach using PSO based optimizer is 1.32 kWh (6.38%), 3.34 kWh (7.88%) and 4.42 kWh (6.43%) in the typical three days in Northeast Monsoon Season, Southeast Monsoon Season and Non-monsoon Season, respectively.

Table 7.3 Comparison of one day total electricity consumption using different control strategies

Conditions	Light-load			Medium-load			Heavy-Load		
	Energy (kWh)	Saving (kWh)	Saving (%)	Energy (kWh)	Saving (kWh)	Saving (%)	Energy (kWh)	Saving (kWh)	Saving (%)
Operation strategy									
<b>Fixed approach</b>	20.69	-	-	42.41	-	-	68.70	-	-
<b>Proposed</b>	19.37	1.32	6.38	39.07	3.34	7.88	64.28	4.42	6.43

Compared with the fixed approach control method, over 6% of totally energy consumption can be saved by applying the proposed hybrid model-based system

optimization approach. And these results demonstrate that the proposed method is more energy efficient. It is noted, the fixed approach method is already optimized in some degree, a larger percentage of energy saving can be achieved if compared with conventional control strategies.

Figure 7.7 shows the identified number of operating towers and the identified number of operating chillers using the proposed hybrid model-based system optimization approach with respect to the building cooling load profile and the weather data of a typical day of Non-monsoon Season (Figure 7.3(c)). It shows that all three towers are in operation from 7 a.m. to 9 p.m., while the number of operating chillers changes between one and three. This observation demonstrates that operating more cooling towers with a lower fan frequency may be an energy efficient means to save power consumption of a HVAC system out-building section. This finding may help us to improve the optimization procedure of the PSO optimizer and thus enhance the computational time as well as reduce the memory demand further in our future work.

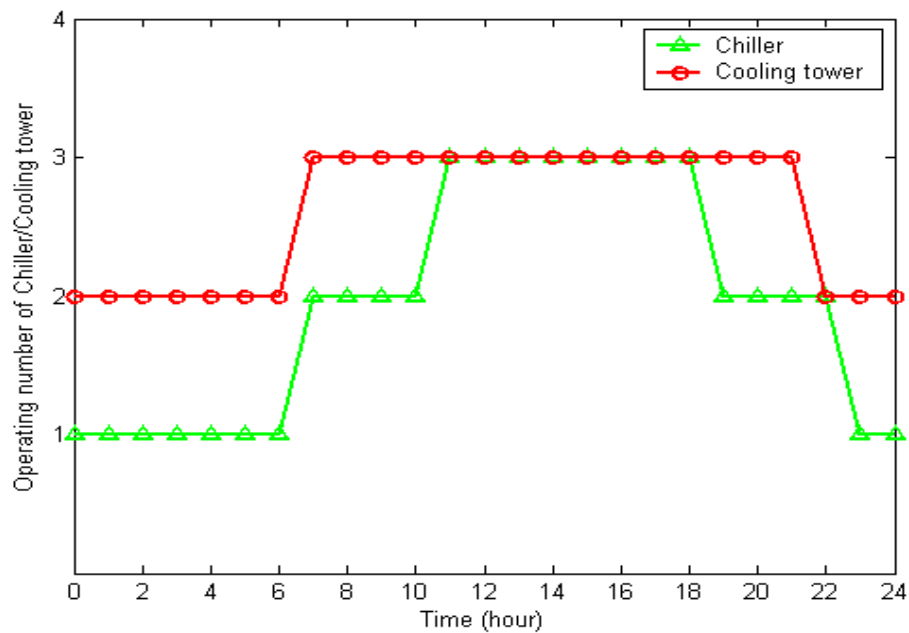


**Figure 7.7 Operating numbers of chillers and cooling towers**

Based on the above study, it can be found that the proposed hybrid model-based system optimization approach can save over 6% of total energy consumption more than the fixed approach method. The proposed method is still simple and easy enough to implement in practice. It is worthwhile to point out that the chilled water supply temperature is not optimized and is maintained as a constant ( $7^{\circ}\text{C}$ ) during the above experiments.

### **7.5 Summary**

In this chapter, the developed hybrid model-based system optimization approach is implemented into an EMCS to operate a laboratorial scale HVAC system. The energy performance evaluation experimental study shows total energy consumption can be saved when applying the hybrid model-based system optimization approach using PSO as an optimization technique compared to that of the conventional fixed approach control method. The daily energy savings when using the proposed hybrid model-based system optimization approach was over 6% as compared with the fixed approach control method. It is worthwhile to note that this part of the energy savings was achieved by applying the system optimization algorithm only and without adding any additional cost. It is also worth pointing out that the fixed approach control method used as the benchmark in this study has already optimized the temperature set point of the condenser water supply temperature. Therefore, the actual energy saving using the proposed hybrid model-based system optimization using PSO as optimization technique could be significantly more than the energy savings presented above since the conventional control strategies utilized in practice might be more simple. These experiments and the comparison studies show these characteristics make the proposed method suitable for online practical and real time optimization applications.

## CHAPTER 8 CONCLUSIONS AND FUTURE WORK

### *8.1 Conclusions*

In this thesis, hybrid modeling and model-based system optimization methodologies for building HVAC systems were presented. Firstly, the existing modeling methodologies and optimization approaches for building HVAC systems were reviewed and the key factors for performing system optimization were identified. Then the mathematical models of the major components were developed, including: 1) a static cooling tower model developed in Chapter 3 based on heat exchange theories. It only involves three parameters for correlation without requiring any geometric information; 2) dynamic cooling tower and cooling coil models proposed in Chapter 4 based not only on the components' inherent physical and mechanical characteristics but also on reasonable approximations of complex heat and mass transfer processes; and 3) a composite refrigeration cycle model developed in Chapter 5 based on the modeling of its components, including evaporator, compressor, expansion valve and condenser. These models are simple and easy-to-use, the experimental test results showed that they could accurately describe the process characteristics. In Chapter 6, with the static component models of cooling towers and refrigeration cycles, the physical constraints of the individual components as well as the interactions among them in the HVAC system were discussed and analyzed. Then, the optimization problems for the HVAC systems out-building section operation with respect to varying cooling load demands and changing ambient environments were formulated. The individual variables need to be optimized including condenser water supply temperature; evaporating and condensing pressure of the refrigeration cycle; PLR of each operating refrigeration cycle; condenser water mass flow rate and air flow rate through each cooling tower.

PSO and GA are then selected as the optimization techniques used for resolving the optimization problem. The fundamental theorem, optimization algorithms, procedure of algorithms implementation and the system architecture were introduced in details. Based on the same HVAC component models and simulation conditions, the comparison studies between PSO based optimizer and GA based optimizer in terms of accuracy, computing time and memory requirement were also given in details. The results show that the PSO based optimizer is superior to the GA based optimizer, hence the hybrid model-based system optimization approach using the PSO based optimizer becomes our proposed method.

In Chapter 7, experimental studies were conducted on a laboratory scale HVAC plant to validate and evaluate the application of proposed hybrid model-based system optimization approach. The experimental results of the energy performance evaluation showed that the overall system energy consumption could be indeed reduced by the proposed method as compared with the traditional fixed approach control methods

## ***8.2 Future work***

Real time control and optimization of the HVAC system is a continuously developing field along with the advance of hardware, software and communication technologies. The intention of this research work is to present hybrid modeling methodologies for HVAC component modeling and to establish a general systematic model-based approach to govern the operation of the HVAC process in terms of minimal energy usage without violating the system physical or interaction constraints. To transfer the technology from the laboratory to real world applications of commercial scale HVAC systems, more efforts are needed, including:

- 1) The compressor model adopted in Chapter 5 is only suitable to predict the performance of centrifugal type refrigeration cycles. More work should be done to investigate the mechanical characteristics of other types of refrigeration cycles, such as reciprocating type refrigeration cycles, scroll type refrigeration cycles, screw type refrigeration cycles, and absorption type refrigeration cycles. Simplified semi-physical or hybrid models for each type of refrigeration cycles with physical significant parameters are desirable for online modeling, simulation and optimization.
- 2) The algorithm of PSO can be further improved and the search ranges of the optimal set points can be fine tuned to enhance the control accuracy, computational cost and memory requirement in future studies, so as to extend this work to deal with larger commercial size HVAC systems.
- 3) The system optimization approach considered herein is limited to cooling systems. Methods similar to those explored here could be applied to heating systems as well. The optimization of set points in heating mode, considering both the effect on heating and cooling systems energy use, needs to be considered. A more fully integrated optimization is a logical continuation of this study.
- 4) This thesis only considers the system optimization approach for the HVAC out-building section. It would be more beneficial to develop the system optimization approach viewing the in-building section [107], even the overall HVAC system, as a whole.
- 5) So far, all the research work within this thesis is for building HVAC systems without cooling storage functions. If the systems have the function of cooling storage and they are operated at time varying tariff structure, and if the system

maintenance cost, maximum operation life cycle of the equipment and integration of renewable energy sources are taken into account, the formulation of the optimization problem should be re-considered and the optimization procedure may become more complicated. It is worth noting that minimizing system operating cost is not always equivalent to minimizing system energy input. How to determine the optimal set points for the multi-objective optimization of HVAC systems will be studied in the future.

- 6) Sophisticated nonlinear controllers for local loop control should be designed based on the developed dynamic models for the purpose of improving the control performance of the EMCS for HVAC system. And the component and system models developed in this thesis could be extended to online adaptive control applications.

## Author's publication

- [1] Jin G.Y., Cai W.J., Wang Y.W. and Yao Y., A simple dynamic model of cooling coil unit, *Energy Conversion and Management* 2006, Volume 47, Issue 15-16, Pages 2659-2672.
- [2] Xiong Q. and Jin G.Y., Iterative decentralized PID tuning based on gain and phase margins for TITO system, *International Journal of Innovative Computing, Information and Control* 2007 Volume 3, Number 2, Pages 385-396
- [3] Jin G.Y., Cai W.J., Lu L., Lee E.L., and Chiang A., A simplified modeling of mechanical cooling tower for control and optimization of HVAC systems, *Energy Conversion and Management* 2007, Volume 48, Issue 2, Pages 355-365.
- [4] Jin G.Y., Ding X.D., Tan P.Y., and Koh T.M., A hybrid water-cooled centrifugal chiller model, *The 6th IEEE conference on industrial electronics and applications*, Beijing, June 2011.
- [5] Jin G.Y. and Ding X.D. Tan P.Y., and Koh T.M., Dynamic control of cooling coil unit in HVAC system, *The 6th IEEE conference on industrial electronics and applications*, Beijing, June 2011.
- [6] Jin G.Y., Cai W.J., Ding X.D. and Lu L., A simple dynamic model for cooling towers, submitted to *Energy Conversion and Management* 2011.
- [7] Jin G.Y., Cai W.J. and Ding X.D., Optimization of HVAC Out Building Section by Particle Swarm Optimization Approach, submitted to *Energy Conversion and Management* 2011.

## References

- [1] ASHRAE, ASHRAE Handbook-Fundamentals, American Society of Heating, Refrigerating and Air-Conditioning Engineers Inc., 1997.
- [2] Wang S.W. and Ma Z.J., Supervisory and optimal control of building HVAC systems: A review. HVAC&R research January 2008, Volume 14, Issue 1, Pages 3-33.
- [3] Pérez-Lombard L., Ortiz J. and Pout C., A review on buildings energy consumption information, Energy and Buildings 2008, Volume 40, Issue 3, Pages 394–398.
- [4] Yuill G.K. and Wray C.P., Overview of the ASHRAE TC 4.7 annotated guide to models and algorithms for energy calculation relating to HVAC equipment. ASHRAE Transactions 1990, Volume 96, Part 2.
- [5] ASHRAE, ASHRAE Handbook—2000 HVAC Systems and Equipment, American Society of Heating, Refrigerating, and Air-Conditioning Engineers, 2000.
- [6] Rocky Mountain Institute Research Associates, Commercial Space Cooling and Air Handling, Technology Atlas, E Source, 1995.
- [7] Burger R., Cooling Tower Technology—Maintenance, Updating and Rebuilding, Fairmont Press, 1995.
- [8] Merkel F., Verdunstungskühlung, VDI Forschungsarbeiten, Berlin, 275 (1925).
- [9] Stoecker W.F., Procedures for Simulating the Performance of Components and Systems for Energy Calculations, ASHRAE, Atlanta, 1976.
- [10] Braun J.E., Klein S.A. and Mitchell J.W., Effectiveness models for cooling towers and cooling coils, ASHRAE Transactions 1989, Volume 95, Part 2, Pages 164-174.
- [11] Bernier M.A., Cooling tower performance: theory and experiments, ASHRAE Transactions 1994, Volume 100, Part 2, Pages 114-121.
- [12] Michel A.B., Thermal performance of cooling towers, ASHRAE Journal 1995, Volume 37, Part 4, Pages 56-61.

- [13] Mick S., Take it to the limit ... or just halfway?, ASHRAE Journal 1998, Volume 40, Part 7, Pages 32-39.
- [14] Soylemez M.S., Theoretical and experimental analyses of cooling towers, ASHRAE Transactions 1999, Volume 105, Part 1, Pages 330-337.
- [15] Hasan A. and Sirén K., Theoretical and computational analysis of closed wet cooling towers and its applications in cooling of buildings, Energy and Buildings 2002, Volume 34, Issue 5, Pages 477-486.
- [16] ASHRAE, HVAC 1 Toolkit: A Toolkit for Primary HVAC System Energy Calculation, American Society of Heating, Refrigerating, and Air-Conditioning Engineers, 1999.
- [17] Kloppers C. and Kröger G., Cooling tower performance evaluation: Merkel, Poppe, and e-NTU methods of analysis, Journal of Engineering for Gas Turbines and Power 2005, Volume 127, Number 1, Pages 1-7.
- [18] Wang Y.W., Cai W.J., Soh Y.C., Li S.Y. and Lu L., A simplified modeling of cooling coils for control and optimization of HAVC systems. Energy Conversion and Management 2004; Volume 45, Issue 18-19, Pages 2915-2930.
- [19] Skimin G.K. Technician's Guide to HVAC Systems. New York: McGraw-Hill, Inc.; 1995.
- [20] Kreith F. and West R.E., CRC Handbook on Energy Efficiency, Boca Raton: CRC Press; 1997.
- [21] Myers G.E., Mitchell J.W. and Lindeman C.F., The transient response of heat exchanger having an infinite capacitance rate fluid. ASME J. Heat Transfer 1970; Volume 92, Issue 2, Pages 269-275.
- [22] Kabelac S., The transient response relations for a serpentine cross-flow heat exchanger with water velocity disturbance. ASHRAE Transactions 1989; Volume 32, Issue 6, Pages 1183-1189.

- [23] Gartner J.R. and Daane L.E., Dynamic response relations for a serpentine cross-flow heat exchanger with water velocity disturbance, ASHRAE Transactions 1969; Volume 75, Part 1, Pages 53–68.
- [24] Bocanegra L.M. and Khan A.Y., Parametric analysis of heat and mass transfer performance of a counterflow, cooling and dehumidification coil. ASME Winter Annual Meeting 1992 November, Pages 8–13.
- [25] Khan A.Y., Heat and mass transfer performance analysis of cooling coils at part-load operating conditions. ASHRAE Transactions 1994; Volume 100, Issue 2, Pages 54–62.
- [26] Yao Y., Thermal analysis of cooling coils based on a dynamic model. Applied Thermal Engineering 2004, Volume 24, Issue 7, Pages 1037-1050.
- [27] Lebrun J., Ding X., Eppe J. P. and Wasacz T., Cooling coil models to be used in transient and/or wet regimes - theoretical analysis and experimental validation. In Proceedings of System Simulation in Buildings '90. Liege, Belgium, 1990.
- [28] Wang S.W., Dynamic simulation of a building central chilling system and evaluation of EMCS on-line control strategies. Building and Environment 1998, Volume 33, Issue 1, Pages 1-20.
- [29] Bi Q., Cai W.J., Lee E.L., Wang Q.G., Hang C.C. and Zhang Y., Robust identification of first-order plus dead-time model from step response. Control Engineering Practice 1999, Volume 7, Issue 1, Pages 71-77.
- [30] Bi Q., Cai W.J., Wang Q.G., Hang C.C., Lee E.L., Sun Yong, Liu K.D., Zhang Y. and Zou B., Advanced controller auto-tuning and its application in HVAC systems. Control Engineering Practice 2000, Volume 8, Issue 6, Pages 633-644.
- [31] Wang J.F. and Hihara E., Prediction of air coil performance under partially wet and totally wet cooling conditions using equivalent dry-bulb temperature method. International Journal of Refrigeration 2003; Volume 26, Issue 3, Pages 293-301.

- [32] Bourouni K., Bassem M.M. and Chaïbi M.T., Numerical study of coupled heat and mass transfer in geothermal water cooling tower. *Energy Conversion and Management* 2008, Volume 49, Issue 5, Pages 988-994.
- [33] Rafat Al-Waked and Masud Behnia., CFD simulation of wet cooling towers. *Applied Thermal Engineering* 2006. Volume 26, Issue 4, Pages 382-395.
- [34] Fisenko S.P., Brin A.A., Simulation of a cross-flow cooling tower performance. *International Journal of Heat and Mass Transfer* 2007, Volume 50, Issue 15-16, Pages 3216-3223.
- [35] Lemouari M. and Boumaza M., Experimental investigation of the performance characteristics of a counterflow wet cooling tower, *International Journal of Thermal Sciences* 2010, Volume 49, Issue 10, Pages 2049-2056.
- [36] Lemouari M., Boumaza M. and Kaabi A., Experimental analysis of heat and mass transfer phenomena in a direct contact evaporative cooling tower, *Energy Conversion and Management*, Volume 50, Issue 6, June 2009, Pages 1610-1617.
- [37] Heidarinejad G., Karami M. and Delfani S., Numerical simulation of counter-flow wet-cooling towers *International Journal of Refrigeration* 2009, Volume 32, Issue 5, Pages 996-1002
- [38] Al-Nimr MA., Dynamic thermal behavior of cooling towers. *Energy Convers Manage* 1998, Volume 39, Issue 7, Pages 631–636.
- [39] Al-Nimr MA., Modeling the dynamic thermal behavior of cooling towers containing packing materials. *Heat Transfer Eng* 1999, Volume 20, Issue 1, Pages 91–96.
- [40] Braun J.E., Mitchell J.W., Klein S.A. and Beckman W.A., Models for variable speed centrifugal chillers. *System simulation in buildings. Proceedings of the international conference in Liege (Belgium)* 1986, Pages 83–111.

- [41] Ng K.C., Bong T.Y. and Chua H.T., Performance evaluation of centrifugal chillers in an air-conditioning plant with the building automation system (BAS). *Proc Inst Mech Engrs* 1994, Volume 209, Pages 249-255.
- [42] Van Houte U. and Van den Bulck E., Modelling chiller performance using simultaneous equation-solving procedures. *International Journal of Refrigeration* 1994, Volume 17, Issue 3, Pages 191-198.
- [43] Browne M.W. and Bansal P.K., Steady-state model of centrifugal liquid chillers. *Int. J. Refrig.* 1998, Volume 21, Issue 5, Pages 343–358.
- [44] Browne M.W. and Bansal P.K., An elemental NTU-e model for vapour-compression liquid chillers. *International Journal of Refrigeration* 2001, Volume 24, Pages 612-627.
- [45] Gordon J.M., Ng K.C. and Chua H.T., Optimizing chiller operation based on finite-time thermodynamics: universal modelling and experimental confirmation. *Int. J. Refrig.* 1997, Volume 20, Issue 3, Pages 191–200.
- [46] Gordon J.M., Ng K.C. and Chua H.T., Centrifugal chillers: thermodynamic modelling and a diagnostic case-study. *Int. J. Refrig.* 1995, Volume 18, Issue 4, Pages 253–257.
- [47] Bourdouxhe J.P., Grodent M. and Lebrun J.J., A toolkit for primary HVAC system energy-calculations [Computer program], Atlanta, GA: American Society of Heating, Refrigerating and Air-Conditioning Engineers; 1995.
- [48] Bendapudi S., Braun J.E. and Groll E.A., Dynamic model of a centrifugal chiller system-model development, numerical study, and validation. *ASHRAE Trans* 2005, Volume 111, Pages 132–148.
- [49] Wong S.P.W. and Wang S.K., System simulation of the performance of a centrifugal chiller using a shell-and-tube type water-cooled condenser and R-11 as refrigerant. *ASHRAE Trans* 1989, Volume 95, Pages 445–454.

- [50] Jia Y., and Reddy T.A., A model-based feed-forward controller scheme for accurate chilled-water temperature control of inlet guide-vane centrifugal chillers. *J. Solar Energy Eng* 2005, Volume 127, Issue 1, Pages 48–52.
- [51] Wang S.W., Dynamic simulation of a central chilling system and evaluation of EMCS on-line control strategies. *Building and Environment* 1998, Volume 33, Issue 1, Pages 1–20.
- [52] Chan K.T., and Yu F.W., Thermodynamic-behaviour model for air-cooled screw chillers with a variable set-point condensing temperature. *Appl. Energy* 2006, Volume 83, Pages 265–279.
- [53] Chan K.T. and Yu F.W., Applying condensing-temperature control in air-cooled reciprocating water-chillers for energy efficiency. *Appl. Energy* 2002, Volume 72, Pages 565–581.
- [54] Yu F.W., and Chan K.T., Improved condenser design and condenser-fan operation for air-cooled chillers. *Applied Energy* 2006, Volume 83, Pages 628–648.
- [55] Yu F.W., and Chan K.T., Economic benefits of improved condenser features for air-cooled chillers serving an air conditioned hotel. *Appl. Therm. Eng* 2006, Volume.26, Pages 1063–1073.
- [56] Yu F.W., and Chan K.T., Modelling of a condenser-fan control for an air-cooled centrifugal chiller. *Applied Energy* 2007, Volume 84, Pages 1117-1135.
- [57] Fong K.F., Hanby V.I., and Chow T.T., a System optimization for HVAC energy management using the robust evolutionary algorithm. *Applied Thermal Engineering* 2009, Volume 29, Pages 2327-2334.
- [58] Koeppel E.A., Klein S.A., Mitchell J.W., and Flake B.A., Optimal supervisory control of an absorption chiller system. *HVAC&R Research* 1995, Volume 1, Issue 4, Pages 325–342.

- [59] Kota N.N., House J.M., Arora J.S., and Smith T.F., Optimal control of HVAC systems using DDP and NLP techniques. *Optimal Control Applications & Methods* 1996, Volume 17, Issue 1, Pages 71–78.
- [60] Wang S.W., and Jin X.Q., Model-based optimal control of VAV air-conditioning system using genetic algorithm. *Building and Environment* 2000, Volume 35, Issue 6, Pages 471–87.
- [61] Bassily A.M., and Colver G.M., Cost optimization of a conical electric heater. *International Journal of Energy Research* 2005, Volume 29, Issue 4, Pages 359–376.
- [62] Gray P., Hart W., Painton L., Phillips C., Trahan M. and Wagner J., 1997. A survey of global optimization methods.  
  
<http://www.cs.sandia.gov/opt/survey/main.html>
- [63] Kaya A., Chen C.S., Raina S., and Alexander S.J., Optimum control policies to minimize energy use in HVAC systems. *ASHRAE Transactions* 1982, Volume 88, Part 2, Pages 235–248.
- [64] Cumali Z., Global optimization of HVAC system operations in real time. *ASHRAE Transactions* 1988, Volume 94, Part 1, Pages 1729–1744.
- [65] House J.M., Smith T.F. and Arora J.S., Optimal control of a thermal system. *ASHRAE Transactions* 1991, Volume 97, Part 2, Pages 991–1001.
- [66] House J.M., and Smith T.F., A system approach to optimal control for HVAC and building system. *ASHRAE Transactions* 1995, Volume 101, Part 2, Pages 647–660.
- [67] Zaheer-Uddin M., and Patel R.V., The design and simulation of a sub-optimal controller for space heating. *ASHRAE Transactions* 1993, Volume 99, Part 1, Pages 554–564.
- [68] Zheng G.R., and Zaheer-Uddin M., Optimization of thermal processes in a variable air volume HVAC system. *Energy (Oxford)* 1996, Volume 21, Part 5, Pages 407–420.

- [69] Zaheer-Uddin M., and Zheng G.R., Optimal control of time-scheduled heating, ventilating and air conditioning processes in building. *Energy Conversion and Management* 2000, Volume 41, Issue 1, Pages 49–60.
- [70] Zaheer-Uddin M., and Zheng G.R., Multistage optimal operating strategies for HVAC systems. *ASHRAE Transactions* 2001, Volume 107, Part 2, Pages 346–352.
- [71] Koeppel E.A., Klein S.A., Mitchell J.W., and Flake B.A., Optimal supervisory control of an absorption chiller system. *HVAC&R Research* 1995, Volume 1, Issue 4, Pages 325–342.
- [72] Kota N.N., House J.M., Arora J.S., and Smith T.F., Optimal control of HVAC systems using DDP and NLP techniques. *Optimal Control Applications & Methods* 1996, Volume 17, Issue 1, Pages 71–78.
- [73] Henze G.P., Dodier R.H., and Krarti M., Development of a predictive optimal controller for thermal energy storage systems. *HVAC&R Research* 1997, Volume 3, Issue 3, Pages 233–264.
- [74] Henze G.P., Kalz D.E., Liu S., and Felsmann C., Experimental analysis of model-based predictive optimal control for active and passive building thermal storage inventory. *HVAC&R Research* 2005, Volume 11, Issue 2, Pages 189–214.
- [75] Wang S.W., and Jin X.Q., Model-based optimal control of VAV air-conditioning system using genetic algorithm. *Building and Environment* 2000, Volume 35, Issue 6, Pages 471–487.
- [76] Xu X.H., Wang S.W., Sun Z.W., and Xiao F., A model-based optimal ventilation control strategy of multi-zone VAV air-conditioning systems. *Applied Thermal Engineering* 2009, Volume 29, Issue 1, Pages 91-104
- [77] Zhang Y., and Hanby V.I., Model-based control of renewable energy systems in buildings. *HVAC&R Research* 2006, Volume 12, Issue S1, Pages 739-760

- [78] Goh W.Y., Lim C.P., Peh K.K., and Subari K., Application of a recurrent neural network to prediction of drug dissolution profiles. *Neural Computing & Applications* 2002, Volume 10, Issue 4, Pages 311–17.
- [79] Curtiss P.S., Brandemuehl M.J., and Kreider J.F., Energy management in central HVAC plants using neural networks. *ASHRAE Transactions* 1994, Volume 100, Part 1, Pages 476–93.
- [80] Massie D.D. Optimization of a building's cooling plant for operating cost and energy use. *International Journal of Thermal Sciences* 2002, Volume 41, Issue 12, Pages 1121–1129.
- [81] Bradford J.D. 1998. Optimal supervisory control of cooling plants without storage. PhD thesis, University of Colorado.
- [82] Curtiss P.S., J.F. Kreider, and M.J. Brandemuehl., Artificial neural networks proof of concept for local and global control of commercial building HVAC systems. *Proceedings of the ASME International*, 1993.
- [83] Gibson G.L. A supervisory controller for optimization of building central cooling systems. *ASHRAE Transactions* 1997, Volume 103, Part 1, Pages 486–493.
- [84] Chow T.T., Zhang G.Q., Lin Z., and Song C.L., Global optimization of absorption chiller system by genetic algorithm and neural network. *Energy and Buildings* 2002, Volume 34, Issue 1, Pages 103–109.
- [85] Xu J., Luh P.B., Blankson W.E., Jerdonek R., and Shaikh K., An optimization-based approach for facility energy management with uncertainties. *HVAC&R Research* 2005, Volume 11, Issue 2, Pages 215–237.
- [86] Braun J.E., Mitchell J.W., and Klein S.A., Performance and control characteristics of a large cooling system. *ASHRAE Transactions* 1987, Volume 93, Part 1, Pages 1830–1852.
- [87] Braun J.E., Methodologies for design and control of central cooling plants. PhD thesis 1988, University of Wisconsin-Madison.

- [88] Braun J.E., Klein S.A., Beckman W.A., and Mitchell J.W., Methodologies for optimal control to chilled water systems without storage. ASHRAE Transactions 1989a, Volume 95, Part 1, Pages 652–662.
- [89] ASHRAE. 2003. 2003 ASHRAE Handbook—HVAC Applications. Atlanta: American Society of Heating, Refrigerating and Air-Conditioning Engineers, Inc.
- [90] Pape F.L.F., Mitchell J.W., and Beckman W.A., Optimal control and fault detection in heating, ventilating and air-conditioning systems. ASHRAE Transactions 1991, Volume 97, Part 1, Pages 729–736.
- [91] Cascia M.A., Implementation of a near-optimal global set point control method in a DDC controller. ASHRAE Transactions 2000, Volume 106, Part 1, Pages 249–263.
- [92] Cassidy M.P. and Stack J.F., Applying adjustable speed AC drives to cooling tower fans. In: Annual Petroleum and Chemical Industry Conference. IEEE; 1988.
- [93] Shelton S.V. and Joyce C.T., Cooling tower optimization for centrifugal chillers. ASHRAE J. 1991, Volume 33, Part 6, Pages 28–36.
- [94] Kirsner W., 3 GPM/Ton condenser water flow rate: Does it waste energy? ASHRAE J 1996, Volume 38, Part 2, Pages 63–69.
- [95] Braun J.E., Klein S.A., Mitchell J.W., and Beckman W.A., Applications of optimal control to chilled water systems without storage. ASHRAE Transactions 1989, Volume 95, Part 1, Pages 663–675.
- [96] Braun J.E., and Diderrich G.T., Near-optimal control of cooling towers for chilled-water systems. ASHRAE Transactions 1990, Volume 96, Part 2, Pages 806–813.
- [97] Braun J.E., A general control algorithm for cooling towers in cooling plants with electric and/or gas-driven chillers. HVAC&R Research 2007a, Volume 13, Issue 4, Pages 581–598.
- [98] Cascia MA., Digital controller for a cooling and heating plant having near-optimal global set point control strategy. US Patent 5963458, 1999.

- [99] Olson R.T., and Liebman S., Optimization of a chilled water plant using sequential quadratic programming. *Engineering Optimization* 1990, Volume 15, Issue 3, Pages 171–191.
- [100] Austin S.B., Chilled water system optimization. *ASHRAE Journal* 1993, Volume 35, Part 7, Pages 50–56.
- [101] Ahn B.C., and Mitchell J.W., Optimal control development for chilled water plants using a quadratic representation. *Energy and Buildings* 2001, Volume 33, Issue 4, Pages 371–378.
- [102] Yao Y., Lian Z.W., Hou Z.J., and Zhou X.J., Optimal operation of a large cooling system based on empirical model. *Applied Thermal Engineering* 2004, Volume 24, Issue 16, Pages 2303–2321.
- [103] Sun J., and Reddy A., Optimal control of building HVAC&R systems using complete simulation-based sequential quadratic programming (CSB-SQP). *Building and Environment* 2005, Volume 40, Issue 5, Pages 657–669.
- [104] Braun J.E., Reducing energy costs and peak electrical demand through optimal control of building thermal storage. *ASHRAE Transactions* 1990, Volume 96, Part 2, Pages 876–888.
- [105] Simmonds P., Thermal comfort and optimal energy use. *ASHRAE Transactions* 1993, Volume 99, Part 1, Pages 1037–1048.
- [106] Lu L., Cai W.J., Soh Y.C., Xie L.H., and Li S.J., HVAC system optimization—condenser water loop. *Energy Conversion and Management* 2004, Volume 45, Issue 4, Pages 613–630.
- [107] Lu L., Cai W.J., Xie L.H., Li S.J., and Soh Y.C., HVAC system optimization—In building section. *Energy and Buildings* 2005, Volume 37, Issue 1, Pages 11–22.
- [108] Lu L., Cai W.J., Soh Y.C., and Xie L.H., Global optimization for overall HVAC systems—Part I: Problem formulation and analysis. *Energy Conversion and Management* 2005, Volume 46, Issue 7–8, Pages 999–1014.

- [109] Lu L., Cai W.J., Soh Y.C., and Xie L.H., Global optimization for overall HVAC systems—Part II: Problem solution and simulations. *Energy Conversion and Management* 2005, Volume 46, Issue 7–8, Pages 1015–1028.
- [110] Fong K.F., Hanby V.I. and Chow T.T., HVAC system optimization for energy management by evolutionary programming. *Energy and Buildings* 2006, Volume 38 Issue 3, Pages 220–231.
- [111] Braun J.E., Near-optimal control strategies for hybrid cooling plants. *HVAC&R Research* 2007. Volume 13, Issue 4, Pages 599–622.
- [112] Braun J.E., A near-optimal control strategy for cool storage systems with dynamic electric rates. *HVAC&R Research* 2007, Volume 13, Issue 4, Pages 557–580.
- [113] Burghardt D.M., *Engineering Thermodynamics with Applications*, HarperCollins Publishers Inc, 1986.
- [114] Waldram JR., *The theory of thermodynamics*. New York: Cambridge University Press, 1985.
- [115] Perry RL., *Thermodynamics for engineering technology*, California, Wadsworth Inc, 1984.
- [116] Holman J.P., *Heat Transfer (Seventh Edition)*, Singapore: McGraw-Hill Book Company, 1992.
- [117] White F.M., *Fluid Mechanics (Second Edition)*, Singapore: McGraw-Hill Book Company, 1986.
- [118] Nocedal J. and Wright S.J., *Numerical Optimization*, Springer-Verlag New York, Inc., 1999.
- [119] Stevens R.A., Fernandez J., and Woolf J., Mean temperature difference in one-,two- and three-pass cross-flow heat exchangers, *Trans, ASME* 1957; Volume 79, Pages 287-297.
- [120] Wang S.K., *Handbook of Air Conditioning and Refrigeration*, McGraw-Hill: New York, 2001.

- [121] Jin G.Y., Cai W.J., Lu L., Lee E.L., and Chiang A., A simplified modeling of mechanical cooling tower for control and optimization of HVAC systems. *Energy Conversion and Management* 2007, Volume 48, Issue 2, Pages 355-365.
- [122] Ding X.D., Cai W.J., Jia L. and Wen C.Y., Evaporator modeling – A hybrid approach. *Applied Energy* 2009, Volume 86, Issue 1, Pages 81-88.
- [123] Bourdouxhe J.P., Grodent M. and Lebrun J.J., Reference guide for dynamic models of HVAC equipment. Atlanta, Georgia: American Society of Heating, Refrigerating and Air-Conditioning Engineers, Inc.; 1998.
- [124] Ding X.D., Cai W.J., Jia L., Wen C.Y. and Zhang G.Q., A hybrid condenser model for real-time applications in performance monitoring, control and optimization, *Energy Conversion and Management* 2009, Volume 50, Issue 6, Pages 1513-1521.
- [125] Yu F.W., Chan K.T., Optimization of water-cooled chiller system with load-based speed control *Applied Energy* 2008, Volume 85, Issue 10, Pages 931-950
- [126] Ma Z.J., Wang S.W., Xu X.H., Xiao F., A supervisory control strategy for building cooling water systems for practical and real time applications, *Energy Conversion and Management* 2008, Volume 49, Issue 8, Pages 2324-2336.
- [127] Ma Z.J. and Wang S.W., An optimal control strategy for complex building central chilled water systems for practical and real-time applications, *Building and Environment* 2009, Volume 44, Issue 6, Pages 1188-1198,
- [128] Ma Z.J. and Wang S.W., Supervisory and optimal control of central chiller plants using simplified adaptive models and genetic algorithm, *Applied Energy* 2011, Volume 88, Issue 1, Pages 198-211.
- [129] Kennedy J. and Eberhart R., Particle Swarm Optimization, *Proceedings of the 1995 IEEE International Conference on Neural Networks*, IEEE Press 1995, Pages 1942-1948.

- [130] Jahanbani Ardakani A., Fattahi Ardakani F. and Hosseinian S.H., A novel approach for optimal chiller loading using particle swarm optimization, *Energy and Buildings* 2008, Volume 40, Issue 12, Pages 2177–2187.
- [131] Holland J.H., *Adaptation in Natural and Artificial Systems*, Cambridge, MA: MIT Press, 1975.
- [132] Goldberg D.E., *Genetic Algorithms in Search, Optimization, and Machine Learning*. Reading, MA: Addison-Wesley, 1989.
- [133] Hollstien R.B., *Artificial Genetic Adaptation in Computer Control Systems*, PhD Thesis, Department of Computer and Communication Sciences, University of Michigan, Ann Arbor, 1971.
- [134] Man K.F., Tang K.S., and Kwong S., Genetic Algorithms: Concepts and Applications, *IEEE Transactions on Industrial Electronics* 1996, Volume 43, Number 5, 1996.
- [135] Department of Automatic Control and Systems Engineering, *Genetic Algorithm Toolbox for Use with MATLAB*, University of Sheffield, 2000.
- [136] Sakawa M., Kato K., Sunada H. and Shibano T., Fuzzy programming for multi objective 0-1 programming problems through revised genetic algorithms, *European Journal of Operational Research* 1997, Volume 97, Pages 149-158.
- [137] TRNSYS official website: <http://sel.me.wisc.edu/trnsys/>